UiT The Arctic University of Norway

Faculty of Biosciences, Fisheries and Economics, Department of Arctic and Marine Biology

Changes in fat metabolism in the seasonal body mass cycle of captive Svalbard rock ptarmigan (*Lagopus muta hyperborea)*

—

Linn Aspelund

BIO-3950 Master's thesis in biology, May 2021

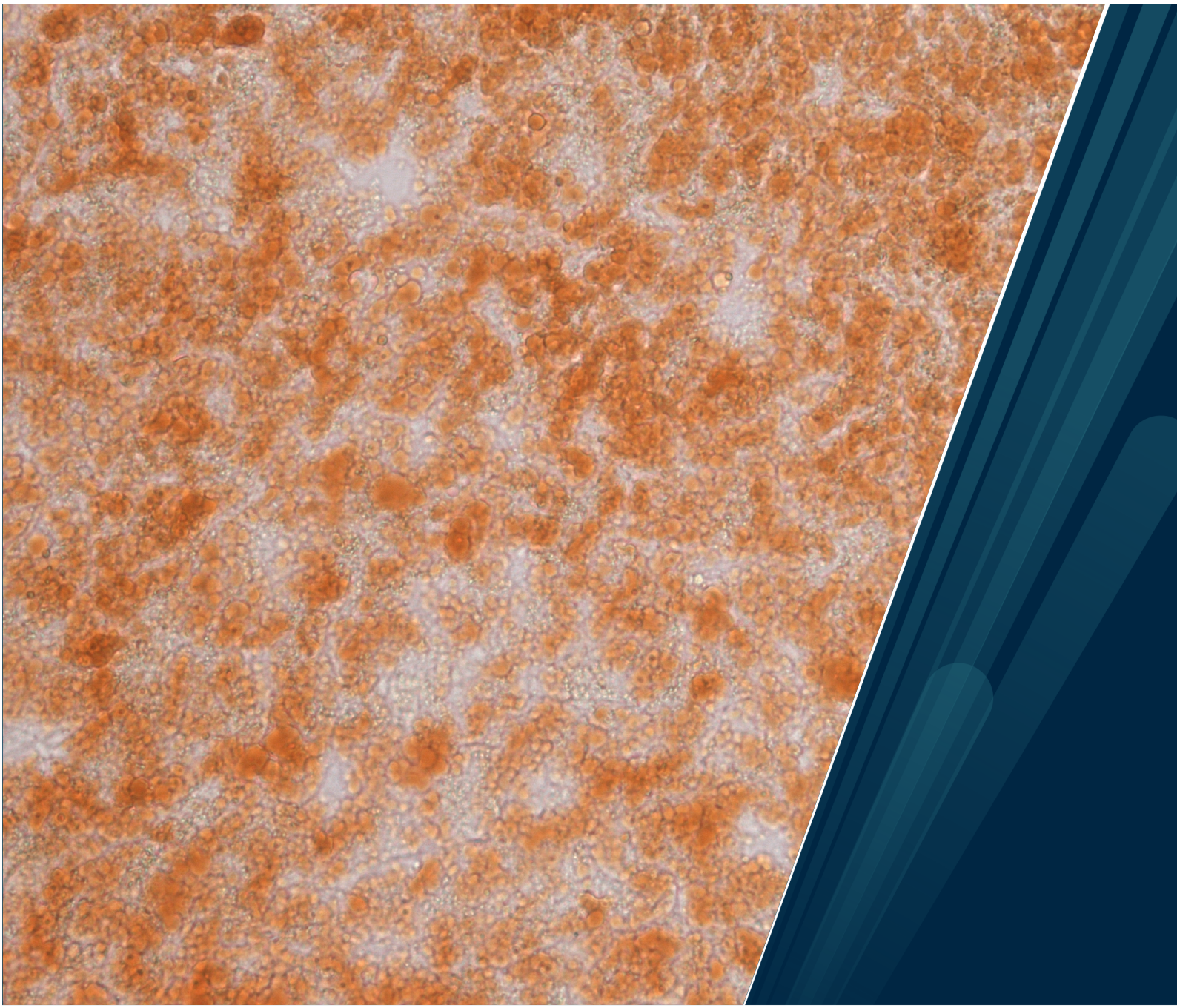

UiT The Arctic University of Norway

Faculty of Biosciences, Fisheries and Economics
Department of Arctic and Marine Biology

Changes in fat metabolism in the seasonal body mass cycle of captive Svalbard rock ptarmigan (*Lagopus muta hyperborea)*

—

Linn Aspelund

BIO-3950 Master's thesis in biology, May 2021

Supervisor:
David Hazlerigg, UiT – the Arctic University of Norway
Co-supervisor:
Daniel Appenroth, UiT – the Arctic University of Norway

Cover photo: Oil Red O stained liver section from Svalbard ptarmigan.

Acknowledgements

First of all, I would like to thank Daniel for allowing me the opportunity to work on this interesting project. Thank you for sharing your knowledge and your passion for these amazing birds. I am grateful for your trust in me to work independently, and always being available when I needed assistance.

I would also like to thank David for your insightful and creative feedback, and for inspiring me to think outside the box.

Thank you to all the members of the Arctic Chronobiology and Physiology research group for showing me the value of collaboration. A special thanks to Anna and Fayiri for all the fun hours spent together in the lab and in the office.

Thank you to my friends for bringing me joy from wherever you are in the world.

Last, but not least, I want to thank my family for your endless support and patience. Thank you for giving me the courage to follow my dreams.

Linn Aspelund

Tromsø, May 2021
Linn Aspelund

Abstract

The Svalbard ptarmigan exhibits profound seasonal variations in body mass. The deposition of fat in the fall is an adaptation that allows the ptarmigan to survive periods of food shortages during the Arctic winter. In this study, previously unexplored molecular aspects of this well-established body mass cycle were investigated. Captive Svalbard ptarmigan fed *ad libitum* and kept under short photoperiod were moved to constant light. Birds were sampled at four different stages in the body mass cycle and longitudinal measurements of physiology and behavior were taken throughout the study. In order to assess molecular control of their body mass cycle I measured the expression of six key elements of fat metabolism by qPCR. The expression of these lipid metabolism genes suggested that fatty acid synthesis was downregulated during the weight-loss phase and upregulated during the weight-gain phase, while lipolysis and fatty acid oxidation was downregulated in the weight-gain phase. Gene expression was also correlated to food intake, suggesting increased lipogenesis and decreased lipolysis and oxidation with high food intake. Results from Oil Red O (ORO) staining indicated that heart and muscle tissues of Svalbard ptarmigan are protected from excess accumulation of fat. ORO staining of liver tissue further revealed that the amount of fat in the liver varied during the BM cycle and was highest when the birds were fat during the short photoperiod. The average size of fat cells was higher in fat birds compared to lean birds, suggesting that the change in fat depots is accomplished through changes in fat cell sizes rather than cell numbers.

Keywords: Svalbard ptarmigan, *Lagopus muta hyperborea*, lipid metabolism, body mass cycle, FAS, ACC, ATGL, MGL, ACS, CPTI.

Table of Contents

List of Tables

List of Figures

List of abbreviations

ACACA	Acetyl-CoA carboxylase (gene)
ACC	Acetyl-CoA carboxylase (enzyme)
ACS	Acyl-CoA synthetase (enzyme)
ACSL1	Acyl-CoA oxidase (gene)
ATGL	Adipose triglyceride lipase (gene/enzyme)
ATP	Adenosine triphosphate
BM	Body mass
CPTI	Carnitine palmitoyl transferase I (enzyme)
CPTIA	Carnitine palmitoyl transferase I (gene)
FA	Fatty acid
FAS	Fatty acid synthase (enzyme)
FASN	Fatty acid synthase (gene)
FFA	Free fatty acid
FI	Food intake
LL	Constant light
MGL	Monoacylglycerol lipase (enzyme)
MGLL	Monoacylglycerol lipase (gene)
ROS	Rain-on-snow
SEM	Standard error of the mean
SP	Short photoperiod
TAG	Triacylglycerol
VFI	Voluntary food intake

1 Introduction

1.1 Svalbard and the Arctic

The Arctic is one of the last places on Earth where vast areas of wilderness still exist. It is a place of long, dark winters and summers with endless sunlight. Many definitions of the Arctic exist (Figure 1). Geographically, the Arctic is the area within the Arctic Circle, which is located at 66°30'N. Above this latitude the sun is above the horizon continuously in the summer and below the horizon continuously in the winter (NSIDC). More useful definitions when it comes to biological systems are the treeline or the 10°C July isotherm because these are distinctions that are important for life in these areas (Blix, 2005).

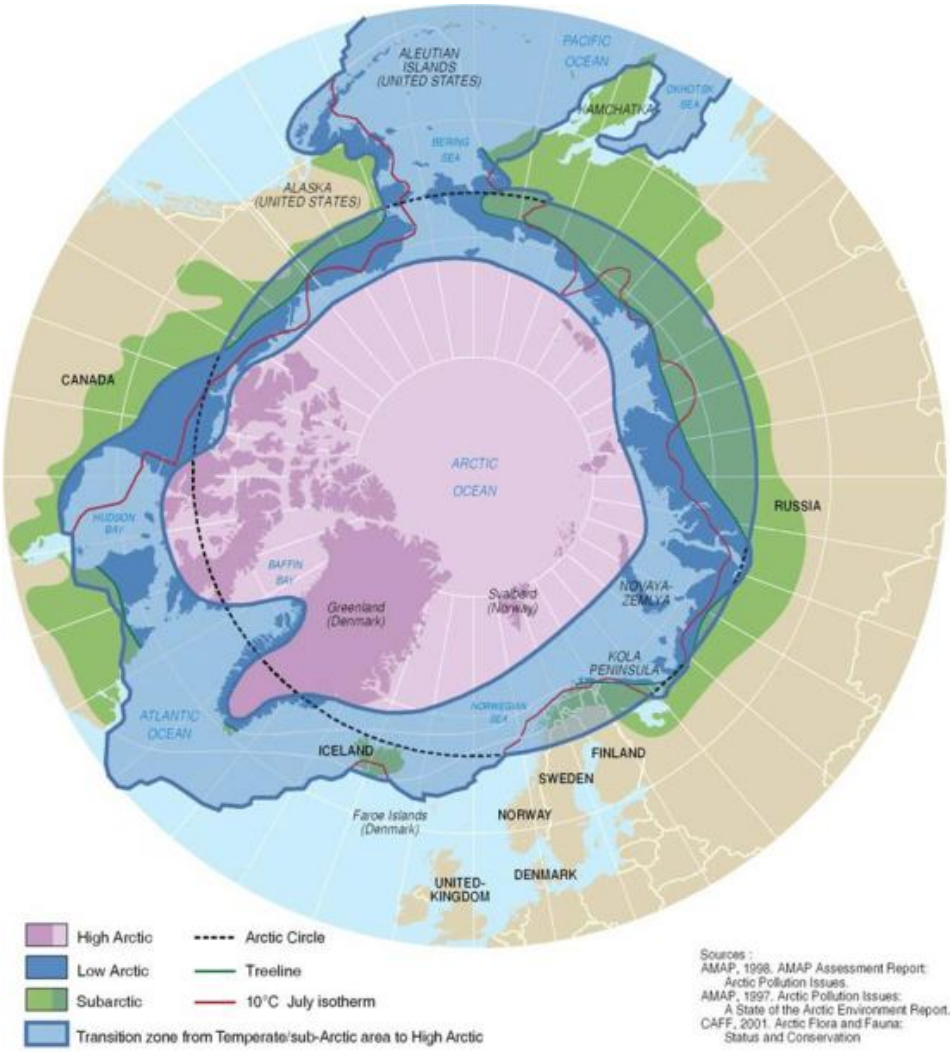

Figure 1. Definitions of the Arctic. How the High Arctic and the Low Arctic are separated, with the Arctic Circle, the treeline, and the 10°C July isotherm marked. Map made by cartographer: Philippe Rekacewicz (UNEP/GRID-Arendal), and available on: https://www.grida.no/resources/7010.

Svalbard is an archipelago located in the High-Arctic between 74°-81°N and 10°-35°E, and the largest island is Spitsbergen (Hisdal, 1998). It is a place that is heavily influenced by its location in the Arctic Ocean when it comes to climate, light conditions, biology and geography, and glaciers cover as much as 60% of the archipelago's surface (Hagen *et al.*, 1993).

1.1.1 Light conditions

Photoperiod is the period of daylight in a day. It is determined by latitude and the time of year, and it is the same every year. These properties make the change in photoperiod the most reliant way for an organism to track the time of year (Sockman & Hurlbert, 2020). As one moves further away from the Equator and closer to the poles, the annual variation in light conditions increases, i.e. the changes in photoperiod varies more between different times of year. The change in photoperiod from the summer solstice and the winter solstice happens more rapidly the further away from the Equator it is. On Svalbard, the sun is above the horizon from the 3rd of May to the 9th of August in the southernmost part of the archipelago, and from the 12th of April to the 30th of August in the northernmost parts (Hisdal, 1998). The polar night in the southernmost parts lasts from the 10th of November until the 1st of February, while it in the northernmost parts lasts from the 19th of October until the 23rd of February (Hisdal, 1998).

Another difference with increasing latitudes is in the duration of civil twilight, which increases further away from the Equator because the sun passes the horizon at a lower angle and it therefore takes longer to pass.

1.1.2 Climate and weather

The Arctic is generally a cold and dry place. However, compared to other places at similar latitudes, Svalbard usually has higher temperatures in the winter because of the warmer air and water that drifts northwards in the Atlantic (Hisdal, 1998). The mean annual temperature on Svalbard was between -5.2 °C and -4.3 °C in the years 1981-2010 (Førland *et al.*, 2011). However, as a place that is especially exposed to global warming, the temperature increased in recent decades with a simultaneous decrease in the annual variability of temperatures (Hølleland & Karlsen, 2020).

The location of Svalbard coincides with an area where cold air masses from the North meet warmer air masses from the South, which can cause extended periods of stormy weather,

especially in the winter (Hisdal, 1998). The Arctic is considered a cold desert because the cold air is not able to hold as much water vapor as warmer air, and this means that precipitation is rare. This holds true for Svalbard too, and the precipitation comes in small amounts at a time (i.e. a drizzle), also in the winter when most precipitation is snow (Hisdal, 1998). Because of the mild air masses coming from the South, it is not uncommon for winter temperatures to reach 0 °C or more in the winter. This might cause rain-on-snow (ROS) events, which can be quite common, especially in the southern parts of the archipelago (Wickström *et al.*, 2020). ROS events can have profound effects on animals, which rely on being able to dig through the snow in order to access food. This is because ROS events can cause the uppermost layer to freeze and become impossible to get through. This layer of ice makes food virtually unavailable to herbivores such as Svalbard reindeer (*Rangifer tarandus platyrhynchus*) and Svalbard ptarmigan (*Lagopus muta hyperborea*) (Hansen *et al.*, 2013; Kohler & Aanes, 2004).

1.1.3 Plant life and animals

The low temperatures and harsh conditions limit the plants and animals that are able to survive and thrive on Svalbard. Only the top layer of the soil is biologically active because it is the only layer that thaws in the spring and summer (Hisdal, 1998). In addition, the permafrost just below the surface prevents water from draining and the short period of high temperatures suitable for growth in the middle of the summer severely limits the plant life. Despite this, more than 160 species of vascular plants grow on Svalbard (Harland, 1997). There are no tall trees or bushes, and all plants here grow close to the ground to protect themselves from the difficult conditions.

The species on Svalbard are adapted to the extreme environmental conditions and are therefore excellent objects for studying Arctic adaptations. Since the documentation of species on Svalbard began, 31 species of mammals have been recorded (Prestrud *et al.*, 2004). Out of these, only eight species are considered common breeders. The Arctic fox (*Vulpes lagopus*), the Polar bear (*Ursus maritimus*) and the Svalbard reindeer (*Rangifer tarandus platyrhynchus*) are the only mammals commonly found on land, while the five other mammal species are pinnipeds and whales. Overall, 202 species of birds have been recorded, and 28 of these are considered common breeders (Prestrud *et al.*, 2004). While maritime ducks such as the Common eider (*Somateria mollissima*) and seabirds such as the Black guillemot (*Cepphus grylle*) overwinter in the Svalbard area, the only landbound bird that spends its entire life on

archipelago, is the Svalbard ptarmigan (Gjertz *et al.*, 1985; Løvenskiold, 1964; Parker & Mehlum, 1991).

1.2 Svalbard Ptarmigan

The Rock ptarmigan (*Lagopus muta*) has a circumpolar distribution, and all its populations can be found all year in tundra or alpine habitats (Sahlman *et al.*, 2009). It has been suggested that this species consists of as many as 23-30 sub-species (Storch, 2000). One of these, is the Svalbard ptarmigan (*L. m. hyperborea*), which in recent years has shown an increase in density and an overall positive population trend (Fuglei *et al.*, 2020). The reason for this is unknown, but possible explanations could include a positive effect of a longer summer on the plant community or changes in predator-dynamics (Henden *et al.*, 2017). The Svalbard ptarmigan is a medium-sized bird with a body mass of 550-1100 g, depending on the season, that has evolved many unique adaptations to life in the High-Arctic. They are expertly camouflaged in the winter with a white plumage, where the males have a black line between the eyes and the beak (Figure 2, left bird). In the spring and summer, the white winter plumage is replaced by a reddish brown plumage. The females shift into their pigmented plumage (Figure 2, right bird) in May, and by late October they molt back to their winter plumage (Stokkan *et al.*, 1986b). The males' plumages are not fully pigmented until the end of August, and only lasts until a rapid molt into the winter plumage in late September or early October (Stokkan *et al.*, 1986b). The difference in molting between males and females has been proposed to be due to an inhibiting function of testosterone on molting (Stokkan *et al.*, 1986b). Inhibiting testosterone levels explains why males do not molt into their pigmented plumage until late summer because that is when their plasma testosterone levels fall. Plumage is also an important way in assessing fitness in a partner or rival. For example, in the Black grouse the plumage is a reliable sign of the males' fitness (Siitari *et al.*, 2007). The Svalbard ptarmigan males' prolonged period with the winter plumage might therefore have evolved due to sexual selection or competition for territories.

Being herbivorous, and living year round on Svalbard, limits the selection of food that these birds have access to. The diet of Svalbard ptarmigan varies depending on the season and what is available. In the middle of the winter, they eat what they are able to access, which are mainly herbs such as saxifrages (Unander *et al.*, 1985). In the spring and the beginning of the summer, the birds are more particular about food choice and will primarily eat the polar willow (*Salix polaris*) (Unander *et al.*, 1985). In July and August, when plants flower, the

ptarmigan will mostly eat flowers, bulbils and leaves which are higher in protein content (Unander *et al.*, 1985).

Figure 2. Captive Svalbard ptarmigan. Male in white winter plumage on the left and female in brown summer plumage on the right (© Ida-Helene Sivertsen).

1.2.1 Life history

The breeding biology of the Svalbard ptarmigan is well-characterized (Steen & Unander, 1985; Unander & Steen, 1985). The first males arrive at the breeding grounds in early March, and until early April the males decide on territories, while the females do not arrive until early April. From the middle of April, the courting behavior begins and usually the males that established a territory the earliest will mate first. The females will start laying eggs in the beginning of June, and usually the first-year females will lay on average 8-9 eggs, while the older females lay on average 9-11eggs in a clutch (Pedersen *et al.*, 2005). After about 21 days of incubation, chicks hatch with an average weight of 16-17g. The chicks double their weight each week, and after only 40 days they weigh approx. 400g. The most important food for young chicks is the bulbils of the alpine bistort (*Polygonum viviparum*), especially in the first few weeks after hatching (Unander *et al.*, 1985).

The Svalbard ptarmigan has few natural predators, and the Arctic fox (*Vulpes lagopus*) might be the most important one (Pedersen *et al.*, 2005; Steen & Unander, 1985). The Arctic skua (*Stercorarius parasiticus*) and the Glaucous gull (*Larus hyperboreus*) can take eggs, while the Snowy owl (*Bubo scandiacus*) can take adults (Unander & Steen, 1985).

1.2.2 Seasonal changes in physiology

1.2.2.1 Body mass (BM)

One of the most striking differences between the Svalbard ptarmigan and other Rock ptarmigan subspecies is that the Svalbard ptarmigan show profound changes in BM throughout the year. One early description of these differences in BM reported visible fat depots in birds shot in September, while fat depots in the birds shot in April were depleted (Grammeltvedt & Steen, 1978). The seasonal changes in the BM have been further described by Mortensen and colleagues (1983). Starting in August, and continuing until November, an increase in BM occurs. Throughout the winter the BM decreases again, and by spring the birds are at their leanest (Figure 3). The birds remain lean throughout the summer, and this cycle is similar in both males and females. However, females have more accumulated fat between March and June due to laying and incubation of eggs. While the total BM vary greatly throughout the year, the fat-free BM remains relatively stable and the BM changes are due to changes in fat mass. At the peak of fat accumulation in late autumn, up to 35% of the ptarmigan's BM consists of fat. These seasonal changes in BM are mainly controlled by photoperiod (i.e. the day length). The fat starts accumulating in the fall when the period of midnight sun ends and reach the maximum level when the period of polar night begins (Mortensen *et al.*, 1983). The fat stores are depleted when the period of polar night ends. During the winter, approx. 30% of the daily energy demand is met by the fat stores while the rest is provided by continued foraging (Mortensen & Blix, 1989). The accumulated fat acts as an emergency energy reserve, and due to the frequent ROS events on Svalbard, it is likely that the ptarmigan will experience periods of food shortage during the winter when they must rely on stored energy for survival. While periods of ROS events have always been a hazard during winter, the current increase in the frequency of these events due to climate change, might challenge the ptarmigan's reliance on stored fat.

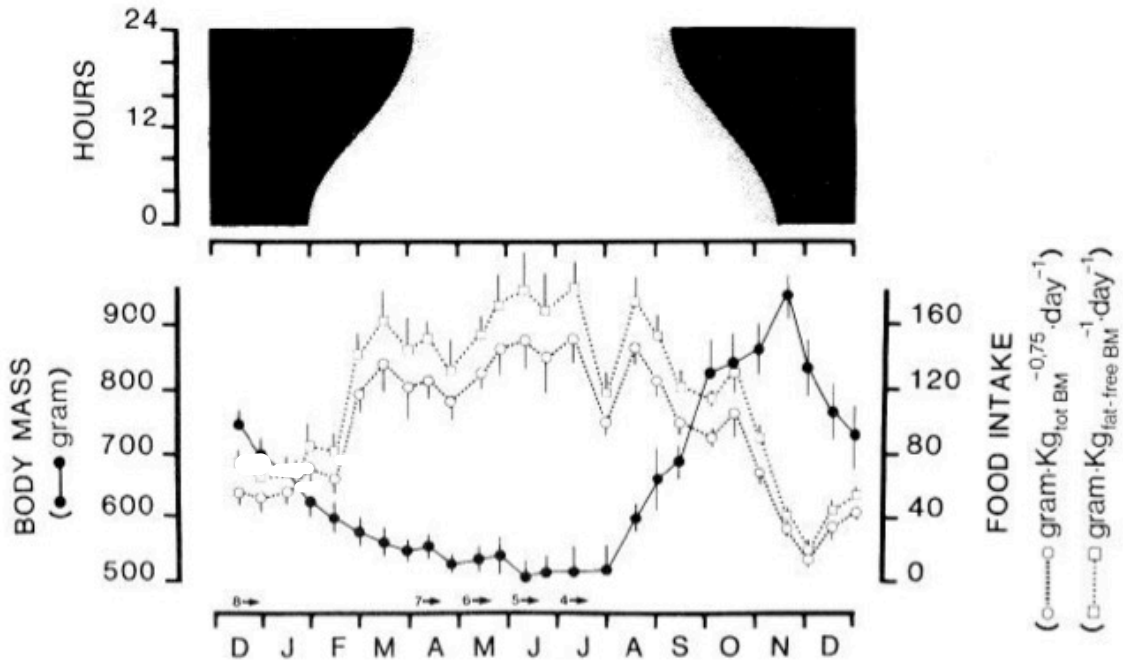

Figure 3. Body mass and food intake. The body mass in grams (closed circles) and food intake in $g \cdot kg_{total}^{-0.75}$/day (open circles) and $g \cdot kg_{fat\text{-}free}^{-0.75}$/day (open squares) in a year for captive Svalbard ptarmigan in natural light and temperature conditions, with *ad libitum* access to food. The arrows at the x-axis denotes sample size. The top panel shows the hours of daylight with black indicating darkness. Figure from (Stokkan *et al.*, 1986a).

1.2.2.2 Food intake (FI) and locomotor activity

In addition to the BM changes, the Svalbard ptarmigan show seasonal variations in their FI (Figure 3). In captivity, the FI is high from March, all throughout summer until August before it rapidly declines and remains low all through the dark winter (Lindgård *et al.*, 1995).

Birds studied in captivity with *ad libitum* access to food also exhibit changes in locomotor activity depending on the time of year (Lindgård *et al.*, 1995). From August/September until February/March the birds are relatively inactive, but once the sun returns they are significantly more active during spring and summer (Figure 4). In addition, birds in captivity show daily activity patterns that also change with the seasons (Stokkan *et al.*, 1986a). In spring and fall, the birds are diurnal, while during the midnight sun in the summer and the polar night in the winter, the birds lose their daily activity pattern.

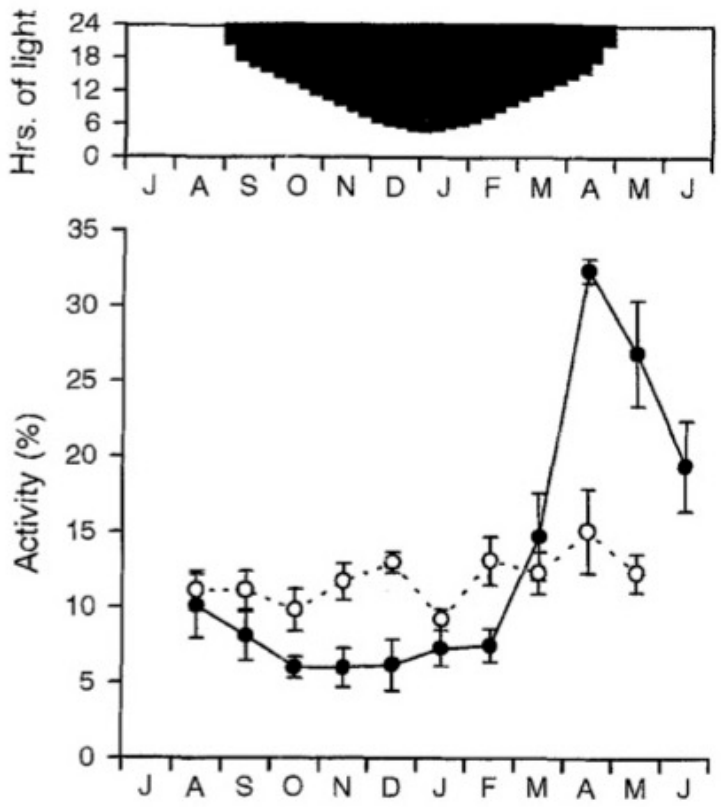

Figure 4. Locomotor activity. The mean locomotor activity level in a year for captive Svalbard ptarmigan in simulated natural light conditions (closed circles, n=4) and constant light (open circles, n=4). The activity is shown as a percentage of a theoretical maximum. The top panel shows the natural photoperiod with black indicating darkness. Figure from Lindgård *et al.* (1995).

1.2.2.3 Wild birds vs. birds in captivity

Svalbard ptarmigan in the wild and kept in captivity under natural light and temperature show the same BM cycle with the decrease in weight beginning in October/November (Mortensen *et al.*, 1983; Stokkan *et al.*, 1986a). However, when birds are kept indoors, even if light conditions simulate natural conditions, the BM stays high as long as the photoperiod is kept short and only starts declining with an increasing photoperiod (Lindgård *et al.*, 1995; Stokkan *et al.*, 1995).

While BM easily can be determined in wild birds, FI and activity level are not so easily measured and are only available for birds in captivity. This means that the observed seasonal changes in both FI and activity might not be the same in wild birds, and one must be careful when drawing conclusions about wild birds from studies done solely on birds in captivity.

1.2.2.4 Photorefractoriness

The increasing daylength in spring is a key factor to activate the reproductive system to initiate breeding in ptarmigan (Stokkan *et al.*, 1986b). However, the birds stop responding to the continuous long days, and breeding is terminated in July after approx. three months of constant light. This is photorefractoriness, which is a term used to describe the condition when the reproductive system has become inactive, despite continuous exposure to a stimulating photoperiod (Nicholls *et al.*, 1988). It is a gradual process, which requires an extended period of long days to proceed. Svalbard ptarmigan starts breeding in the beginning of June and become long-day refractory in July (Stokkan *et al.*, 1986b). Captive ptarmigan become long-day refractory earlier than in the wild, and terminate breeding in the beginning of June (Stokkan *et al.*, 1988). It also appears that for the increase in BM to happen in the autumn, the ptarmigan must first become photorefractory (Stokkan *et al.*, 1995).

1.2.2.5 Sliding set-point theory

BM remains relatively constant over long periods of time in many species of animals. This set-point for BM is finely tuned by adjusting the expenditure and consumption of energy (Mrosovsky & Powley, 1977). It has been proposed that the set-point is a sliding one in animals with a seasonal BM cycle, and depends on where in this cycle the animal is, i.e. the time of year (Mrosovsky & Fisher, 1970). The sliding set-point theory has been studied in the Siberian hamster (*Phodopus sungorus*), in which BM increases before the hibernation period and slowly decreases throughout the winter until spring (Mrosovsky & Fisher, 1970). These hamsters, when starved, lost weight at a fast rate. When food was returned the BM was not brought back to pre-starvation levels, but rather to a level appropriate to the time of the year.

The fact that *ad libitum* fed Svalbard ptarmigan in captivity show a seasonal BM cycle suggests that also these birds have a seasonal sliding set-point for BM where the BM is regulated according to the season. This is also evident from experiments where birds have been exposed to periods of starvation during the phase in the BM cycle when the birds decrease in weight (Mortensen & Blix, 1985). After periods of starvation, the birds increase their FI to gain back the BM that was lost. However, the birds do not go back to pre-starvation levels, but instead reach a BM that is similar to controls that have not been starved (Figure 5).

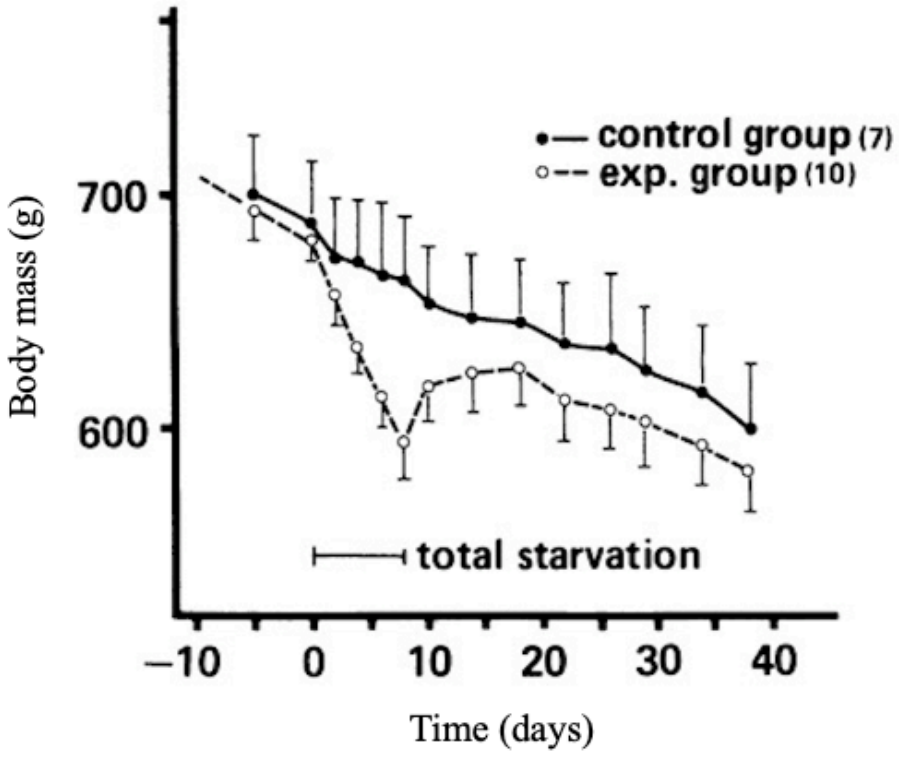

Figure 5. Sliding set-point of body mass. The BM (grams) of captive Svalbard ptarmigan in response to starvation. All birds in the control group (closed circles) were fed *ad libitum* throughout the experiment, and so were the birds in the experimental group (open circles) except for the duration of the starvation (7 days, from day 0 to day 7). Figure from Mortensen and Blix (1985).

1.3 Lipid metabolism

The aforementioned studies have described the seasonal BM cycle in Svalbard ptarmigan in great detail and have also explored its relation to VFI and activity levels. However, the molecular aspects of the BM cycle in Svalbard ptarmigan remain completely unexplored. Molecular details of lipid metabolism have been studied in other species of animals that also exhibit a seasonal BM cycle such as hibernators and migratory birds (Morin & Storey, 2009; Sharma & Kumar, 2019). The BM in many hibernators increase before the hibernation season, and the accumulated fat is used as fuel during hibernation when the animals do not feed (John, 2005). Molecular characteristics of fat tissue during the seasonal BM cycle have been described in hibernators, and so has the pattern of fatty acid (FA) synthesis being more active during the pre-hibernation fattening phase, whereas lipolysis and FA oxidation being more active during hibernation (Dark *et al.*, 1989; Mostafa *et al.*, 1993). Pre-migratory hyperphagia in migratory birds ensures enough fuel to make the migratory trek to their

overwintering grounds or back again to their breeding grounds (Odum, 1960). Also in migratory birds have details of lipid metabolism been described, which showed the same trends as in hibernators with a heavier reliance on FA synthesis during pre-migratory hyperphagia and on FA oxidation for fuel during migration (Sharma & Kumar, 2019).

1.3.1 Energy balance

For any animal to be in energy balance, the energy consumption must equal the energy expenditure. Energy intake consists of food, while energy expenditure depends on the costs of locomotor activity, thermoregulation, reproduction, and, especially, the basal metabolic rate of the animal (Blix, 2005). In any seasonal environment including the Artic, the ambient temperature and food availability show seasonal variability. Animals inhabiting these environments have evolved adaptations that allow them to cope with these seasonally changing factors that might greatly affect their ability to remain in energy balance. With the increased energy costs of thermoregulation at low ambient temperatures combined with shortage of available food, it seems almost inevitable that polar animals will have to cope with a negative energy balance during the long winter. Many Arctic animals, including the Svalbard ptarmigan, solve this problem by depositing fat in preparation for the winter and the likely negative energy balance that comes with it.

In the long-term, fat is stored as triacylglycerols (TAGs), which consist of three fatty acids (FAs) and a backbone of glycerol (Appling *et al.*, 2016). These molecules are excellent for energy storage because 1 gram of stored fat contains six times the amount of calories than what is found in 1 gram of carbohydrates (Appling *et al.*, 2016). Stored fat is not only used as an energy reserve, but can also function as insulation and protection.

The growth of adipose tissue can happen in two ways, the number of cells might increase (hyperplasia) or the size of each cell might increase (hypertrophy). In chickens, the growth of fat in younger birds is mainly due to hyperplasia, while as the birds get older, growth is mainly due to hypertrophy of fat cells (Buyse & Decuypere, 2014). When the adipose tissue decreases in chickens, this is mainly due to hypotrophy, i.e. the delipidation of fat cells (Buyse & Decuypere, 2014). In a hibernator with a seasonal body mass cycle, the Edible dormouse (*Glis glis*), the pre-hibernation growth of fat is due to hypertrophy of fat cells, while the depletion of fat during hibernation is due to hypotrophy (Mrosovsky *et al.*, 1987).

1.3.2 Fatty acid synthesis (Figure 6A)

To be able to utilize energy from fat, FAs need to be available in the bloodstream for uptake into the cells. There are three sources of FAs in the bloodstream: directly from the diet, from stored TAGs, and from *de novo* synthesis.

Dietary fats are hydrolyzed by lipases, and the resulting free FAs (FFA) are taken up by the mucosal cells in the gut where the FAs are esterified with glycerol to create TAGs. TAGs subsequently form lipoproteins by binding with phospholipids, cholesterol or apolipoproteins (Buyse & Decuypere, 2014). In mammals, these lipoproteins (chylomicrons) are released into the lymphatic system, but because the avian lymphatic system is poorly developed, the lipoproteins (portomicrons) are released into the hepatic portal vein in birds (Buyse & Decuypere, 2014; Zaefarian *et al.*, 2019).

FAs can also be synthesized *de novo*, and in birds the main site of this process is the liver. FA synthesis starts with excess glucose in the bloodstream entering the cells' cytoplasm where glycolysis happens. Glycolysis results in two pyruvate molecules for each glucose molecule, and these are actively transported into the inner mitochondrial matrix (Appling *et al.*, 2016). In the matrix, the enzyme pyruvate dehydrogenase oxidizes pyruvate to generate acetyl-CoA, which is a two-carbon molecule that is further processed in the citric acid cycle (Appling *et al.*, 2016). The citric acid cycle generates the electrons that set up the proton gradient used for ATP synthesis (i.e. generates energy) (Appling *et al.*, 2016). However, in times of excess glucose (i.e. excess energy intake), the acetyl-CoA can enter an alternative pathway: FA synthesis. The enzymes needed for the synthesis of FAs from acetyl-CoA are found in the cytoplasm. For acetyl-CoA to be able to move from the mitochondrial matrix to the cytoplasm, it must bind with oxaloacetoacetate to create the molecule citrate, for which the membrane has pores (Appling *et al.*, 2016). Once in the cytoplasm, citrate is broken apart again and acetyl-CoA is further processed. A non-reversible step of FA synthesis is the creation of malonyl-CoA from acetyl-CoA, which is carried out by the enzyme, acetyl-CoA carboxylase (ACC) (Appling *et al.*, 2016). This reaction requires energy in the form of ATP. The next step is the polymerization of malonyl-CoA molecules, through several chemical reactions, to form the FA palmitate (Appling *et al.*, 2016). All the steps of generating palmitate from malonyl-CoA are activated by the enzyme fatty acid synthase (FAS) (Buyse & Decuypere, 2014). The FAs are then attached to a glycerol backbone to generate TAGs, which are carried by lipoproteins in the blood (Buyse & Decuypere, 2014).

The TAGs within the lipoproteins are hydrolyzed by the enzyme lipoprotein lipase, which is synthesized by adipose and muscle cells (Buyse & Decuypere, 2014). The FFAs resulting from this reaction, can be taken up by adipose cells where they are stored as TAGs or they can generate energy in muscle cells by FA oxidation (Buyse & Decuypere, 2014).

1.3.3 Lipolysis (Figure 6B) and fatty acid oxidation (Figure 6C)

Lipolysis is the hydrolyzation of the stored TAGs to FFAs and glycerol, and takes place primarily in adipose cells. Three lipases are responsible for this process. The adipose triglyceride lipase (ATGL) is important in the first step of breaking apart the TAG to diglyceride and a FFA, while hormone-sensitive lipase (HSL) is responsible for breaking apart the diglyceride to monoglyceride and another FFA (Appling *et al.*, 2016). Monoacylglycerol lipase (MGL) breaks apart the monoglyceride to a FFA and glycerol. The FFAs are released into the bloodstream where they can be taken up by the cells that need the fuel they provide, such as muscle cells.

Once the FA is inside the cytosol of the cell, FA oxidation begins with an activation step where the enzyme acyl-CoA synthetase (ACS) converts the FA to a fatty acyl-CoA (Appling *et al.*, 2016). Next, the fatty acyl-CoA needs to be attached to carnitine to be able to move across the mitochondrial membranes and into the matrix. This process is carried out by carnitine acyl transferase I (CPTI), while CPTII breaks apart the fatty acyl-CoA and the carnitine in the matrix (Appling *et al.*, 2016). Inside the matrix, the oxidation happens where through a cycle of repeating steps the fatty acyl-CoA is oxidized to an acetyl-CoA, which can then enter the citric acid cycle and generate ATP for energy use (Appling *et al.*, 2016). The ATP yield from one molecule of FA, e.g. palmitate, is 129 ATP molecules, while one glucose molecule generates only 30-32 ATP, which is one of the reasons why fat is such an efficient way of storing energy (Appling *et al.*, 2016).

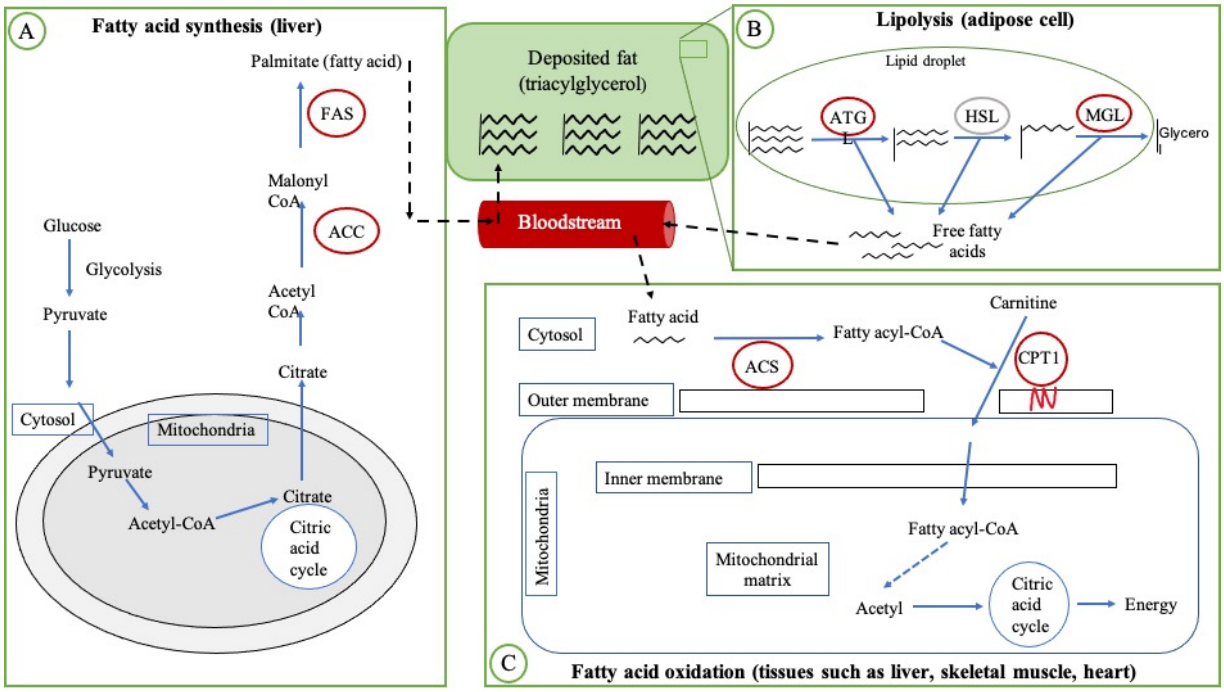

Figure 6. Overview of the lipid metabolism pathway. Schematic illustration of (A) fatty acid synthesis, (B) lipolysis, and (C) fatty acid oxidation with enzymes measured in this study circled in red. FAS: fatty acid synthase; ACC: acetyl-CoA carboxylase; ATGL: adipose triglyceride lipase; HSL: hormone-sensitive lipase; MGL: monoacylglycerol lipase; ACS: acyl-CoA synthetase; CPTI: carnitine palmitoyl transferase I.

1.4 Aims of the project

Birds (and mammals) with a pronounced BM cycle often accumulate excess amounts of fat, but in contrast to human obesity, no adverse health effects have been observed in these animals (Olsen *et al.*, 2021). It is therefore of interest for obesity research to understand what mechanisms are involved in the regulation of the BM cycle of animals such as the Svalbard ptarmigan.

It has been well-established how the BM changes throughout the year and with photoperiod in Svalbard ptarmigan, both in the wild and in captivity. Therefore, these birds make an excellent model for studying the molecular aspects of these changes in BM. In the following experiment, I aimed to examine how the BM is regulated on the molecular level in liver and fat tissue in the Svalbard ptarmigan. Based on what is already known about lipid metabolism regulation in hibernators and migratory birds, I hypothesize that in the Svalbard ptarmigan gene expression of key enzymes involved in lipogenesis (ATGL and MGL) and FA oxidation (ACS and CPTI) is upregulated during weight-loss prior to reproduction. While the gene expression of key enzymes involved in FA synthesis (ACC and FAS) is upregulated during the weight-gaining phase after reproduction is terminated in preparation for the next winter. I also aimed to relate these molecular findings to physiology and behavior. Lastly, I aimed to validate a histopathological staining technique (Oil Red O) to assess the fat state of the birds.

In this study, longitudinal measurements of BM, VFI and activity were recorded in captive Svalbard ptarmigan, and at four stages in the BM cycle birds were sampled. In order to examine molecular aspects, the gene expression of key lipid metabolism enzymes (as indicated in Figure 6) in liver and fat tissue was measured. In addition histopathological stainings of liver, heart, muscle and fat tissues were produced to assess their role in lipid metabolism in Svalbard ptarmigan.

2 Materials and methods

2.1 Experimental set-up and samplings

2.1.1 Animal care and housing

Svalbard ptarmigan (*Lagopus muta hyperborea*) bred in Tromsø (69°39'N, 18°57'E) were housed inside in approved animal care facilities at the University of Tromsø. The birds were housed in temperature and light controlled rooms with water and food provided *ad libitum*. There was daily housekeeping and the cages were cleaned once a week. The temperature in the rooms were kept between 4 and 9 °C, i.e. well within the birds' thermoneutral zone. Red illumination (Northlight 36-6557, 15 lm, Clas Ohlson, Insjön, Sweden) was on at all times, and fluorescent strip lights (Osram, L 58 W 830 Lumilux, approx. 1000 lx at floor level) provided the controlled lighting. The birds were kept in accordance with EU directive 2010/63/EU under license obtained from the Norwegian Food Safety Authority (Mattilsynet, FOTS 14209).

2.1.2 Experimental design

The experiment started in November 2019, and 33 birds were entrained to a short photoperiod (SP), which consisted of 5 hours of light and 19 hours of darkness (L:D 5:19). Throughout the experiment, various measurements were taken and a total of four samplings were done. The birds were kept on an SP until 29.02.2020 when the lighting was changed to constant light (LL). At the first sampling (20.02.2020), fat winter birds were sampled while still on an SP (n=7). At the second sampling (10.03.2020), birds that were rapidly losing weight after being moved to LL were sampled (n=8). The third sampling (08.05.2020) took place when the birds were reproductive and at their leanest (n=7). The last sampling (07.08.2020) took place when the birds had become photorefractive and started to gain weight again (n=8). Three birds were left at the end of the experiment, and not sampled. The sex- and age-ratios at each sampling are provided in Table 1. The experimental set up is summarized in Figure 7.

Table 1. The sex- and age-ratios at each sampling point.

	Old males	**Old females**	**Young males**	**Young females**
Sampling 1	2	1	2	2
Sampling 2	3	1	2	2
Sampling 3	2	1	2	2
Sampling 4	3	1	2	2

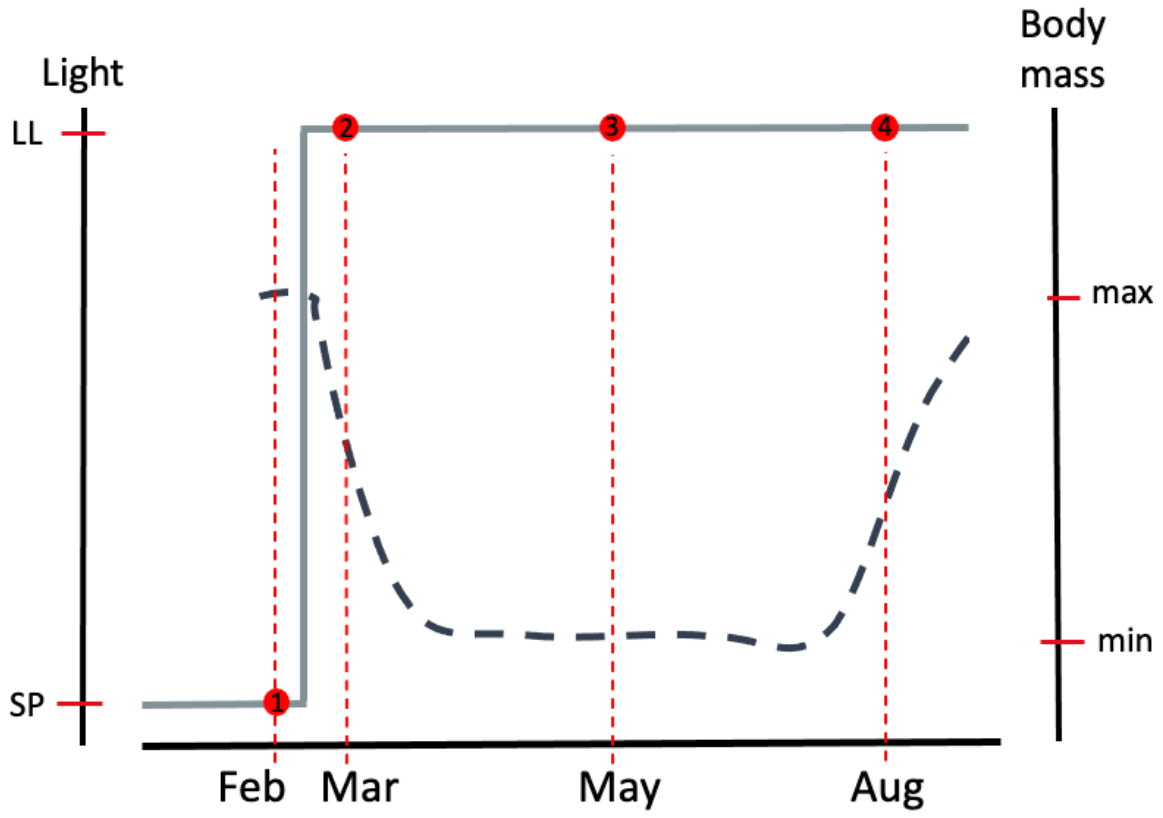

Figure 7. Experimental design. The light conditions (grey line), a short photoperiod (SP) until 29/02/20 when the birds were moved to constant light (LL) and the expected body mass cycle (stippled line) relative to seasonal maximum and minimum weights. The 4 sampling points at 20/02/20, 10/03/20, 18/05/20, and 07/08/20 are illustrated by the red stippled lines. A total of 30 birds were sampled, and the number of birds sampled at each point were 7 at sampling 1 and 3 and 8 at sampling 2 and 4.

2.1.3 Measurements

Body mass, locomotor activity, and food intake were measured throughout the whole experiment. Body mass was measured once a week by the use of a laboratory scale (Mettler PL3000, 612421). The voluntary food intake (VFI) was measured in a 24-hour period twice a week (i.e. 48 hours each week) by weighing the food given, and then weighing the food left after 24 hours to calculate the amount eaten. Activity was measured continuously by using homebuilt infrared sensors mounted on a homebuilt circuit board, which was attached to an Actimetrics CL200 USB interface coupled with a computer. The computer was equipped with ClockLab data acquisition software (version 2.61). The amount of pigmented plumage was measured once a week by taking a dorsal picture of the bird and measuring the pigmentation with the threshold function in ImageJ (Schneider *et al.*, 2012). The egg laying was monitored daily by visual inspection.

2.1.4 Samplings

Each bird was weighed prior to euthanasia by decapitation. A blood sample was collected in a heparinized tube. The sample was centrifuged, and the plasma frozen and stored at -80 °C until further analysis. The liver was removed and weighed. Liver, fat and muscle (*pectoralis*) tissue were collected within 10 minutes of euthanasia, frozen on dry ice and later stored at -80 °C. Liver and muscle tissue, and the heart were collected for ORO staining and frozen on dry ice, and later stored at -80 °C. The gonads and the fat mass were measured *post mortem*.

2.1.5 Testosterone

The frozen plasma samples were used to measure testosterone. Quantitative levels of testosterone were measured by an enzyme immunoassay, a competitive ELISA (MyBioSource.com, ref: MBS9711529), as per manufacturer's instructions.

2.1.6 Data analysis

The raw data was sorted and organized in Microsoft® Excel (version 16.45), and graphed and analyzed in GraphPad Prism (version 9.0.0, 2020).

2.2 Oil Red O staining

2.2.1 Tissue preparation and cutting

Oil Red O (ORO) is a dye that is soluble in fat (i.e. a lysochrome), and can therefore be used to image and quantify lipids in tissue samples (Mehlem *et al.*, 2013). The ORO will only stain triglycerides and cholesteryl oleate, but no other lipids such as lipid membranes (Ramirez-Zacarias *et al.*, 1992). The staining was done following the protocol developed by Mehlem and colleagues (2013), with some modifications. The liver, heart, muscle, and fat samples were frozen to -80 °C shortly after sampling, and kept frozen until sectioning. The samples were not flash-frozen in liquid nitrogen as described in the protocol. The liver and muscle samples were cut into approximately 4x4 mm cubes before being mounted, the fat tissue was cut into 3x3 mm cubes, and an approximately 5mm thick slice was cut from the apex of the hearts and mounted. The tissues were mounted on objects with Tissue-Tek® (Sakura FineTek; REF: 4583) before sectioning in a cryostat (Leica CM3050 S) (Figure 8A). For the liver, muscle and heart samples, the cutting temperature was kept at -18 °C, each section was 12 µm thick, and 3 sections from each tissue was put on VWR SuperFrost® Plus microscope slides. The fat samples were cut at -30 °C into 30 µm thick sections. The critical step in the cutting process was to not allow the sections to dry out at room temperature (RT), because

this resulted in the sections cracking and caused the staining to fail (Figure 9). Therefore, each section was stained with ORO immediately after sectioning.

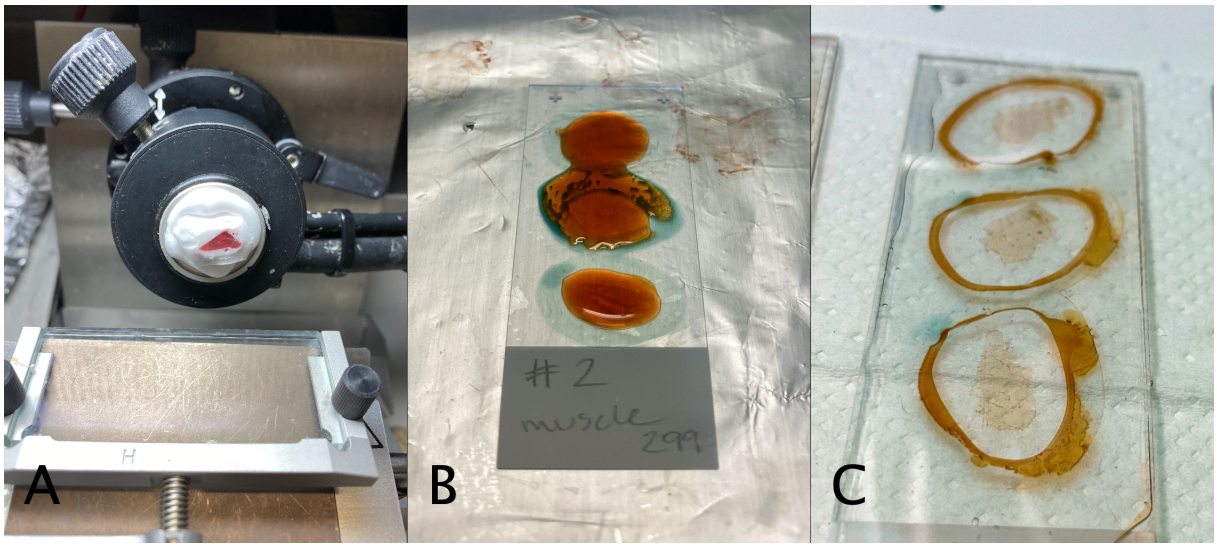

Figure 8. ORO workflow. Muscle tissue embedded in Tissue-Tek ready for sectioning (A), tissue sections imbedded in ORO (B), and the stained sections ready for imaging (C).

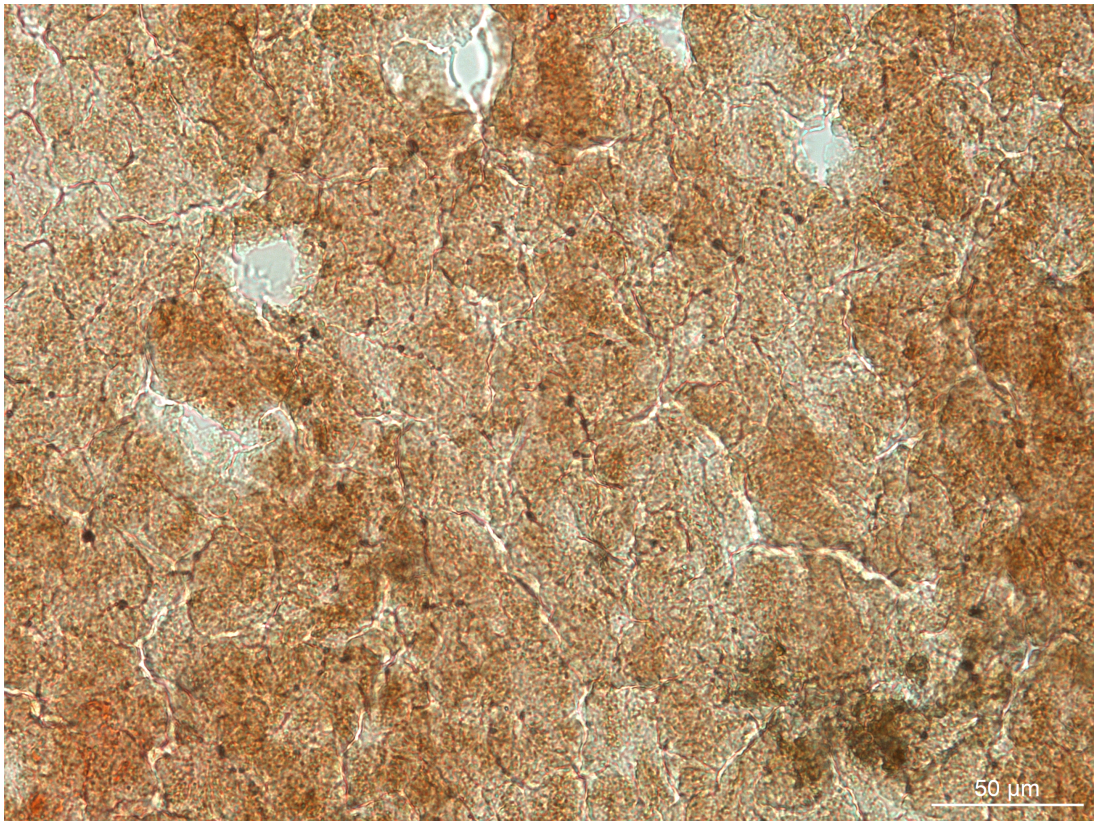

Figure 9. Failed ORO staining. Due to the cracking of the section before staining, the ORO staining of this liver sample (bird-ID: 135-98) failed. Image shows an area of 0.096 mm^2 at 20x magnification, scale bar: 50 µm.

2.2.2 ORO staining

An ORO stock solution was made in advance by mixing 400 ml of 99% isopropyl alcohol and 2.5 g of ORO with magnetic stirring at RT for 2 h. Then, an ORO working solution was made by mixing 1 part distilled water with 1.5 parts stock solution. The solution was filtered using a Rapid-Flow filter unit (ThermoScientific Nalgene) with a 0.45 µm aPES membrane and used within 6 hours. Each section on the slide was traced around with a liquid blocker pen (PAP pen from Abcam), and then incubated with approx. 500 µl ORO solution for 5 min (Figure 8B). After incubation, the slides were rinsed carefully for 5 min under running tap water before they were mounted with Kaiser's glycerol gelatine mounting medium (kept at 40 °C) and cover slips. The mounted slides were left to dry for 10 min before the edges were sealed with clear nail polish (Figure 8C).

2.2.3 Imaging

The stained sections were imaged within 24 h of mounting to avoid drying and precipitation of the ORO. The images were captured using a Leica DMRBE microscope with a PL FLUOTAR lens (20x/0.50 PH 2) and a Leica DFC420 camera. The camera settings were controlled in the computer program LAS Core. A minimum of 3 images were captured for each sample (i.e. one slide with 3 sections per bird per tissue). At 20x magnification the image captured showed an area of 0.096 mm^2.

2.2.4 Quantification – liver, muscle and heart samples

One image of high quality was selected for each sample, and if one sample had more than one such image, the first image in the series was analyzed. An image of high quality was considered one with a section without cracking or any precipitation of the ORO. The images were analyzed with the software ImageJ (Schneider *et al.*, 2012), and the analyses followed the protocol as described by Mehlem and colleagues (2013). Each image was converted to an 8-bit image before the threshold function was employed on each sample. The threshold range that suited most images was set for all images. This measured the amount of red in each image in area (i.e. how much the ORO had stained), and therefore the amount of fat in a section. The total red area was also measured by setting the maximum threshold to the highest possible (i.e. 100% of the image was red). This was done so that results could be presented as a percentage of the total red in the whole image. The image analyses were done before the images were annotated so that it was not known which sampling group each sample belonged to during the analyses.

2.2.5 Quantification – fat samples

Several images were captured for each sample and used for the quantification of the size of the adipose cells. In ImageJ (Schneider *et al.*, 2012) the freehand selection tool was used to trace around each cell in the image and measure the area of the cell. For each sample, seven or more cells were traced and measured. The cell area was averaged for each sample and this mean was used for further analysis.

2.2.6 Data analysis

The data was analyzed and graphed in GraphPad Prism (version 9.0.0, 2020). For the liver, muscle and heart, an ordinary one-way ANOVA with a Tukey's multiple comparisons test was performed to test for differences between the four sampling groups. For the fat, the birds tested were sorted into two groups: lean birds with a body fat percentage of 6% or less and fat birds with a body fat percentage of 11% or more. An unpaired t-test was performed to look at the difference between the two groups.

2.3 qPCR

2.3.1 Primer design

To design primers for the six genes of interest, the gene sequence was first located in the genome browser Ensembl.org for chicken (*gallus gallus*) (Release 101, (Yates *et al.*, 2020)). This sequence was then compared to an unpublished brain transcriptome of the Icelandic rock ptarmigan (*Lagopus muta*) by using a basic local alignment tool (BLAST). This also gave the location of the gene sequence in the transcriptome. The location of the gene sequence was then further used to design primers for that specific gene. The web tool Primer3web (version 4.1.0, (Untergasser *et al.*, 2012)) was used to design appropriate primers and settings were set as follows: primer length between 18-27 nucleotides, the primer melting temperature (Tm) between 53-54°C, the GC content between 40-60% and the product length between 70 and 150 nucleotides. Then, primers were checked for having the same Tm in the "Promega Tm calculator" (Promega Corporation, 2020) and the reverse primer was put in the reverse complement. The primers were then located in the gene sequence. Primers were only picked if they spanned an exon-exon barrier (i.e. included nucleotides from 2 adjacent exons). Primer pairs were then put in Primer-Blast (Ye *et al.*, 2012) to check for gene specificity (i.e. that the primers targeted the right gene) and self-complementarity. The primers and their sequences can be found in Table 2. The primers were ordered from Sigma-Aldrich and were, upon arrival, hydrated and diluted with RNase-free H_2O to a concentration of 10 µM.

Table 2. Primers for genes of interest. The sequence (5'→3'), length of amplicon (bp), melting temperature (Tm; °C) and GC content (%).

Gene (enzyme)	**Primer**	**Sequence** (5'→3')	**Length of amplicon (bp)**	**Tm (°C)**	**%GC**
ACACA (ACC)	ACACAfor1	CATCTTCCATTATGTCCTGG	117	60	45
	ACACArev1	CTCAGTGTCTTCATTAGTCG		60	45
CPTIA (CPTI)	CPTIAfor3	GTTTCCAGACGTCTTTACC	95	60	47
	CPTIArev3	TTCATCATTCATAAGTGGCC		60	40
ATGL (ATGL)	ATGLfor2	TATTAGATGGATGAGGGAGC	107	60	45
	ATGLrev2	CAAGATGATAGTAAAGCCTGG		60	43
ACSL1 (ACS)	ACSL1for1	GTTCTGATATCATTCCTGCC	95	60	45
	ACSL1rev1	CCTTGAAAGAATCCTATCCG		60	45
FASN (FAS)	FASNfor5	TTCCTACTACATGGCATCC	102	60	47
	FASNrev5	ATAGATGTACTGATCCACCG		60	45
MGLL (MGL)	MGLLfor1	CTAATCTCTCCTCTGGTGG	146	60	53
	MGLLrev1	TCCATCTCCTTCTTGTTCC		60	47
PPIB (PPIB)	PPIBfor	CTGACGAGAACTTCAAGC	96	60	50
	PPIBrev	TGGTGATGAAGAACTGGG		61	50

2.3.2 RNA extraction – liver

Two RNA samples were extracted from liver tissue for each subject by using an RNeasy Mini Kit from QIAgen, and the protocol was followed as per manufacturer's instructions. Concentration and purity was measured using a NanoDrop (Thermo Scientific 2000c). Following the extraction, a DNase treatment was performed by using DNase I buffer (New England BioLabs, #B0303S) and DNase I (New England BioLabs, #M0303S) (Table 3). Samples were then put at 37 °C for 10 min, and then 0.9 µl of EDTA 0.05M was added to each tube before a deactivation step at 75 °C for 10 min.

Table 3. DNase treatment recipe. Concentrations added to each tube.

Buffer	0.8 µl
DNase	0.1 µl
RNA	x µl to equal 2 µg
RNase-free H_2O	x µl to a final volume of 9 µl

After the DNase treatment, a cDNA conversion was done by using a High Capacity RNA-to-cDNA kit (Applied biosystems by Thermo Fisher Scientific) (Table 4), and then put at 37 °C for 1h and 95 °C for 5 min.

Table 4. cDNA conversion recipe. Concentrations added to DNase-treated RNA and the final volume in each tube**.**

RT Buffer Mix	10 µl
RT Enzyme Mix	1 µl
Final volume	20 µl

2.3.3 RNA extraction – fat

One RNA sample was extracted from white adipose tissue (WAT) for each subject using a combined method consisting of a QIAzol® method and an RNeasy Mini Kit (QIAgen). A frozen sample (30 mg) of WAT in 1 ml of QIAzol® Lysis Reagent (QIAgen; Cat #: 79306) was homogenized in a TissueLyser II (QIAgen) for 4 min at 20 Hz. The sample was then allowed to sit at RT for 5 min before being centrifuged for 10 min at 12000x g at 4 °C. A lipid layer was then visible at the top, and was carefully avoided for the next step. 950 µl of the RNA sample was transferred to a new tube, and 200 µl of chloroform (Sigma-Aldrich; product #: 372978) was added. The tube was shaken for 15 s, and allowed to incubate at RT for 3 min. The sample was then centrifuged at 12000x g for 15 min at 4 °C. This created a phase separation with a clear, aqueous phase at the top which contained the RNA. Between 300 and 400 µl of this top phase was transferred to a new tube, while carefully avoiding disruption of the other layers. The same volume (300-400 µl) of 70% ethanol was added to the tube and mixed. The sample was then transferred to an RNeasy Mini Spin Column, and the manufacturer's instructions were followed.

The DNase treatment and cDNA conversion were done as described above.

2.3.4 Primer efficiency

To test the primers' efficiency, a serial dilution was prepared with a test-sample of liver-cDNA (Figure 10). The dilutions were then used to prepare a GoTaq qPCR with each primer pair (Table 5), and then the qPCR reaction was run on a BIO RAD CFX Connect Real-Time System (Table 6). The melting curves generated were analyzed, and if a primer pair only creates one peak this is a good indication that there is only one amplicon and that the primers

are specific. The efficiency of each primer pair was calculated by plotting the log of the concentrations of cDNA against the C_T-value and establishing a standard curve. The efficiency of each primer pair was then calculated:

$$Primer\ efficiency = -1 + 10^{(-1/slope)} \quad (1)$$

Where the slope is the standard curve. Primer pairs were considered acceptable if the efficiency was above 90%. The efficiencies of the primer pairs used are found in Table 7.

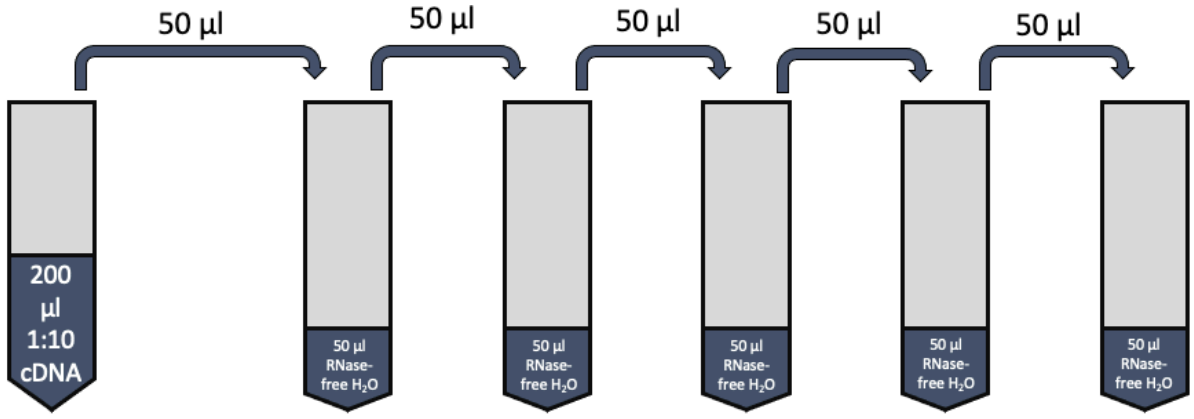

Figure 10. Serial dilution for primer efficiency test. Started with a test-sample of liver-cDNA (200 µl) in a 1:10 dilution and 5 tubes with 50 µl of RNase-free water in each. 50 µl was then transferred from the first tube to the next and mixed before 50 µl of the mixture was transferred to the next tube and so forth.

Table 5. GoTaq qPCR for primer efficiency. Concentrations added in each well on the qPCR plate.

RNase-free H2O	6.9 µl
GoTaq	10 µl
Forward primer	1 µl
Reverse primer	1 µl
CxR (reference dye)	0.1 µl
Template (cDNA)	1 µl

Table 6. GoTaq qPCR program.

Temperature	Duration	Cycles
95 °C	2 min	1
95 °C	15 sec	40
60 °C	1 min	
65 °C	Gradually increase in temperature from 65°C to 95°C in increments of 0.5°C, each step lasting 5 seconds.	
95 °C		

Table 7. Primer efficiency results.

Gene	Efficiency
ACACA	91.5%
CPTIA	91.7%
ATGL	92.2%
ACSL1	95.1%
FASN	95.4%
MGLL	90.7%

2.3.5 Primer specificity

The primers were verified to ensure that they amplified the right gene sequences. First, a GoTaq PCR was prepared for each primer pair (Table 8), and was put in the thermocycler on the program described in Table 9. The PCR products were then ligated into a pCR®-Blunt II-TOPO® plasmid (Table 10) and allowed to incubate at RT for 5 min before being put in -20 °C. A growth medium was prepared by mixing 500 ml of distilled water and 20 g of LB Broth with agar (Sigma; L3147), and LB Broth was made by mixing distilled water and 12.5 g of LB Broth (Sigma; L3522). The growth medium and the broth were then autoclaved and let cool slightly before adding 0.5 ml of Kanamycin in each flask. The growth medium was put on plates and sealed with parafilm for storage at 4 °C.

Table 8. GoTaq PCR recipe. Concentrations added in each well on the qPCR plate.

RNase free water	7.0 µl
GoTaq	10 µl
Forward primer	1 µl
Reverse primer	1 µl
cDNA	1 µl

Table 9. GoTaq PCR thermocycler program.

Temperature	**Duration**	**Cycles**
94 °C	3 min	1
94 °C	45 sec	30
56 °C	45 sec	
72 °C	45 sec	
72 °C	10 min	1

Table 10. Ligation recipe. Concentrations added to each tube.

pCR®-Blunt II-TOPO® plasmid (Invitrogen; P/N: 100023351)	1 µl
PCR product	1 µl
Salt solution (Invitrogen; P/N: 46-0205)	1 µl
RNase-free H_2O	3 µl

A transformation was performed by thawing 12 tubes with 25 µl of NEB® 5-Alpha Competent *E. coli* (NEB; C2987I) on ice before adding 2 µl of the ligated plasmid into each tube. Each tube was left on ice for 30 min before a heat shock at 42 °C for 30 sec, and then 5 min on ice. 475 µl of SOC Outgrowth Medium (New England BioLabs; #B9020S) was added to each tube, which were then put in a shaking incubator at 37 °C at 250 rpm for 60 min. The plates prepared previously were moved from 4 °C to 37 °C, and then 475 µl of the solution was put on each plate. The plates were left to dry bottom up at 37 °C for 60 min, then turned around and left overnight at 37 °C.

A Falcon tube (15 ml) was prepared with 7 ml of LB Broth with Kanamycin for each sample. A single colony from each plate was carefully moved into a tube. The tubes were loosely closed, to allow air exchange, and left in a shaking incubator at 37 °C at 120 rpm overnight.

On the following day, DNA was extracted from the bacterial culture by using a QIAprep® Spin Miniprep Kit (QIAgen, REF: 27106) according to the manufacturer's instructions. DNA concentrations and purities were measured using a NanoDrop (Thermo Scientific 2000c). Then, the samples were prepared for sequencing by using a BigDye reaction, as described in Table 11, and the reaction was performed in a thermocycler (Eppendorf® Mastercycler, Z316083; Table 12). Samples were sent to a sequencing-team for sequencing.

Table 11. BigDye reaction recipe. Concentrations added to each tube.

M13 Forward Primer (Invitrogen; P/N: 100026030)	0.5 µl
BigDye 3.1	0.5 µl
5x sekvens-buffer	3 µl
DNA	x µl to equal 100 ng
RNase-free H_2O	x µl to a final volume of 20 µl

Table 12. BigDye Thermocycler program.

Temperature	Duration	Cycles
96 °C	5 min	1
96 °C	10 sec	30
50 °C	5 sec	
60 °C	4 min	

The DNA sequences from each primer pair were aligned with the corresponding gene sequence from the reference genome in the plasmid editor program ApE (v2.0.61; (Davis, 2020)) to confirm that the primer pair amplified the right sequence.

2.3.6 qPCR

For the liver samples, the sample with the highest purity and RNA concentration for each bird was used in the qPCR analysis. For the fat, there was only one sample for each bird. All samples were run in duplicates for each gene, and the qPCR wells were loaded as described in

Table 5. The qPCR program used for the genes of interest is described in Table 6. The housekeeping gene, *PPIB*, was used to normalize results, and the qPCR program used for this gene is found in Table 13.

Table 13. qPCR program for the housekeeping gene (*PPIB*).

Temperature	Duration	Cycles
95 °C	2 min	1
95 °C	15 sec	40
57 °C	15 sec	
60 °C	1 min	
65 °C	Gradually increase in temperature from 65°C to 95°C in increments of 0.5°C, each step lasting 5 seconds.	
95 °C		

2.3.7 Data analysis

The relative gene expression in fold change was calculated using the $2^{-\Delta\Delta C_T}$ method described by Livak and Schmittgen (2001). The C_T-values from the qPCR reactions were used to derive the gene expression in the following way. First, the C_T-values from the two technical replicates were averaged for every sample, before the ΔC_T was calculated:

$$\Delta C_T = C_T(gene\ of\ interest) - C_T(housekeeping\ gene) \quad (2)$$

The housekeeping gene *PPIB* was used as a control for experimental variability. The ΔC_T-values for each sample and gene were then used to calculate the $\Delta\Delta C_T$:

$$\Delta\Delta C_T = \Delta C_T(test) - \Delta C_T(control) \quad (3)$$

Where the average ΔC_T-values in sampling group 1 was used as the control, meaning that the gene expression results in groups 2, 3 and 4 were expressed as relative to group 1. Lastly, the fold change in gene expression was calculated:

$$Fold\ change = 2^{-\Delta\Delta C_T} \quad (4)$$

GraphPad Prism (version 9.0.0, 2020) was used for graphing and statistical analyses. Fold change was log2 transformed for data to approximate normal distribution, one of the

assumptions for a one-way ANOVA. For each gene of interest, an ordinary one-way ANOVA with a Tukey's multiple comparisons test was performed to look for differences between the four sampling groups.

2.4 Correlation analysis in R

All measurements from the samplings except testosterone level, plumage and egg-laying were organized with the results from the qPCR and ORO staining to look for correlating parameters. For each individual bird, activity and VFI from the last week before sampling were averaged. This data was then analyzed using RStudio. The corrplot package was used to create a correlation matrix, before individual correlation plots for significant correlations ($p<0.01$) were made with the ggscatter function in the ggpubr package (Kassambara, 2020; Wei *et al.*, 2017). The r script is found in Appendix C. Pearson's correlation coefficient (r) for linear correlation is a statistical measure of how closely two variables are related (Emerson, 2015). This statistical analysis results in a number between -1 and 1, with -1 meaning a perfect negative relationship, 1 meaning a perfect positive relationship and 0 meaning that there is no relationship between the two variables. Values 0.5 from 0 are considered high (Emerson, 2015). A correlation matrix is a table of the correlation coefficient between any two variables for a set of variables.

The same dataset prepared for the correlation analysis were used to look for age- and sex-differences within sampling groups. T-tests were run for all variables in each sampling group for both age- and sex-differences.

3 Results

The raw data and the results of statistical tests can be found in Appendices A and B.

3.1 Body mass, VFI, and activity

The body mass (BM) measurements were the main parameter used to establish the four sampling points. Fat winter birds were sampled while the BM was high during the short photoperiod (SP). After being switched to constant light (LL), the birds lost weight rapidly, and were sampled. For the third sampling, reproductive behaviors were also used to determine the sampling date (see next section). Once the birds started gaining weight and terminating reproduction, i.e. became photorefractory, the 4th sampling took place. At the beginning of the study, the old birds maintained a seasonal maximum BM at 926 ±17.8 g (n=16) in SP, and rapidly lost weight when they were moved to LL (Figure 11). The animals reached their seasonal minimum of 589.3 ±39.0 g (n=6) three months after being moved to LL, before they started to gain weight again (Figure 11). At the beginning of the study, the yearlings (n=17) had a mean BM that was 325.8 ±23.78 g, significantly lower than the old birds (n=16; unpaired t-test, $p<0.0001$) (Figure 11). In contrast to the old birds, the yearlings increased significantly in BM during the SP, the mean BM was 110.1 ±11.88 g (n=17) more after 3 months in the SP, than at the beginning of the study (paired t-test, $p<0.0001$) (Figure 11). In the remainder of the study, the yearlings followed a similar pattern to the old birds, and reached a seasonal minimum of 526.8 ±22.8 g (n=5) at the same time (Figure 11).

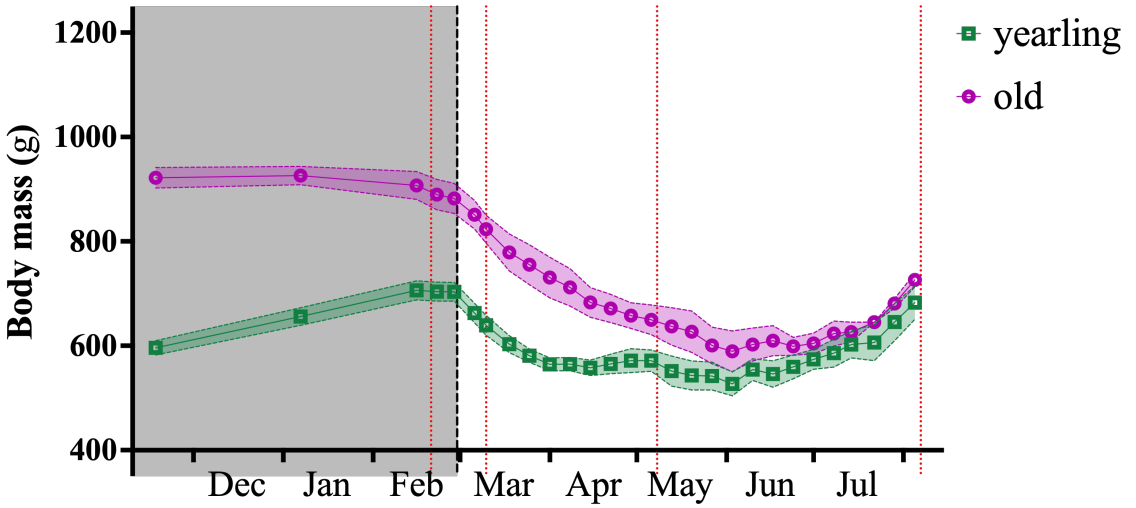

Figure 11. Body mass. Body mass in grams in captive Svalbard ptarmigan fed *ad libitum* while kept on a short photoperiod (grey background) and after being moved to constant light (at the black stippled vertical line). Birds were sampled at four time points, illustrated by the red stippled vertical lines; n= 33 before the 1st sampling, n=26 between the 1st and 2nd sampling, n=18 between the 2nd and 3rd sampling, and n=10 between the 3rd and 4th sampling. The BM of yearlings (green squares) and old birds (purple circles) is expressed as mean ±SEM.

The voluntary food intake (VFI) varied throughout the study in both yearlings and old birds (Figure 12A). The VFI was low in the SP and after being moved to LL, linear regression showed that the VFI increased for the rest of the study ($p<0.0001$). The equations were 0.2527x+27.6 and 0.2906x+20.3 for yearlings and old birds, respectively. The intercept was significantly higher in yearlings ($p<0.001$ by unpaired t-test based on means of regression analysis for each bird) while the slopes did not differ significantly ($p=0.071$).

The activity level was low in SP, and both yearlings and old birds had the lowest activity on the same day: 08.02.20. The yearlings had a mean ±SEM activity level of 9088 ±793 counts per day (n=17), and the old birds had an activity level of 6050 ±626 counts per day (n=16), which was significantly lower than the yearlings (unpaired t-test, $p<0.01$). Immediately after being moved to LL, the activity steeply increased and remained high from March until May before gradually decreasing to very low levels towards the end of the study (Figure 12B).

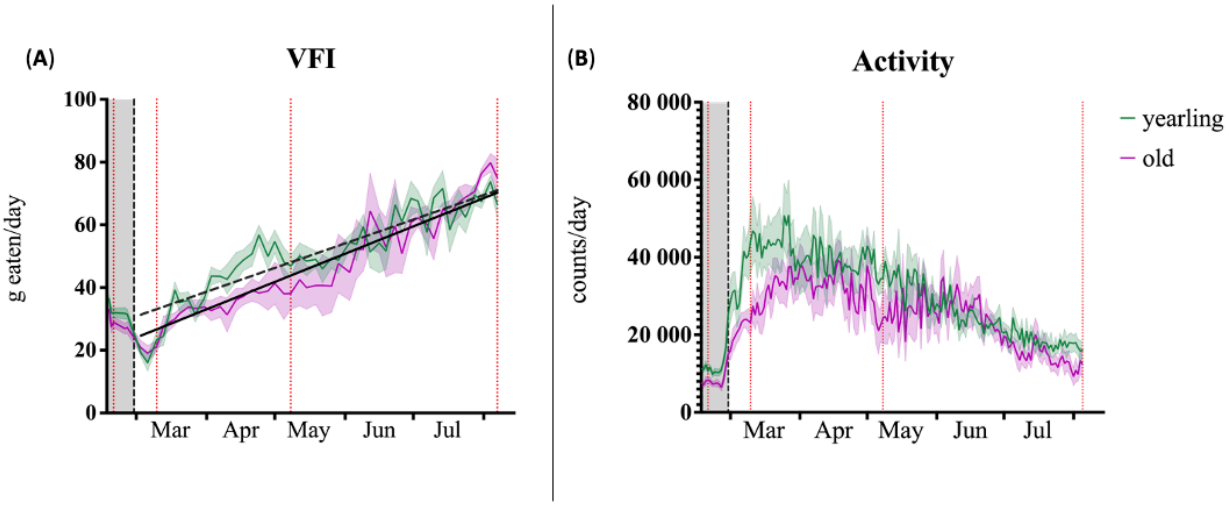

Figure 12. Food intake and activity. (**A**) The voluntary food intake (VFI) in grams eaten per day and (**B**) activity in counts per day for captive Svalbard ptarmigan fed *ad libitum* while kept on a short photoperiod (grey background) and after being moved to constant light (at the black stippled vertical line). Birds were sampled at four time points, illustrated by the red stippled vertical lines; n= 33 before 1st sampling, n=26 between 1st and 2nd sampling, n=18 between 2nd and 3rd sampling, and n=10 between 3rd and 4th sampling. The VFI and activity of yearlings (green lines) and old birds (purple lines) are expressed as mean ±SEM. Linear regression on the mean VFI for each day was calculated from the onset of LL, and both slopes significantly increased ($p<0.0001$). The equations were 0.2527x+27.6 and 0.2906x+20.3 for yearlings (black stippled line) and old birds (black solid line), respectively.

3.2 Plumage

Svalbard ptarmigan alternate between two plumages, a white one in winter and a pigmented one in the spring/summer. During SP and for the first month after being moved to LL, all birds had their white winter plumage (Figure 13). The females exhibited a rapid molt into their pigmented plumage after 6 weeks in LL, and remained in their summer plumage for 14 more weeks when they started molting into their winter plumage again (Figure 13). The males started molting slowly and incompletely in after 6 weeks in LL. After 13 more weeks, the males reached their most pigmented state with approx. 75% pigmentation (n=6) (Figure 13). As with the females, the males started the molting into their winter plumage after 5 months in LL (Figure 13).

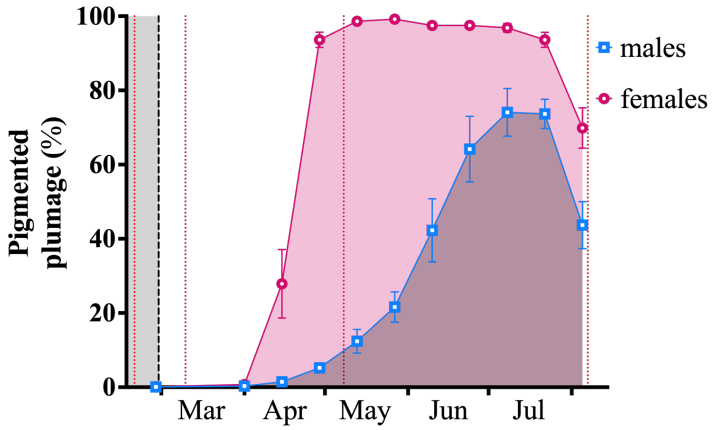

Figure 13. Plumage. The mean ±SEM percentage of pigmented plumage for captive Svalbard ptarmigan fed *ad libitum* while kept on a short photoperiod (grey background) and after being moved to constant light (at the black stippled vertical line). Birds were sampled at four time points, illustrated by the red stippled vertical lines. For males (blue squares) n=16 between samplings 1 and 2, n=11 between samplings 2 and 3, and n=6 between samplings 3 and 4. For females (pink circles) n=10 between samplings 1 and 2, n=7 between samplings 2 and 3, and n=4 between samplings 3 and 4.

3.3 Reproductive activity

The first female ptarmigan started to lay eggs 2 months after being moved to LL, and after almost 3 months, all females were laying eggs (n=4; Figure 14). All egg-laying had seized 4 months after being moved to LL (n=4). The ovaries were regressed at the 1st and 2nd sampling with a mean weight ±SEM of 0.15 ±0.02 g and 0.21 ±0.09 g, respectively. The ovaries matured and the mean weight had increased significantly to 23.1 ±3.4 g (n=3; Tukey's multiple comparisons test *post hoc*; $p<0.0001$) at the 3rd sampling, while at the 4th sampling the ovaries had regressed again to a mean weight of 0.34 ±0.13 g (Figure 14).

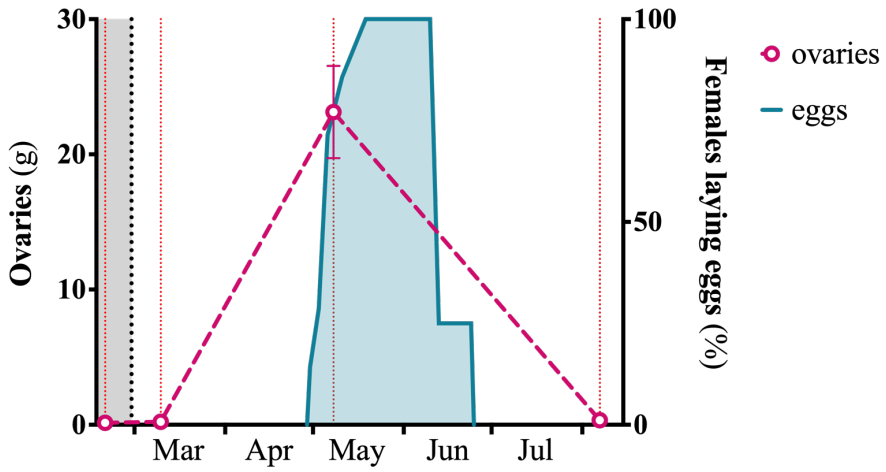

Figure 14. Ovaries weight and egg-laying activity. The mean ±SEM weight of ovaries in grams (pink circles) for female captive Svalbard ptarmigan fed *ad libitum* while kept on a short photoperiod (grey background) and after being moved to constant light (at the black stippled vertical line). Birds were sampled at four time points, illustrated by the red stippled vertical lines; n=3 at each sampling. The percent of all females laying eggs is shown in blue (n=7 before sampling 3, and n=4 after sampling 3).

In the male ptarmigan, the testes were regressed at sampling 1 and 2 with a mean weight ±SEM of 0.073 ±0.01 g (n=4) and 0.12 ±0.02 g (n=5), respectively (Figure 15). The testes had matured at sampling 3 with a mean weight of 2.04 ±0.38 g (n=4; Tukey's multiple comparisons test *post hoc*, $p<0.0001$), before they regressed again at sampling 4 to 0.38 ±0.09 g (n=5). The level of testosterone increased from undetectable levels (n=4) at the 1st and 1.09 ±0.49 ng/µl (n=5) at the 2nd sampling to 2.1 ±0.42 ng/µl (n=3; Tukey's multiple comparisons test *post hoc*, $p<0.01$) at the 3rd sampling before being back to 0.0036 ±0.004 ng/µl (n=5) at the 4th sampling (Figure 15).

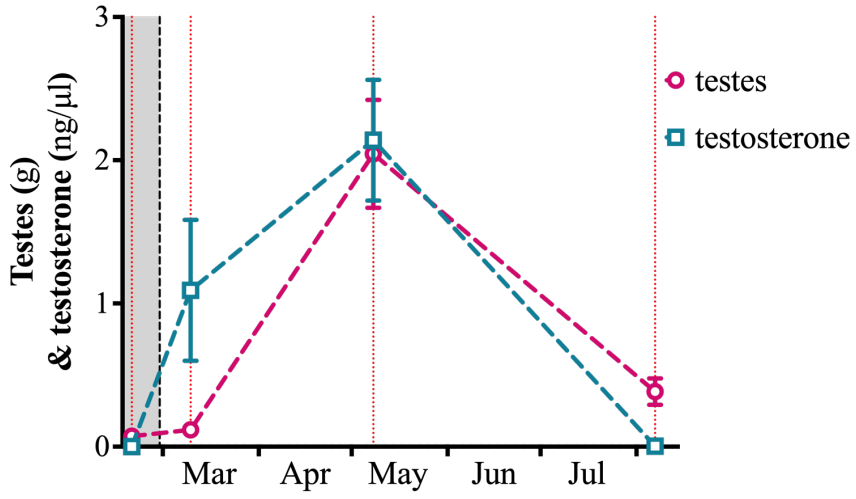

Figure 15. Testes weight and testosterone level. The mean ±SEM testes weight in grams (pink circles) and testosterone level in ng per µl (blue squares) for male captive Svalbard ptarmigan fed *ad libitum* while kept on a short photoperiod (grey background) and after being moved to constant light (at the black stippled vertical line). Birds were sampled at four time points, illustrated by the red stippled vertical lines; n=4 (4) at sampling 1; n=5 (5) at sampling 2 and 4; n=4 (3) at sampling 3 for testes (and testosterone).

3.4 Liver

The mean ±SEM liver mass was 6.1 ±1.1 g (n=3) for the old birds and 5.5 ±0.38 g (n=4) for the yearlings at the 1st sampling, and decreased to 4.4 ±0.63 g (n=4) for the old birds and 4.9 ±0.27 g (n=4) for the yearlings at the 2nd sampling (Figure 16). The liver mass then increased to 7.2 ±1.5 g (n=3) for the old birds and 7.5 ±1.2 g (n=4) for the yearling at the 3rd sampling, and to 9.4 ±0.44 g (n=4) for the old birds and 9.6 ±1.4 g (n=4) for the yearling at the 4th sampling (Figure 16). A two-way ANOVA was performed and revealed a significant difference between means in the different sampling groups ($p<0.001$), but no difference between yearlings and old birds ($p=0.94$). A Tukey's multiple comparisons test performed *post hoc* showed that in yearlings there was a difference between groups 1 and 4 ($p<0.05$) and groups 2 and 4 ($p<0.01$), and in old birds there was a difference between groups 2 and 4 ($p<0.01$). Additionally, in sampling 3, the mean ±SEM liver mass of 9.7 ±0.64 g in females (n=3) was significantly higher than the liver mass of 5.6 ±0.50 g in males (n=4, unpaired t-test, $p<0.001$).

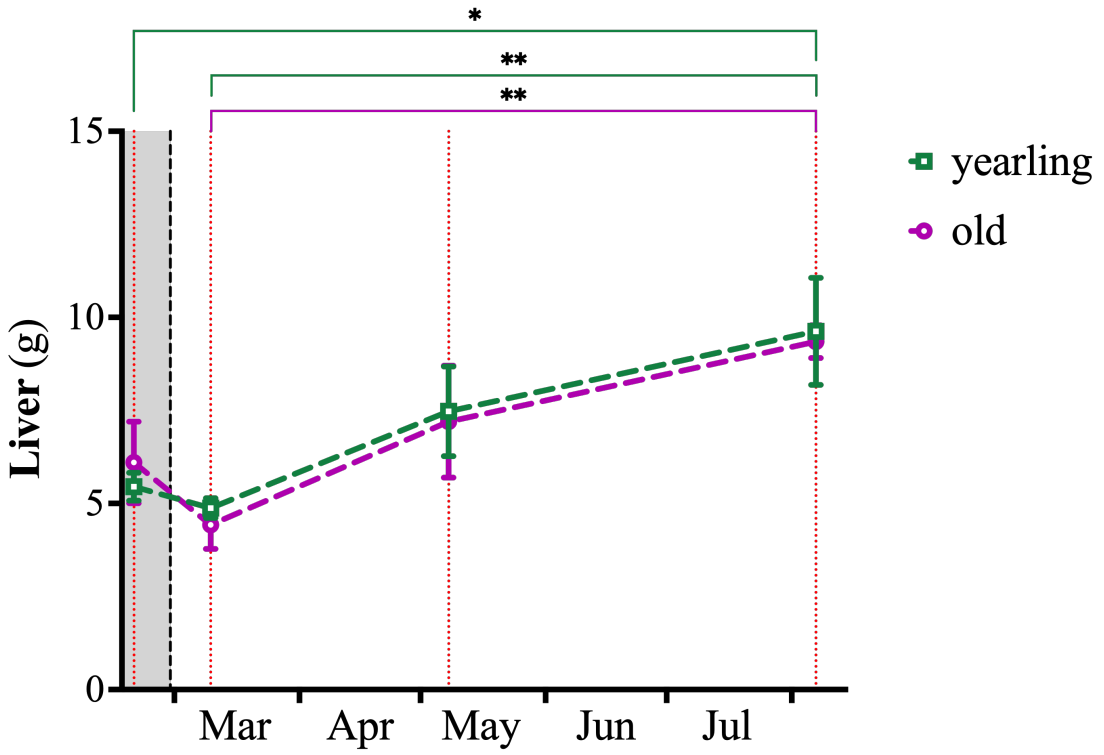

Figure 16. Liver mass. The liver mass in grams of captive Svalbard ptarmigan fed *ad libitum* at four sampling points in the body mass cycle while kept on a short photoperiod (grey background) and after being moved to constant light (at the black stippled vertical line). Birds were sampled at four time points, illustrated by the red stippled vertical lines. The liver mass of yearlings (green squares) and old birds (purple circles) is expressed as mean ±SEM. n=16 (n=4 at each sampling for yearlings and n=14 (n=3 at samplings 1 and 3, and n=4 at samplings 2 and 4) for old birds. A Tukey's multiple comparisons test was performed *post hoc*. **p<0.01, *p<0.05.

The Oil Red O (ORO) staining revealed significant differences among means in the four sampling groups (one-way ANOVA, $p<0.05$; Figure 17A). In sampling group 1, an average ±SEM of 36.9 ±7.8 % of the sampled area was stained (n=7); in group 2, 17.0 ±2.4 % of the area was stained (n=8); in group 3, 12.7 ±2.0 % of the area was stained (n=7); and in group 4, 26.2 ±5.4 % of the area was stained (n=8). A *post hoc* Tukey's multiple comparisons test showed a significant difference between groups 1 and 2 ($p<0.05$) and groups 1 and 3 ($p<0.05$). Stained sections from sampling groups 1 and 4 could be observed with noticeably more ORO staining, i.e. red coloration than stained sections from groups 2 and 3 (Figure 17B). In sampling group 3, the males had had a mean stain of 16.4 ±1.4 % (n=4), which was significantly higher than the females' of 7.7 ±1.5 % (n=3, unpaired t-test: $p<0.01$).

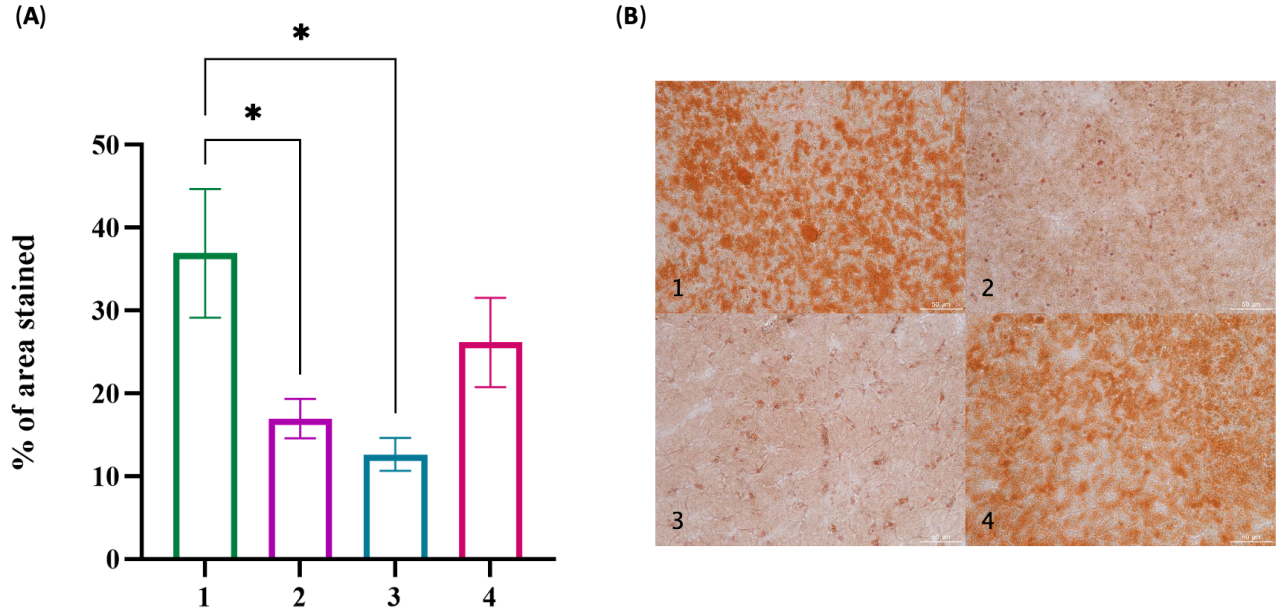

Figure 17. ORO liver. Oil Red O (ORO) staining of liver tissue from captive Svalbard ptarmigan fed *ad libitum* at four sampling points in the body mass cycle. Birds were sampled while being kept on a short photoperiod (1: fat winter birds; n=7), shortly after being moved to constant light (2: birds rapidly losing weight; n=8), when reproductive (3: lean summer birds; n=7) and when photorefractive (4: birds gaining weight; n=7). **(A):** The % area in a section stained by ORO expressed as mean ±SEM. A one-way ANOVA was performed and showed significant difference among means ($P<0.05$). A Tukey's multiple comparisons test was performed *post hoc* and showed significant differences (*$p<0.05$) between groups 1 and 2 and groups 1 and 3. **(B):** Representative images of the ORO stained sections from the 4 different groups (Bird-ID: 1=R30, 2=R26, 3=R28, 4=R7). Each image is at 20x magnification, shows an area of 0.096 mm^2 and scale bars = 50 µm.

3.5 Fat

At each sampling, the amount of dissected fat followed the same pattern as the BM cycle. The amount of fat was highest in SP, had decreased shortly after the birds were placed in LL, and was lowest when the birds were reproductive before increasing again when breeding was terminated as the birds became photorefractive. At sampling 1, the mean ±SEM was 123.3 ±22.9 g (n=3) for old birds and 59.0 ±9.8 g (n=4) for yearlings; at sampling 2, it was 107.8 ±17.7 g (n=4) for old birds and 52.2 ±15.2 (n=4) for yearlings; at sampling 3, it was 29.2 ±12.9 g (n=3) for old birds and 22.4 ±7.7 g (n=4) for yearlings; and at sampling 4, it was 53.5 ±7.6 g (n=4) for old birds and 58.6 ±8.5 g (n=4) for yearlings (Figure 18). A two-way ANOVA and a Tukey's multiple comparisons test performed *post hoc* revealed a significant difference between sampling groups in old birds: group 1 and 3 ($p<0.001$), 1 and 4 ($p<0.01$), 2 and 3 ($p<0.01$) and 2 and 4 ($p<0.05$). No differences were found between sampling groups in yearlings.

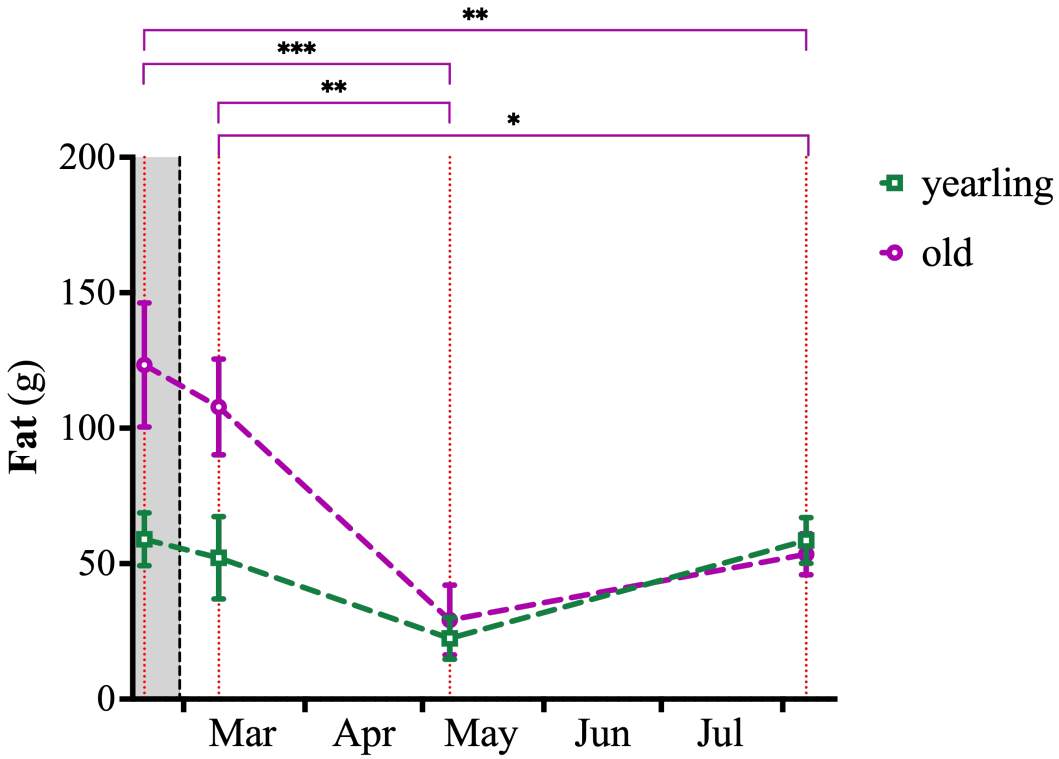

Figure 18. Fat mass. The mass of dissectible fat in grams of captive Svalbard ptarmigan fed *ad libitum* at four sampling points in the body mass cycle while kept on a short photoperiod (grey background) and after being moved to constant light (at the black stippled vertical line). Sampling points were at the red stippled vertical lines. The fat mass of yearlings (green squares) and old birds (purple circles) is expressed as mean ±SEM. n=16 (n=4 at each sampling for yearlings and n=14 (n=3 at samplings 1 and 3, and n=4 at samplings 2 and 4) for old birds. A Tukey's multiple comparisons test was performed *post hoc*. ***p<0.001, **p<0.01, *p<0.05.

In order to assess morphological differences in white adipose tissue, fat sections were stained with ORO. The stained sections were categorized into lean birds if the bird's body fat percentage was ≤6% or fat birds if the bird's body fat percentage was ≥11%. ORO stained sections from lean birds revealed fat cells that had an average area ±SEM of 2643.91 ±205.8 μm^2 (n=8), while fat cells in fat birds had a significantly larger average area of 5207.63 ±582.7 μm^2 (n=7; unpaired t-test, p<0.001; Figure 19A). The average cell area increased with body fat percentage according to the linear regression equation: Y=260.6x + 1607 (significantly non-zero, p<0.0001) (Figure 19C).

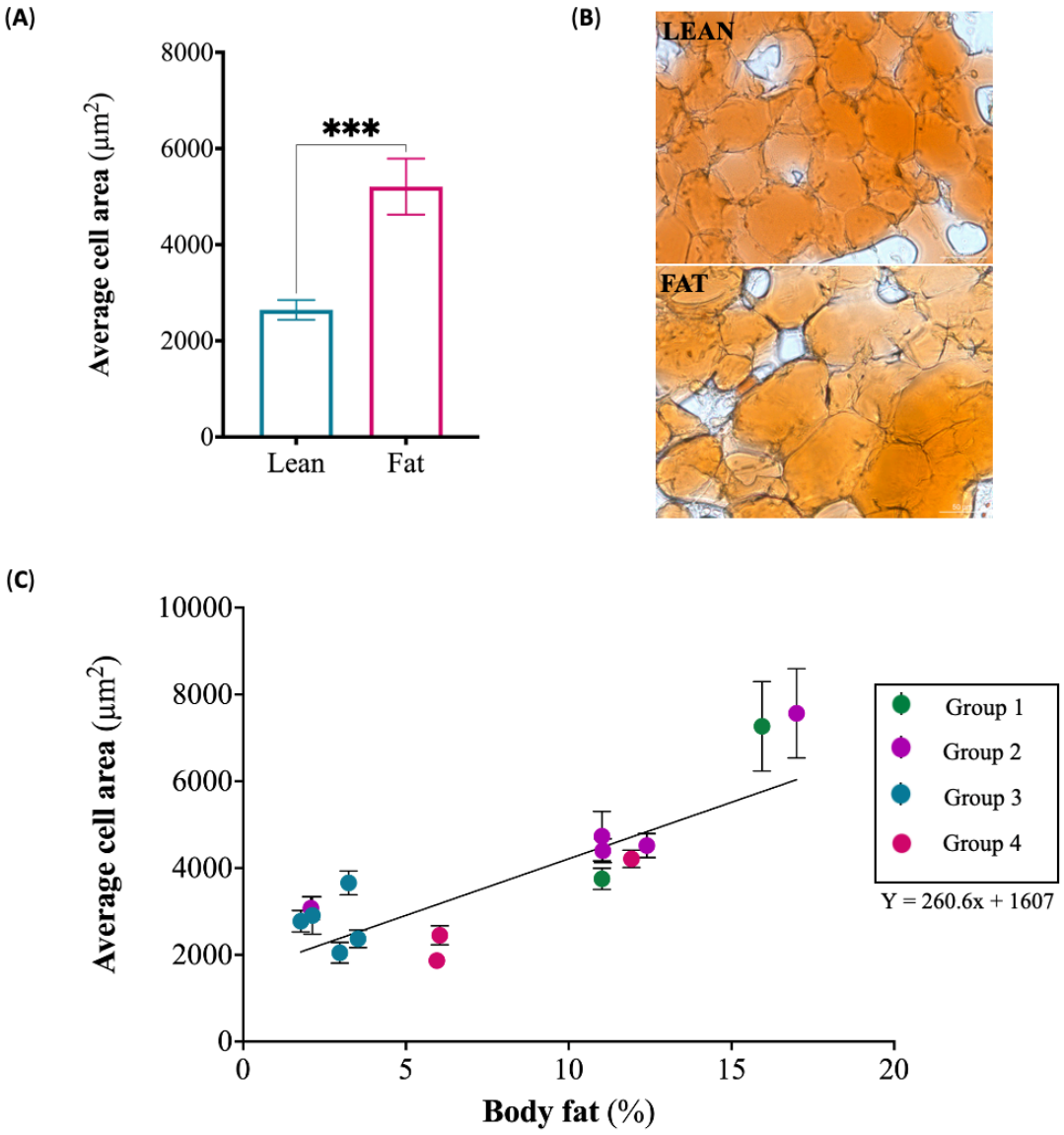

Figure 19. ORO adipose tissue. Oil Red O (ORO) staining of white adipose tissue from captive Svalbard ptarmigan fed *ad libitum*. **(A):** The average cell area in µm^2 expressed as the mean ±SEM. Birds with body fat ≤6% were lean (n=8), and birds with body fat ≥11% were fat (n=7). For each bird the average cell area was calculated from measurements from 7 to 21 individual cells. An unpaired t-test was performed and found a significant difference between lean and fat birds (***p<0.001). **(B):** Representative images of ORO stained sections for a lean (Bird-ID: R34) and a fat (Bird-ID: 294-98) bird. Each image is at 20x magnification, shows an area of 0.096 mm^2 and scale bars = 50 µm. **(C)**: The average cell area in µm^2 plotted against body fat as a percentage of BM. Equation of linear regression: Y=260.6x + 1607 (p<0.0001).

3.6 ORO staining of heart and muscle

In order to examine if fat was stored in the heart at different stages of the BM cycle, ORO staining was performed on sections of heart tissue. Generally, very small amounts of the heart sections were stained with ORO. In sampling group 1, a mean ±SEM of 1.51±0.69 % (n=7) of the section area was stained; in group 2, 0.91±0.30 % (n=8) of the section area was stained; in group 3, 2.0±0.71 % (n=7) of the section area was stained; and in group 4, 2.37±0.42 % (n=8) of the section area was stained (Figure 20A). A one-way ANOVA showed no significant differences (p=0.24) in means between the four sampling groups, nor could any obvious differences in staining be observed in the imaged sections (Figure 20B).

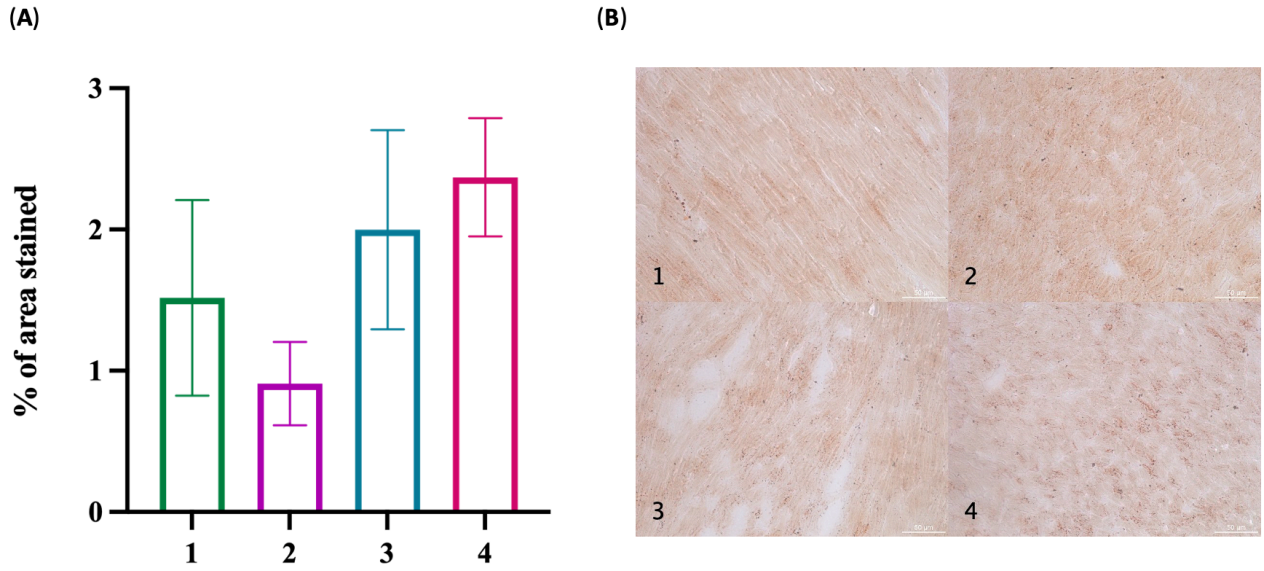

Figure 20. ORO heart. Oil Red O (ORO) staining of heart tissue from captive Svalbard ptarmigan fed *ad libitum* at the four sampling points in the body mass cycle. Birds were sampled while being kept on a short photoperiod (1: fat winter birds; n=7), shortly after being moved to constant light (2: birds rapidly losing weight; n=8), when reproductive (3: lean summer birds; n=7) and when photorefractive (4:birds gaining weight; n=7). **(A):** The % area in a section stained by ORO expressed as mean ±SEM. **(B):** Representative images of ORO stained heart sections from the four sampling groups (Bird-ID: 1=183-98, 2=184-98, 3=R27, 4=G176). Each image is at 20x magnification, shows an area of 0.096 mm^2 and scale bars = 50 µm.

ORO staining was also performed on muscle tissue from the *Pectoralis* muscle in the birds' chest. As with the heart tissue, only small amounts of the sections were stained with great variability within sampling groups. In sampling group 1, a mean ±SEM of 2.7 ±0.75 % (n=7) of the section area was stained; in group 2, 4.8 ±1.4 % (n=8) of the section area was stained; in group 3, 8.6 ±2.5 % (n=7) of the section area was stained; and in group 4, 7.6 ±1.9 % (n=8)

of the section area was stained (Figure 21A). A one-way ANOVA showed no significant differences (p=0.099) in means between the four sampling groups, nor could any obvious differences in staining be observed in the sections (Figure 21B).

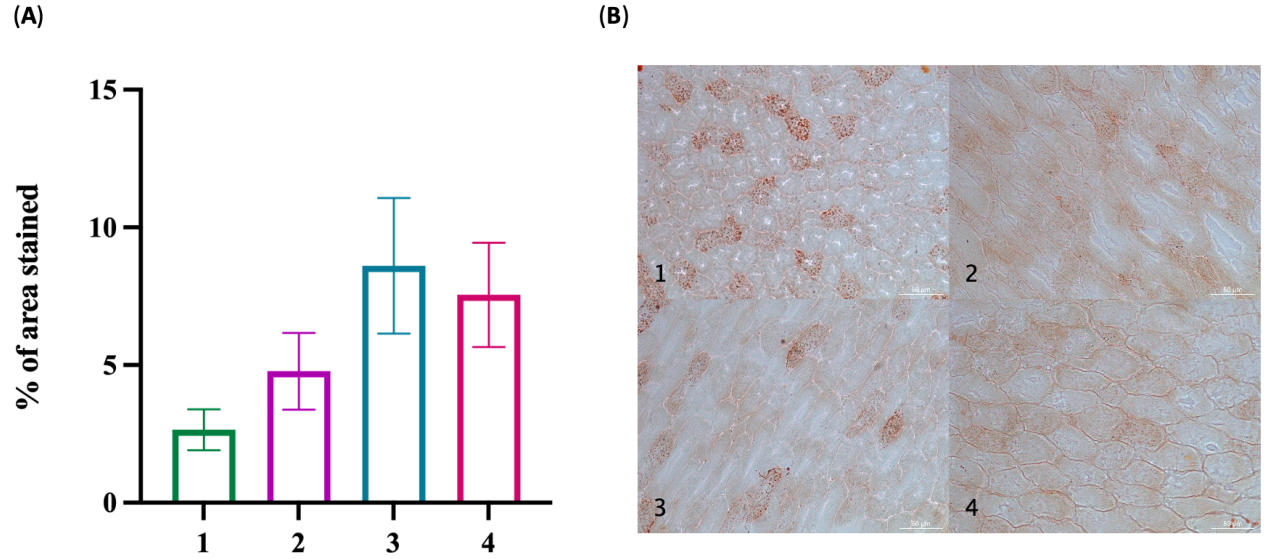

Figure 21. ORO muscle. Oil Red O (ORO) staining of muscle tissue from captive Svalbard ptarmigan fed *ad libitum* at the four sampling points in the body mass cycle. Birds were sampled while being kept on a short photoperiod (1: fat winter birds; n=7), shortly after being moved to constant light (2: birds rapidly losing weight; n=8), when reproductive (3: lean summer birds; n=7) and when photorefractive (4: birds gaining weight; n=7). **(A):** The % area in a section stained by ORO expressed as mean ±SEM. **(B):** Representative images of ORO stained muscle sections from the four sampling groups (Bird-ID: 1=294-98, 2=184-98, 3=296-98, 4=291-98). Each image is at 20x magnification, shows an area of 0.096 mm^2 and scale bars = 50 µm.

3.7 qPCR

The gene expression of six lipid metabolism genes were measured with qPCR to examine the molecular regulation of fat deposition and mobilization. The enzymes encoded by these genes and their function are described in Figure 22. All results of gene expression are presented as the log2 fold change from group 1 unless otherwise stated. In the liver, a one-way ANOVA revealed significant differences among means between the four sampling groups for all genes except for the lipolytic genes *ATGL* and *MGLL*. The relative gene expression and the results of Tukey's multiple comparisons test performed *post hoc* are presented in Figure 23 for the liver. *ACACA* gene expression was significantly lower in group 2 (-1.1 ±0.32) than in group 4 (0.21 ±0.15, $p<0.05$). *FASN* expression was significantly lower in group 2 (-1.4 ±0.45)

compared to group 1 (0 ±0.32, $p<0.05$) and group 4 (0.08 ±0.2, $p<0.05$). For *ACSL1*, relative gene expression had significantly decreased from 0 ±0.31 in group 1 to -1.4 ±0.6 in group 3 ($p<0.05$). For *CPTIA*, the gene expression in group 4 was -1.1 ±0.32, a significant decrease from 0.38 ±0.28 in group 2 ($p<0.05$). In group 3, the gene expression of *ATGL* was significantly higher in males (1.92 ±0.4 fold change, n=4) than in females (0.457 ±0.1 fold change, n=3; unpaired t-test: $p<0.05$). In group 4, the gene expression of *ACACA* was significantly higher in females (1.63 ±0.1 fold change, n=3) than in males (0.954 ±0.04 fold change, n=5; unpaired t-test: $p<0.01$).

In the fat tissue, a one-way ANOVA revealed significant differences among means between the four sampling groups for all genes except for *ACACA* and *ACSL1*. The relative gene expression in log 2 fold change from group 1 and the results of Tukey's multiple comparisons test performed *post hoc* are presented in Figure 24. Gene expression of *FASN* was significantly lower in group 2 (-0.63 ±0.08) compared to group 4 (0.25 ±0.13, $p<0.01$). *ATGL* expression was significantly lower in group 4 (-1.0 ±0.12) compared to both group 2 (0.09 ±0.31, $p<0.05$) and group 3 (1.2 ±0.41, $p<0.001$). *MGLL* expression was also lower in group 4 (-0.48 ±0.18) than in group 2 (0.21 ±0.18, $p<0.05$). For *CPTIA*, the gene expression in group 4 (-1.2 ±0.18) was significantly lower than in both group 1 (0 ±0.16, $p<0.01$) and in group 2 (-0.14 ±0.12, $p<0.05$). In sampling group 3, the gene expression of *FASN* was significantly higher in yearlings (1.19 ±0.2 fold change, n=4) than in old birds (0.640 ±0.03 fold change, n=3; unpaired t-test: $p<0.05$).

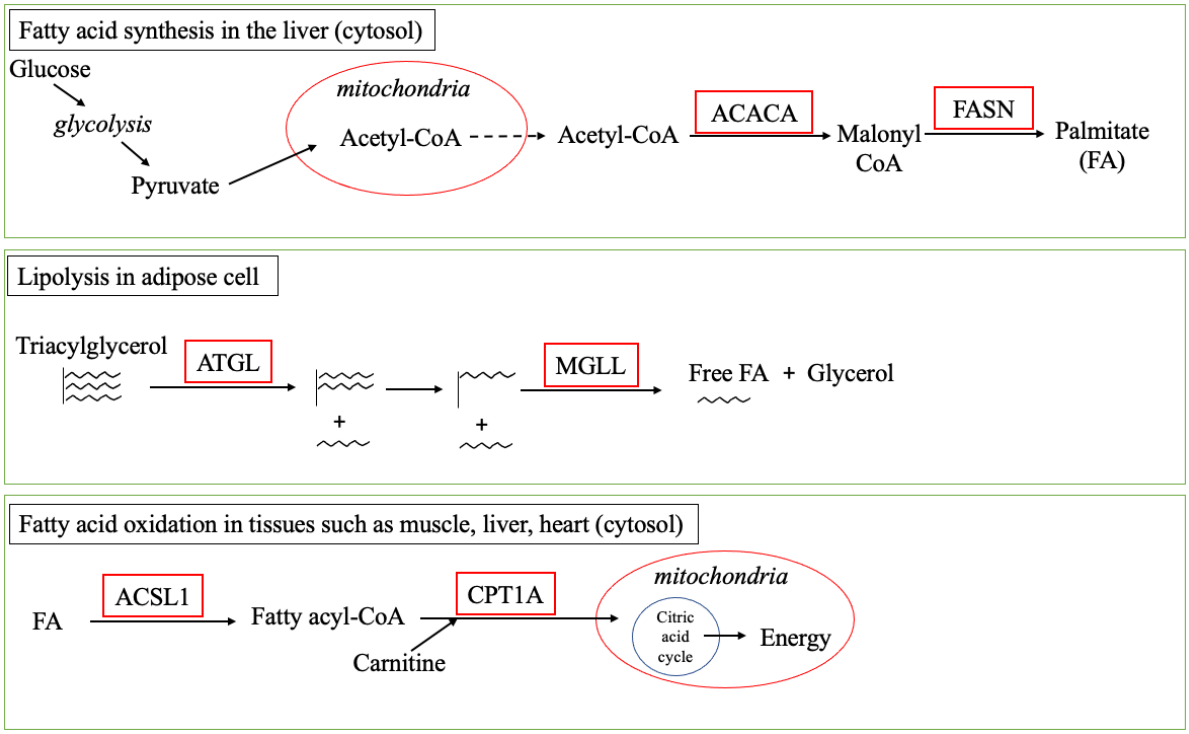

Figure 22. Schematic illustration of the function of key lipid metabolism enzymes. The illustrated function of two key enzymes (genes) in fatty acid synthesis: Acetyl-CoA carboxylase (*ACACA*) and fatty acid synthase (*FASN*), two key enzymes (genes) in lipolysis: adipose triglyceride lipase (*ATGL*) and monoacylglycerol lipase (*MGLL*), and two key enzymes (genes) involved in the fatty acid oxidation pathway taking place in tissues such as skeletal muscle, the liver, and the heart: acyl-CoA synthetase (*ACSL1*) and carnitine palmitoyl transferase I (*CPTIA*). The stippled arrow illustrates that there are several steps in the pathway not shown.

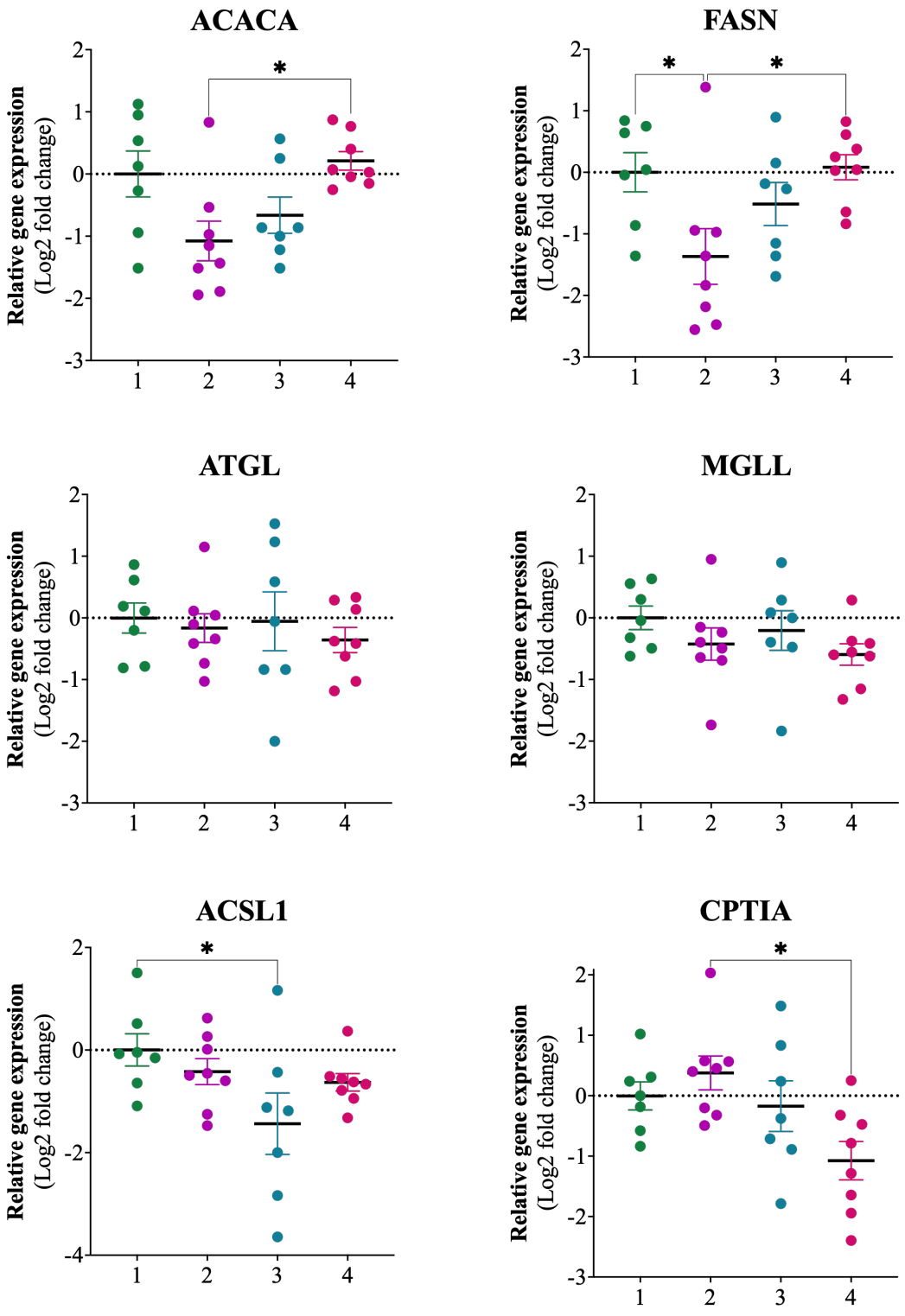

Figure 23. qPCR results liver. The relative gene expression of genes encoding key lipid metabolism enzymes in liver tissue in captive Svalbard ptarmigan sampled at four time points in their body mass cycle. Sampling points indicated on the x-axis: 1 – fat winter birds (n=7), 2 – birds rapidly losing weight (n=8), 3 – lean summer birds (n=7), and 4– photorefractive birds gaining weight (n=8). Results are shown as mean ±SEM of log2 fold change from group 1 with each circle representing one bird. A one-way ANOVA was performed for each of the genes, and when significant, a Tukey's multiple comparisons test was done *post hoc*. *p<0.05.

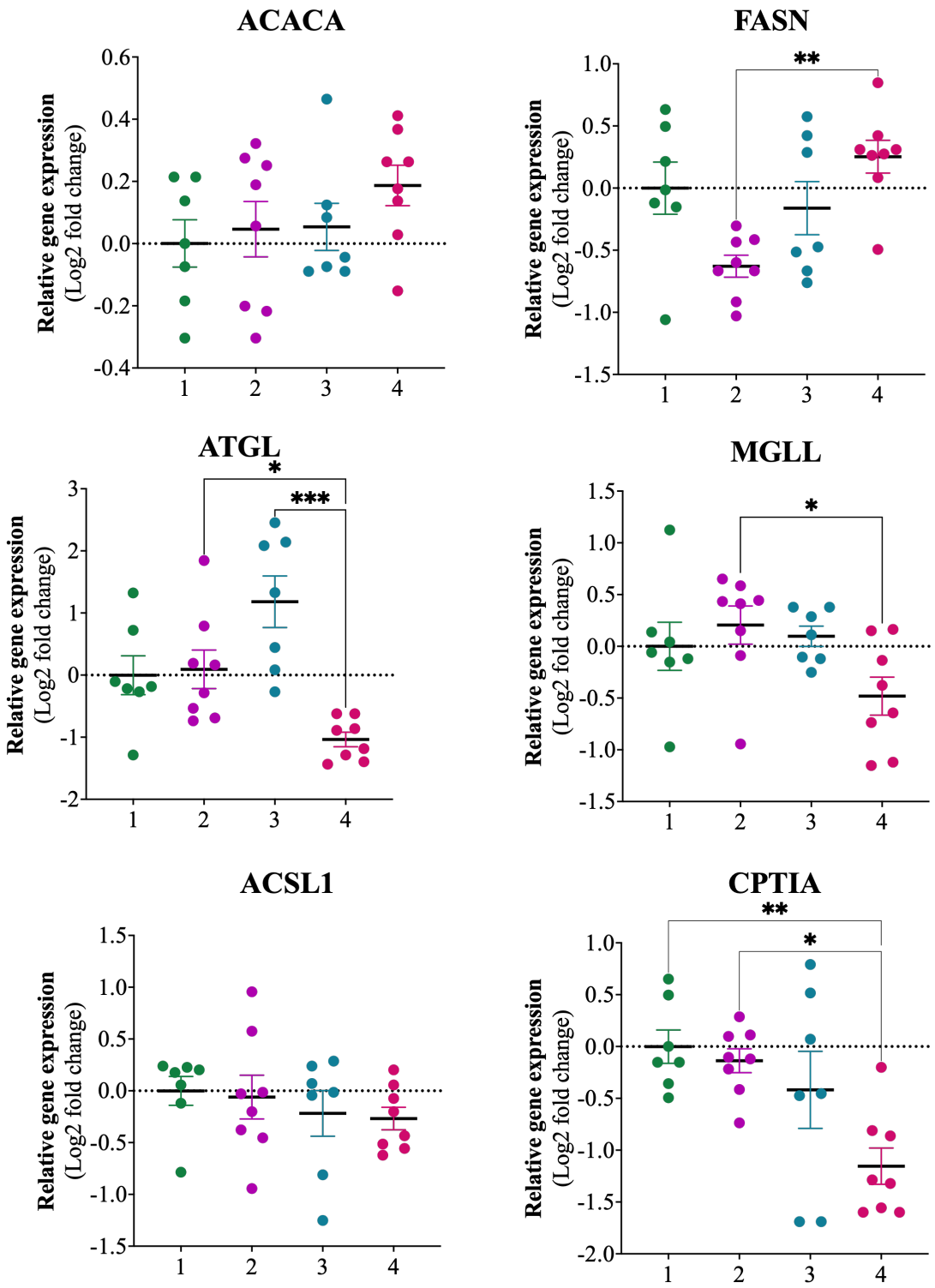

Figure 24. qPCR results fat. The relative gene expression of genes encoding key lipid metabolism enzymes in white adipose tissue in captive Svalbard ptarmigan sampled at four time points in their body mass cycle. Sampling points indicated on the x-axis: 1 – fat winter birds (n=7), 2 – birds rapidly losing weight (n=8), 3 – lean summer birds (n=7), and 4– photorefractive birds gaining weight (n=8). Results are shown as mean ±SEM log2 of fold change from group 1 with each circle representing one bird. A one-way ANOVA was performed for each of the genes, and when significant, a Tukey's multiple comparisons test was done *post hoc.* *p<0.05, **p<0.01, ***p<0.001.

3.8 Correlation: gene expression and measurements of physiology and behavior

In order to assess relationships between the different parameters, a correlation matrix was created (Figure 25). This revealed significant relationships between the gene expression of several of the genes. Where there was a correlation, the expression of lipolytic (*ATGL* and *MGLL*) and FA oxidative (*ACSL1* and *CPTIA*) genes correlated positively. Lipolytic and FA oxidative genes correlated negatively with lipogenic (*ACACA* and *FASN*) genes (Appendix C, Figure C. 1). The exceptions to this were the expression of *FASN* correlated positively with the expression of *MGLL* in the liver (R= 0.57, p<0.001) and the expression of *ACSL1* correlated positively with the expression of *ACACA* in the fat (R = 0.53, p<0.01) (Appendix C, Figure C. 2).

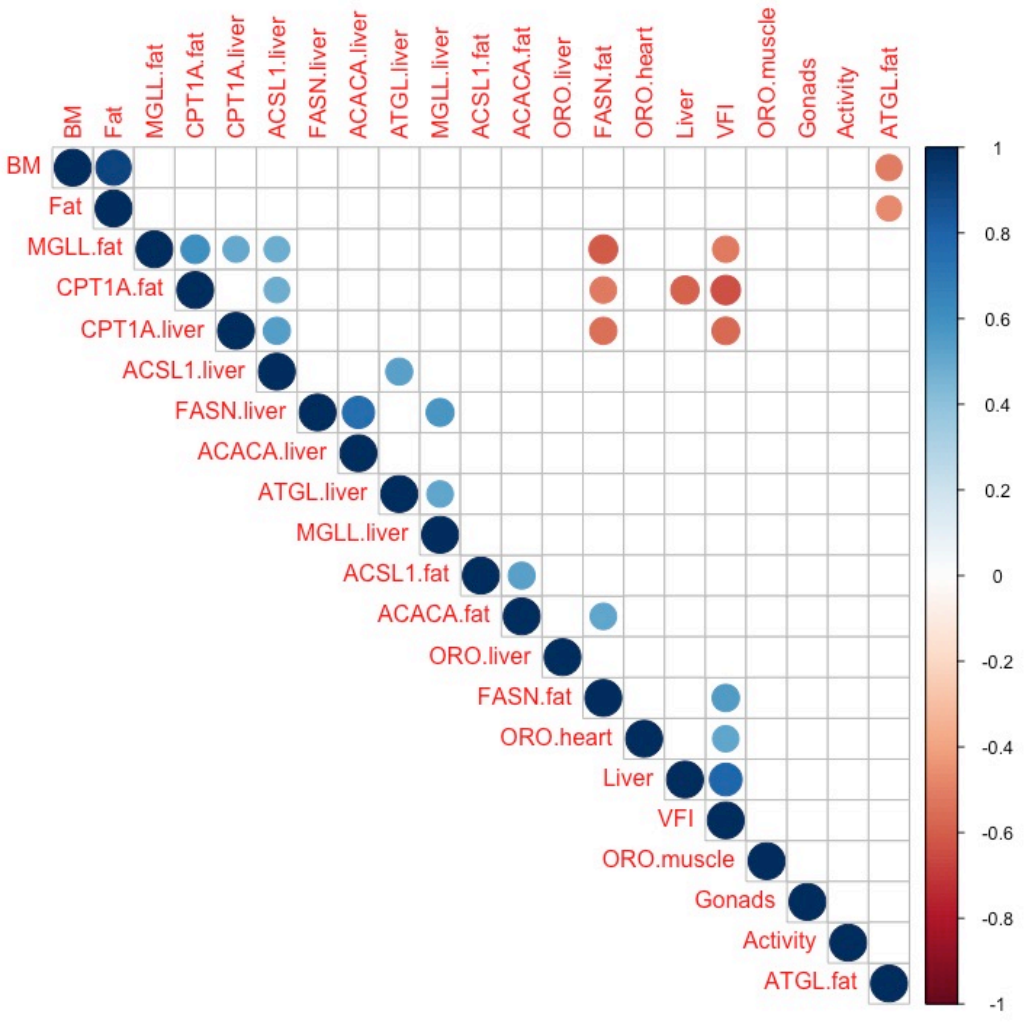

Figure 25. Correlation matrix. Circles show significant correlation (p<0.01) and the bigger the circle the lower the p-value. Pearson's coefficient is shown with color, red indicates a negative correlation and blue indicates a positive correlation. Created with the corrplot package in RStudio.

The VFI correlated negatively with *MGLL* (lipolysis) in fat (R= -0.51, p<0.01) and positively with *FASN* (FA synthesis) in the fat (R= 0.55, p<0.01) (Figure 26A-B). VFI correlated negatively with gene expression of the FA oxidation gene *CPTIA* in liver (R= -0.56, p<0.01) and in fat (R= -0.64, p<0.001) (Figure 26C-D). The VFI also correlated positively with liver weight (R= 0.78, p<0.0001) (Figure 27A). The gene expression of *ATGL* (lipolysis) in the fat correlated negatively with BM (R= -0.5, p<0.01) (Figure 27B).

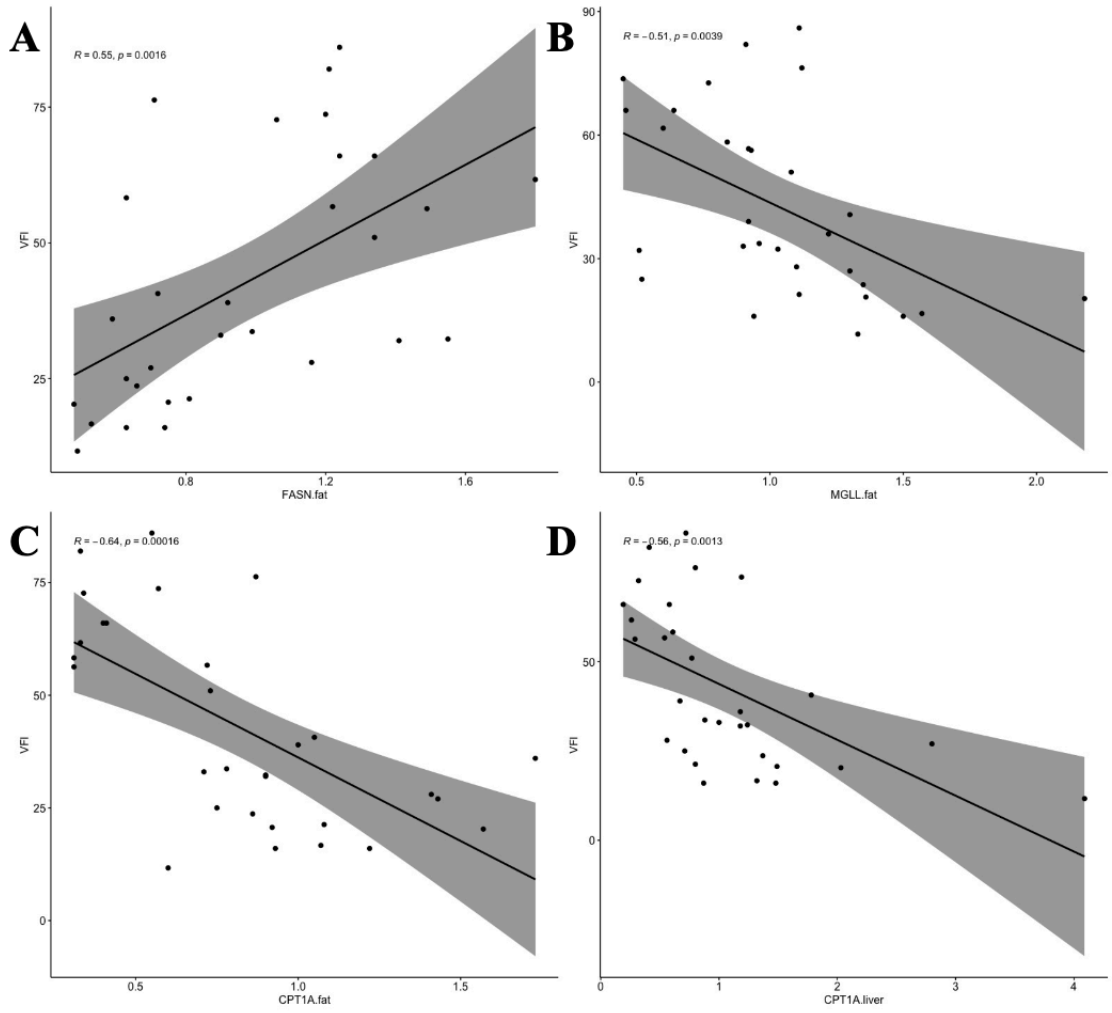

Figure 26. Food intake correlates with gene expression. The VFI (grams eaten per day) plotted against (**A**) *FASN* expression in fat (R= 0.55, p<0.01), (**B**) *MGLL* expression in fat (R= -0.51, p<0.01), (**C**) *CPTIA* expression in fat (R= -0.64, p<0.001) and (**D**) *CPTIA* expression in liver (R= -0.56, p<0.01) in fold change with 95% confidence interval.

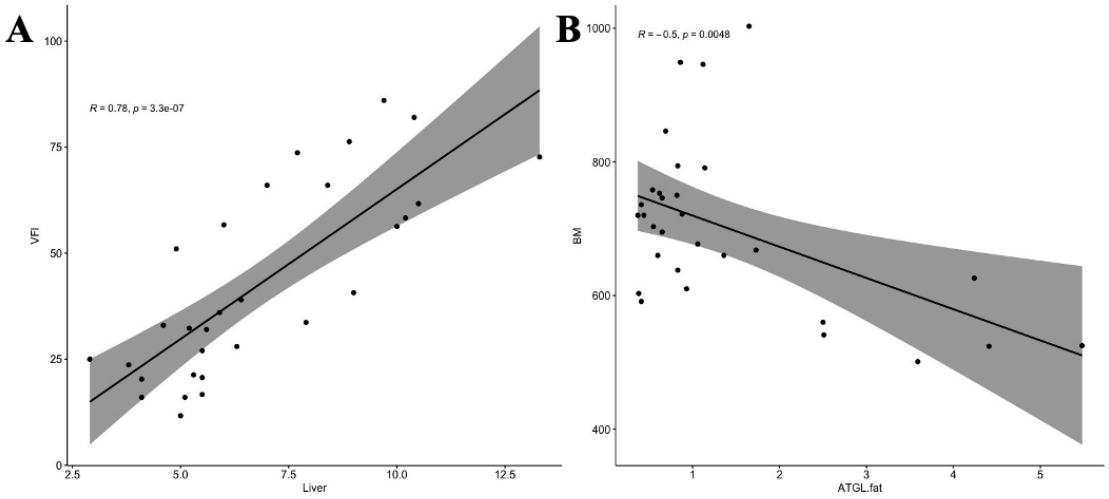

Figure 27. Food intake correlates with liver mass and BM correlates with *ATGL* expression in fat. (**A**) The VFI (grams eaten per day) plotted against liver mass (grams) (R=0.78, p<0.0001) and (**B**) The BM (grams) plotted against *ATGL* gene expression in fat tissue in fold change (R= -0.5, p<0.01) with 95% confidence intervals.

4 Discussion

4.1 Patterns of physiology and behavior

In this study, molecular aspects of the BM cycle in the Svalbard ptarmigan have been investigated. Four sampling points were established during the BM cycle. The first sampling took place in SP when birds were fat, the second sampling took place shortly after the birds had been moved to LL and were losing weight. The third sampling took place 3 months after the birds had been moved to LL. At this point, BM was at the seasonal minimum and the birds were displaying reproductive behavior. The last sampling took place when the birds had been exposed to LL for about 5 months, and had become photorefractive (terminating reproduction and gaining weight). The BM cycle in the birds in this study was similar to previous studies on captive Svalbard ptarmigan (Lindgård *et al.*, 1995; Stokkan *et al.*, 1995).

VFI and activity were also similar previous studies (Lindgård *et al.*, 1995). VFI was low in SP, and after a brief decline shortly after moving to LL, VFI gradually increased. This initial decrease in VFI after the switch to LL could be a stress response to the abrupt change in photoperiod. The activity was also low in SP, but rapidly increased after the birds had been moved to LL, and remained high until reproduction (after approx. 3 months in LL) when it started to decline as the birds became photorefractive.

While the changes in BM could be explained, at least in part, by these alterations in VFI and activity, sliding set-point experiments have shown that the BM cycle is not just a passive response to VFI and activity (Mortensen & Blix, 1985; Stokkan *et al.*, 1995). Birds that had been exposed to starvation increased their VFI to regain BM. However, the BM did not revert to pre-starvation levels, but rather to a BM appropriate for the season, as evident in control birds not exposed to starvation.

The variations in pigmented plumage in the birds in this study followed the annual changes in plumage described by Stokkan *et al.* (1986b). The females molted rapidly and completely from their white winter plumage to their brown summer plumage after approx. 2 months in LL, while the males molted later and incompletely. The males reached maximum pigmentation (75%) after 4.5 months in LL, and both males and females started molting back into their winter plumage after 5 months in LL.

The four sampling points were verified with reproductive measurements. The gonads were regressed at the first and second sampling, while they were developed at the third sampling

before regressing again at the last sampling. Egg-laying behavior was also consistent with this pattern: the first females started laying eggs shortly before the third sampling, and all females had stopped laying eggs 1 month before the last sampling. The testosterone level was regressed at the first sampling, had slightly increased in the second sampling, and peaked in the third sampling before regressing again in the fourth sampling. All these reproductive measurements, including the lag from movement to LL and the onset of reproduction, concur with previous studies describing the breeding cycle in wild Svalbard ptarmigan (Stokkan *et al.*, 1986b). On the basis of this, the molecular aspects investigated in this study can be related back to these changes in physiology and behavior during the BM cycle.

4.2 Liver mass and lipid content

Liver mass in wild birds is high in the fall when fat deposition is at its highest and declines to a seasonal minimum in February (Mortensen *et al.*, 1983). In this study, the liver mass was low in the first sampling, and decreased insignificantly in the second sampling. In the third sampling, there was no significant increase. Liver mass was at its highest in the last sampling when the birds were gaining weight. Since the liver is the main site of *de novo* lipogenesis in birds, it is expected that liver mass correlates with fat deposition. This is what happens in the Eared grebe, a migrating waterbird. In the fall, the grebe deposits large amounts of fat and show profound changes in body compositions, including an increase in liver mass (Jehl Jr, 1997).

ORO staining of liver tissue revealed significant differences in lipid content between different stages of the BM cycle in Svalbard ptarmigan. ORO staining of liver samples is commonly used to diagnose steatosis (i.e. abnormal retention of fat within an organ) in both livestock such as cows, humans, and laboratory animals such as rats and mice (Gerspach *et al.*, 2017; Levene *et al.*, 2012; Pummoung *et al.*, 2021). Whereas, as a diagnostic tool, ORO staining reveal abnormal lipids in liver tissue, in the Svalbard ptarmigan the fat within the liver is part of the normal annual BM cycle. Images from sampling groups 1 and 4 show clear staining of lipids comparable to images of diseased livers from other animals that do not exhibit seasonal variations in BM. However, Svalbard ptarmigan seem to use their liver as a fat storage organ in the winter for easy access for the utilization of the energy in this fat stored in the liver. At the 4th sampling point, when the birds are depositing fat for the winter, they have excess amounts of fat in the liver for another reason. Because *de novo* FA synthesis primarily

happens in the liver, the elevated amount of fat seen at the 4th sampling point is likely an image of newly synthesized fat that is in the process of being moved to fat depots elsewhere.

Migratory birds also store fat in the liver, and like the Svalbard ptarmigan seemingly suffer no pathological effects (King & Farner, 1965; Sharma & Kumar, 2019). One mechanism behind this has been investigated in the Landes goose, a goose species bred for the production of foie gras (fatty liver) and a descendant of a migratory species (Geng *et al.*, 2016). In their study, Geng *et al.* (2016) examined possible reasons for how the geese seemed to be protected from developing pathologies associated with excess fat accumulation in the liver, e.g. inflammation. They investigated the effects of the cytokine adiponectin. Adiponectin has anti-inflammatory effects in fatty livers and it is only released by fat cells. Its expression has been shown to decrease in obese humans. Geng *et al.* (2016) showed that the expression of adiponectin was suppressed in fat tissue in overfed geese compared to normal fed geese. However, the expression of this cytokine in liver tissue did not differ between the two groups of geese, but the expression of adiponectin receptors were increased in the livers of overfed compared to normally-fed geese. The authors suggested that this overexpression of adiponectin receptors might enhance the liver's sensitivity to adiponectin and in this way avoid inflammation. The ORO staining revealed that the Svalbard ptarmigan store excess amounts of fat in their livers. It is therefore probable that a similar protective mechanism exists in Svalbard ptarmigan because they rely on accumulating excess amounts of fat in the liver that in other animals are pathological.

In wild females, the liver mass peaks prior to egg-laying in May/June, while in males liver mass remains low during the breeding season (Mortensen *et al.*, 1983). In this study, both liver mass and ORO staining showed significant sex-differences in the reproductive season (sampling point 3). The females had a significantly higher liver mass than males. While liver mass was higher in females than in males, ORO staining of the liver revealed that males had a significantly higher fat content than the females. These differences in liver components in the reproductive season are likely due to the liver's involvement in egg production. In laying hens, lipogenesis in the liver is increased because of the stimulating effects of high estrogen secretion (Hermier, 1997). This is because in the process of making egg yolk, the laying hens synthesize the lipoprotein, vitellogenin, in the liver which is delivered to the ovaries to be part of the energy requirement of the developing chick inside the egg (Alvarenga *et al.*, 2011). The liver also synthesizes other proteins for the eggs (Pulliainen & Tunkkari, 1984), which is another explanation for the higher liver mass in females during the egg-laying season.

However, ORO staining of the liver revealed a higher fat content in the males' livers, which could be explained by high mobilization rates in females so that as soon as proteins and lipoproteins are synthesized they are transported directly to the ovaries and used in the production of eggs preventing an accumulation of lipids in the liver.

4.3 Fat mass

The amount of fat follows that of BM: when the BM is high, so is the amount of dissectible fat. A clear difference arose between yearling and old birds. In old birds, the dissectible fat mass was highest in SP and decreased drastically until sampling 3. Dissectible fat were significantly lower in groups 3 and 4 compared to groups 1 and 2. While in yearlings, there were no significant changes in fat mass between sampling groups. This is likely due to the fact that yearlings are not yet fully grown, and are still growing non-fatty tissue such as muscles.

Cell area as a measure for cell size was significantly larger in fat birds compared to lean birds. This supports the theory that the growth of adipose tissue is due to hypertrophy (i.e. increase in cell size) and not hyperplasia (i.e. increase in cell number). As the birds deposit fat, the main way this happens is with an increase in fat cell size, but to conclusively say this, data on cell number are needed. In chicken, a fat line and a lean line was bred and in the fat line adipocyte number increased more than adipocyte size compared to the lean chicken line (Guo *et al.*, 2011). In humans, adipocyte size seems to only increase up to a moderate level of obesity, suggesting that adipocytes reach a maximum size, while in more severe cases of obesity the number of adipocytes increases with the degree of obesity (Hirsch & Batchelor, 1976). The theory that hyperplasia only occurs when existing adipocytes have reached a maximum size is also supported by evidence from experiments on rats done by Björntorp *et al.* (1982).

Adipocyte hyperplasia occurs in some forms of obesity. However, it seems that the growth of adipose tissue is limited to adipocyte hypertrophy in animals that rely on seasonally deposition of large amounts of fat. This might be because seasonal deposition of fat is not severe enough to need adipocyte hyperplasia to occur to keep growing. This is also likely to be adaptive because of the easier regulation of cell size compared to the regulation of cell number during short term changes in fat mass. If it is indeed harder to reduce the number of adipocytes than reducing their size, hyperplasia in animals that seasonally deposit large amounts of fat risks not being able to lose all this deposited fat when it is not needed in

subsequent seasons (Mrosovsky *et al.*, 1987). However, if these animals are resistant to adipocyte hyperplasia, they are protected from this risk of an increasing number of adipocytes.

4.4 Lipid content in heart and muscle

ORO staining of heart and muscle did not show any differences during the BM cycle in the amount of fat deposited in these tissues. In muscle tissue, less than 10% of the area was stained, while in heart tissue, less than 3% was stained. This suggests that even in SP when Svalbard ptarmigan are fat, they do not deposit any extra fat in the heart or muscle tissue.

Migratory birds do not store any fat in and around their hearts (Odum & Perkinson Jr, 1951), nor do they appear to store any significant amounts of fat in their muscles at the peak of fat deposition prior to migration (Bauchinger & Biebach, 2001). An efficient system for fat mobilization is crucial for birds that rely on the energy from fat during migration. These birds also need their muscles and heart to work effectively, and therefore it is important that the excess amounts of fat in their bodies do not interfere with the cardiovascular system (Weber, 2009). This is a likely reason that fat is stored in a designated area (subcutaneously), and not within important areas for flying.

While migratory birds and Svalbard ptarmigan do not store significant amounts of fat in muscle and heart, obese animals do. Obese mice accumulate significantly more fat in both skeletal and cardiac muscle than their lean counterparts, as measured by ORO staining (Hagberg *et al.*, 2012).

The ORO staining of the heart and muscle in this study showed high variation within groups, and numerous sections were incomplete and the quantification had to be done on an insert of the image. The muscle samples were taken from the same muscle, the pectoralis, but the sample was not labeled with a posterior/anterior or dorsal/ventral marking, so that care was not taken to ensure the sectioning was done in the same direction and area of each sample. This resulted in some sections being cross-sections of the muscle fibers, while other samples were longitudinal sections. This could have made a difference in the staining between samples.

4.5 ORO – reflections on the method

ORO staining is a commonly used method for eluding lipid details in various organs and tissues, especially the liver. It is considered, in combination with digital image analysis, one of the best and most accurate ways of detecting and quantifying liver steatosis in mammals (Levene *et al.*, 2012). Its accuracy is considerably higher than the previously preferred method of using hematoxylin-eosin stained sections (Ge *et al.*, 2010). In this study, ORO staining proved a useful tool for viewing lipid content in the liver at various stages in the Svalbard ptarmigan's BM cycle.

In muscle, ORO staining might not be the preferred method for measuring fat content because it cannot be used on live cells and it can be challenging to use when multi-labeling approaches are needed (Spangenburg *et al.*, 2011). A cell permeable lipophilic fluorescent dye, BODIPY (493/503) can be used on both frozen muscle and on live or fixed cells (Spangenburg *et al.*, 2011). It is the preferred dye to measure intramuscular fat and the relative intramuscular distribution of fat because it penetrates cells and it can easily be used with other staining procedures, e.g. to differentiate between different types of muscle fibers (Prats *et al.*, 2013).

There are many advantages with the use of ORO staining to image lipids in various tissues. It is cheap and requires equipment that is present in most research labs. It also does not require any highly hazardous materials that might require special training prior to use. In addition, computerized quantification produces reproducible results efficiently and quickly. However, the staining process can be labor-intensive depending on the tissue, and the ORO easily precipitates which requires a new solution to be prepared before each day of use. But probably, the most laborious step is the preparation of the sections, which requires some experience with the use of a cryostat to produce adequate sections for staining. Especially fat tissue is difficult to work with and usually requires fixation to be able to obtain sections that can be used for staining procedures.

The most common method to fix fat tissue is with paraffin, but because the de-paraffinization process removes most lipids, ORO staining cannot be used afterward (Mehlem *et al.*, 2013). Parlee *et al.* (2014) have described a method to standardize the analysis of volume and number of adipocytes in fat tissue by the use of hematoxylin-eosin staining following paraffin fixation. This method still requires training in sectioning technique and is as labor-intensive as ORO, but it is a more reliable way of imaging fat tissue.

Despite the above mentioned issues, I showed that ORO staining of fat tissue could be used to distinguish between the fattest and the leanest birds (Figure 19A). However, as an alternative to measure dissectible fat to determine a bird's fatness, it is not precise enough (Figure 19C).

There are ways of quantifying fat that are non-invasive and can be performed on awake birds in the wild. The easiest and most accurate of these methods is the quantitative magnetic resonance (QMR), which can measure fat, wet lean mass, and total water within a scanned volume (Guglielmo *et al.*, 2011). This rapid and easy-to-use method makes longitudinal studies of body composition possible in both the lab and field in birds such as the Svalbard ptarmigan. It does not require any laboratory work, or the sacrifice of the animal under study, and is therefore preferable to both histopathological methods such as ORO or hematoxylin-eosin staining and dissection.

4.6 Gene expression

Prior to this study, the hypotheses were that FA synthesis, lipolysis and FA oxidation would be affected by the photoperiod and the stage in the BM cycle the Svalbard ptarmigan were in. This is indeed what the results of this study show (Table 14). Fat winter birds in sampling group 1 were sampled as a control, and fold change gene expression was measured relative to this group at the three other sampling groups. The activity of the FA synthesis genes *ACACA* and *FASN* was upregulated during the weight-gaining phase (sampling group 4) compared to the weight-loss phase (sampling group 2) of the BM cycle. The activity of the lipolysis genes *ATGL* and *MGLL* was downregulated during the weight-gaining phase in fat tissue. However, seasonal differences in lipolytic gene activity were not observed in liver tissue. The activity of the FA oxidative gene *CPTIA* was downregulated when the birds were losing weight.

Table 14. Summary of gene expression results. The change in activity of the genes measured in sampling group 4 (birds gaining weight) compared to sampling group 2 (birds losing weight).

	Gene	**Liver tissue**	**Fat tissue**
Fatty acid synthesis	*ACACA*	↑	-
	FASN	↑	↑
Lipolysis	*ATGL*	-	↓
	MGLL	-	↓
Fatty acid oxidation	*ACSL1*	-	-
	CPTIA	↓	↓

Fatty acid synthase (FASN) is a crucial enzyme in *de novo* FA synthesis, and its activity in liver tissue has been investigated in several species of migratory birds (Guglielmo, 2018; Sharma & Kumar, 2019; Zajac *et al.*, 2011). The FASN activity doubled prior to spring migration in wild Red-headed buntings and Western sandpipers (Guglielmo, 2018). Zajac *et al.* (2011) found that in the white-throated sparrow FASN activity in the liver was higher in captivity compared to wild birds. The authors stated that this might be an artifact of the captive birds being fed *ad libitum*, and therefore increasing FA synthesis capacity to be able to convert excess food intake to fat. FASN activity in the liver and adipose tissue has also been investigated in a hibernating mammal, the marmot (Mostafa *et al.*, 1993). In this species, FASN activity was higher in early spring when the animals were emerging from hibernation and in mid-summer when feeding on a high-carbohydrate diet compared to during hibernation in the winter. These studies provide evidence that animals are capable of changing FA synthesis capabilities during the year as needed. This seems to also be the case for Svalbard ptarmigan. High *FASN* activity in the fat correlated with high VFI, which seems to suggest that surplus energy is converted to fat for storage in anticipation to periods with less food.

FASN activity in sampling group 3 was higher in yearlings than in old birds, which suggests that the yearlings start upregulating FA synthesis earlier than old birds. This might be because the yearlings have a lower BM than old birds, and to have enough deposited fat by winter they need to start this process earlier.

Adipose triglyceride lipase (ATGL) catalyzes the first step in breaking down stored fat to use for energy. Its activity in Svalbard ptarmigan correlates negatively with levels of fat, meaning that in fat birds, *ATGL* activity is low. *ATGL* activity is at its highest when the birds are at their leanest at the third sampling point. In starved humans and seals, ATGL activity is upregulated (Viscarra & Ortiz, 2013; Viscarra *et al.*, 2012). Concurrently with the increase in ATGL, hormone-sensitive lipase (HSL) decreased, and the authors of these papers suggested that this was an adaptive mechanism in animals regularly exposed to starvation. The reason for this is that the activity of ATGL, which breaks down triglycerides, ensures that lipolysis is maintained, while HSL breaks down diglycerides and monoglycerides, and therefore the inhibition of this enzyme ensures that the lipid stores are not emptied prematurely (Viscarra & Ortiz, 2013). It would be of interest to study the Svalbard ptarmigan under food restriction to see if ATGL (and HSL) activity follows the same pattern as other starved animals. MGLL hydrolyzes monoacylglycerol and its activity in Svalbard ptarmigan is negatively correlated with VFI, so that when VFI is low, the mobilization of FAs is high. *HSL* gene expression

could not be measured in this study because the gene sequence was not found in the reference genome. The sequences of *ATGL* and *HSL* should be studied to look for similarities or evidence that ATGL might have resumed some of the functions of HSL or that this enzyme is not found in Svalbard ptarmigan.

The expression of *ATGL* in the liver was significantly higher in males than in females. The higher activity of *ATGL* in males could be explained by the higher fat content in males' livers and that the males are still mobilizing their fat from the winter. Another reason for the difference in *ATGL* activity could be that lipolysis is inhibited in females to conserve fat needed for egg production.

Carnitine palmitoyl transferase I (CPTIA) is crucial for FA oxidation. Its activity in Svalbard ptarmigan shows that during the autumnal fattening, FA oxidation is inhibited. In migratory bunting, CPTI activity has been found to be higher during the night in the migratory state (Sharma & Kumar, 2019), which is to be expected because this is when the bird would need to utilize fat stores for energy. This agrees well with the data from Svalbard ptarmigan which show a negative correlation between VFI and *CPTIA* activity in both the liver and fat. With a higher VFI, the bird's energy demand is met by its food consumption, and therefore it does not need to oxidize stored fat for energy. In the liver, *ACSL1* expression was lowest in the third sampling, which differs from the expression of *CPTIA*. However, *ACSL1* is one isozyme out of many in a large gene family of acyl-CoA synthetases where all known members catalyzes the breakdown of FAs into fatty acyl-CoA (Ellis *et al.*, 2010). Different isozymes of this family act on different lengths of FAs and are believed to affect what metabolic pathway the fatty acyl-CoA enters next. There might be other isozymes of this family that is more active during FA oxidation or act on specific FAs that are abundant in the liver in Svalbard ptarmigan.

Interestingly, the gene expression of *FASN* correlated positively with the expression of *MGLL* in the liver. There is no obvious explanation for this relationship, and because of the high variation within sampling groups and low variation between groups, it could be a coincidence rather than causation. In addition, the gene expression of *ACSL1* positively correlated with *ACACA* in fat tissue. These are not the rate-limiting enzymes for FA oxidation and FA synthesis, respectively, and might therefore not be tightly regulated because their activity relies on other enzymes' activities. It is therefore likely that the statistical correlation is not based on biological causation.

A summary of the lipid metabolism pathway and for which genes activity seemed to be affected by photoperiod and VFI is found in Figure 28 for liver tissue and in Figure 29 for fat tissue.

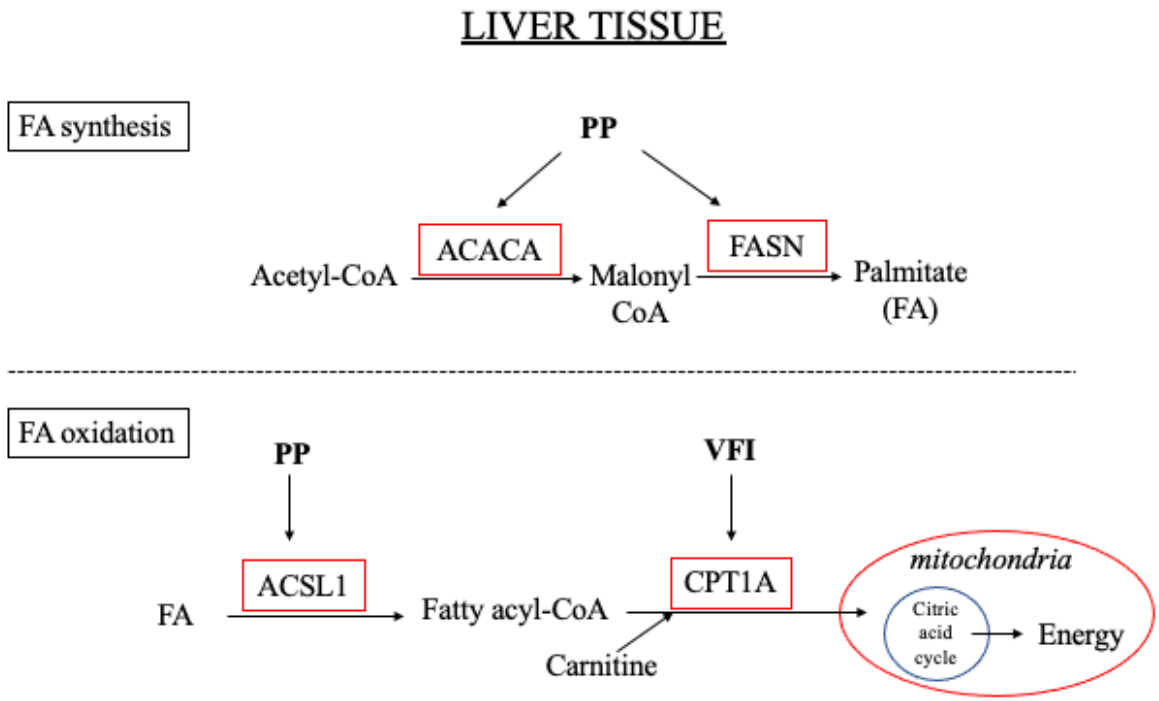

Figure 28. The gene expression of fatty acid (FA) synthesis and FA oxidation genes in liver tissue is affected by voluntary food intake (VFI) and photoperiod (PP).

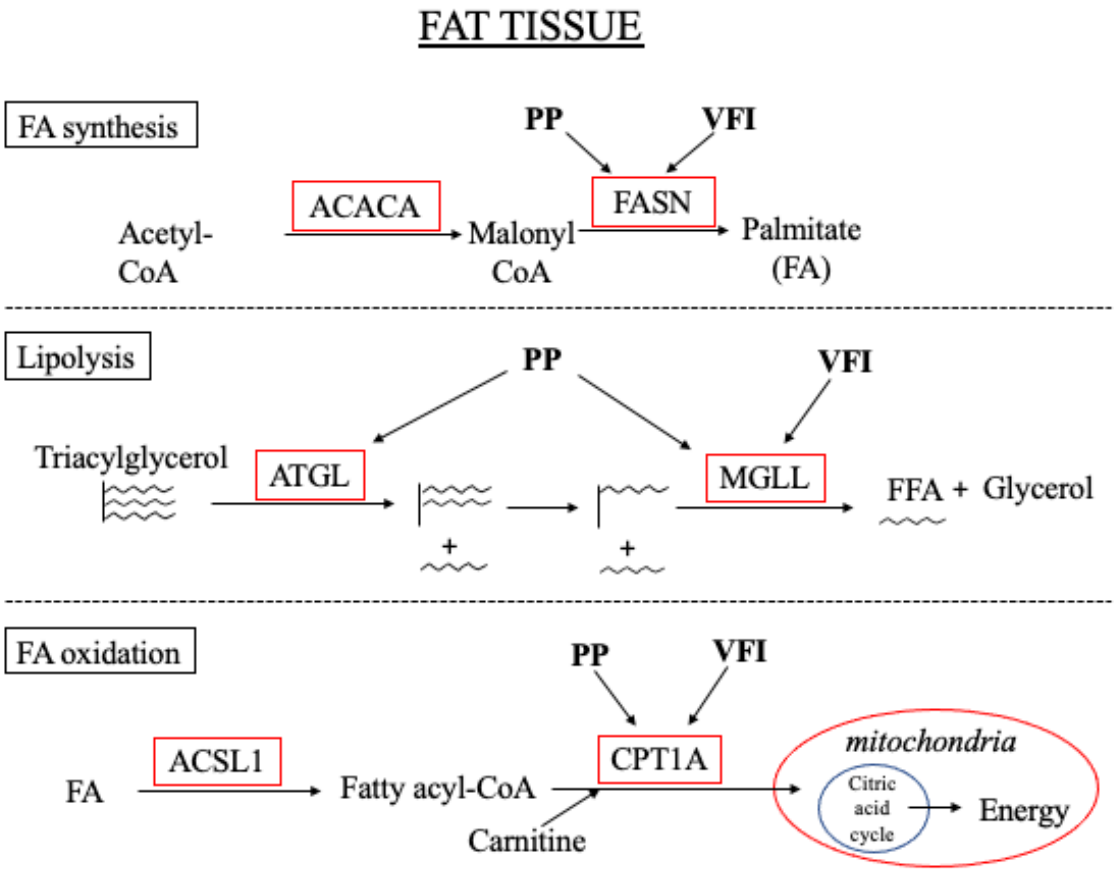

Figure 29. The gene expression of fatty acid (FA) synthesis lipolysis and FA oxidation genes in fat tissue is affected by voluntary food intake (VFI) and photoperiod (PP).

4.7 Future outlook

While this experiment has taken a step toward discovering the molecular underpinnings of the BM cycle in the Svalbard ptarmigan, a great deal of work remains. BM was remarkably uniform within age groups, while both VFI and activity showed great variation throughout the study. It is therefore of interest to investigate the relationship between these three parameters on an individual level to see if any clear relationships emerge. This could also be done with the ORO stains and gene expression data because all these measurements contained great variation within sampling groups.

The birds in this study were fed *ad libitum* and the high intragroup variation in gene expression might be due to the lack of food restriction. Therefore, an experiment where starvation or food restriction is included should be designed and repeat the measures of gene

expression. This would also better distinguish effects of VFI and photoperiod on gene expression.

It is also of interest to look at plasma concentrations of certain components/metabolites of lipid metabolism, such as FFAs, cholesterol and lipoproteins, to better understand the effects of the profound seasonal variations in fat content in these birds. A comparison to species that do not show seasonal variations in BM is crucial to elude how the ptarmigan can store excess amounts of fat without any obvious ill-health effects.

In this study, gene expression of a small subset of well-characterized lipid metabolism enzymes were measured. However, future research should look into the possibilities of techniques such as RNA-sequencing to reveal variations in previously unknown genes that could be of interest.

5 Conclusion

This is the first study to describe molecular aspects of the lipid metabolism in peripheral tissue in the Svalbard ptarmigan. I have presented evidence that the Svalbard ptarmigan possesses the means to alter the activity of lipogenesis and lipolysis in terms of changes in the expression of key lipid metabolism genes with regard to the time of year and behavior such as VFI. These birds also store significant amounts of fat in preparation for winter, and while this is evident in the liver, tissues such as the heart and skeletal muscle seem to contain some sort of mechanism that protects them from excess storage of fat. I have also assessed the usefulness of histopathology staining of fat tissue to determine the fat state in these birds.

Works cited

Alvarenga, R., Zangeronimo, M., Pereira, L., Rodrigues, P., & Gomide, E. (2011). Lipoprotein metabolism in poultry. *World's Poultry Science Journal, 67*(3), 431-440.

Appling, D. R., Anthony-Cahill, S. J., & Mathews, C. K. (2016). *Biochemistry: concepts and connections* (J. Zalesky, Ed. 1 ed.). Pearson.

Bauchinger, U., & Biebach, H. (2001). Differential catabolism of muscle protein in garden warblers (Sylvia borin): flight and leg muscle act as a protein source during long-distance migration. *Journal of Comparative Physiology B, 171*(4), 293-301.

Björntorp, P., Karlsson, M., & Pettersson, P. (1982, 1982/04/01/). Expansion of adipose tissue storage capacity at different ages in rats. *Metabolism, 31*(4), 366-373. https://doi.org/https://doi.org/10.1016/0026-0495(82)90112-3

Blix, A. S. (2005). *Arctic animals and their adaptations to life on the edge*. Tapir Academic Press.

Buyse, J., & Decuypere, E. (2014). Adipose tissue and lipid metabolism. In C. G. Scanes (Ed.), *Sturkie's Avian Physiology* Elsevier Science & Technology.

Dark, J., Stern, J. S., & Zucker, I. (1989). Adipose tissue dynamics during cyclic weight loss and weight gain of ground squirrels. *American Journal of Physiology-Regulatory, Integrative and Comparative Physiology, 256*(6), R1286-R1292.

Davis, M. (2020). *ApE - A plasmid Editor, v2.0.61*. https://jorgensen.biology.utah.edu/wayned/ape/

Ellis, J. M., Frahm, J. L., Li, L. O., & Coleman, R. A. (2010). Acyl-coenzyme A synthetases in metabolic control. *Current opinion in lipidology, 21*(3), 212-217. https://doi.org/10.1097/mol.0b013e32833884bb

Emerson, R. W. (2015). Causation and Pearson's correlation coefficient. *Journal of visual impairment & blindness, 109*(3), 242-244.

Fuglei, E., Henden, J.-A., Callahan, C. T., Gilg, O., Hansen, J., Ims, R. A., . . . Merizon, R. A. (2020). Circumpolar status of Arctic ptarmigan: Population dynamics and trends. *Ambio, 49*(3), 749-761.

Førland, E. J., Benestad, R., Hanssen-Bauer, I., Haugen, J. E., & Skaugen, T. E. (2011). Temperature and precipitation development at Svalbard 1900–2100. *Advances in Meteorology, 2011*, 1-14. https://doi.org/10.1155/2011/893790

Ge, F., Lobdell, H. t., Zhou, S., Hu, C., & Berk, P. D. (2010). Digital analysis of hepatic sections in mice accurately quantitates triglycerides and selected properties of lipid droplets. *Experimental biology and medicine (Maywood, N.J.), 235*(11), 1282-1286. https://doi.org/10.1258/ebm.2010.010095

Geng, T., Yang, B., Li, F., Xia, L., Wang, Q., Zhao, X., & Gong, D. (2016). Identification of protective components that prevent the exacerbation of goose fatty liver: characterization, expression and regulation of adiponectin receptors. *Comparative Biochemistry and Physiology Part B: Biochemistry and Molecular Biology, 194*, 32-38.

Gerspach, C., Imhasly, S., Klingler, R., Hilbe, M., Hartnack, S., & Ruetten, M. (2017). Variation in fat content between liver lobes and comparison with histopathological scores in dairy cows with fatty liver. *BMC Veterinary Research, 13*(1), 98. https://doi.org/10.1186/s12917-017-1004-9

Gjertz, I., Mehlum, F., & Gabrielsen, G. W. (1985). Food sample analysis of seabirds collected during the 'Lance'-cruise in ice-filled waters in Eastern Svalbard 1984.

Grammeltvedt, R., & Steen, J. B. (1978). Fat Deposition in Spitzbergen Ptarmigan (Lagopus mutus hyperboreus). *ARCTIC, 31*(4), 496-498. https://doi.org/10.14430/arctic2676

Guglielmo, C. G. (2018). Obese super athletes: fat-fueled migration in birds and bats. *Journal of Experimental Biology, 221*(Suppl_1). https://doi.org/10.1242/jeb.165753

Guglielmo, C. G., McGuire, L. P., Gerson, A. R., & Seewagen, C. L. (2011). Simple, rapid, and non-invasive measurement of fat, lean, and total water masses of live birds using quantitative magnetic resonance. *Journal of Ornithology, 152*(1), 75.

Guo, L., Sun, B., Shang, Z., Leng, L., Wang, Y., Wang, N., & Li, H. (2011). Comparison of adipose tissue cellularity in chicken lines divergently selected for fatness. *Poultry science, 90*(9), 2024-2034.

Hagberg, C. E., Mehlem, A., Falkevall, A., Muhl, L., Fam, B. C., Ortsäter, H., . . . Lu, L. (2012). Targeting VEGF-B as a novel treatment for insulin resistance and type 2 diabetes. *Nature, 490*(7420), 426-430.

Hagen, J. O., Liestøl, O., Roland, E., & Jørgensen, T. (1993). *Glacier atlas of Svalbard and Jan Mayen* (Vol. 129). Norwegian Polar Institute.

Hansen, B. B., Grøtan, V., Aanes, R., Sæther, B.-E., Stien, A., Fuglei, E., . . . Pedersen, Å. Ø. (2013). Climate events synchronize the dynamics of a resident vertebrate community in the high Arctic. *Science, 339*(6117), 313-315.

Harland, W. B. (1997). Svalbard. *Geological Society, London, Memoirs, 17*(1), 3-15. https://doi.org/10.1144/GSL.MEM.1997.017.01.01

Henden, J.-A., Ims, R. A., Fuglei, E., & Pedersen, Å. Ø. (2017). Changed Arctic-alpine food web interactions under rapid climate warming: implication for ptarmigan research. *Wildlife Biology, 2017*(SP1).

Hermier, D. (1997). Lipoprotein metabolism and fattening in poultry. *The Journal of nutrition, 127*(5), 805S-808S.

Hirsch, J., & Batchelor, B. (1976). Adipose tissue cellularity in human obesity. *Clinics in endocrinology and metabolism, 5*(2), 299-311.

Hisdal, V. (1998). *Svalbard nature and history*. Norwegian Polar Institute.

Hølleland, S., & Karlsen, H. A. (2020). Decline in temperature variability on Svalbard. *Journal of Climate, 33*(19), 8475-8486.

Jehl Jr, J. R. (1997). Cyclical changes in body composition in the annual cycle and migration of the Eared Grebe Podiceps nigricollis. *Journal of Avian Biology*, 132-142.

John, D. (2005). Annual lipid cycles in hibernators: integration of physiology and behavior. *Annuual Review of Nutrition, 25*, 469-497.

Kassambara, A. (2020). *Package 'ggpubr'.* In R.

King, J. R., & Farner, D. S. (1965). Studies of fat deposition in migratory birds. *Annals of the New York Academy of Sciences, 131*(1), 422-440.

Kohler, J., & Aanes, R. (2004). Effect of winter snow and ground-icing on a Svalbard reindeer population: results of a simple snowpack model. *Arctic, Antarctic, and Alpine Research, 36*(3), 333-341.

Levene, A. P., Kudo, H., Armstrong, M. J., Thursz, M. R., Gedroyc, W. M., Anstee, Q. M., & Goldin, R. D. (2012). Quantifying hepatic steatosis–more than meets the eye. *Histopathology, 60*(6), 971-981.

Lindgård, K., Stokkan, K. A., & Näslund, S. (1995). Annual changes in body mass in captive Svalbard ptarmigan: role of changes in locomotor activity and food intake. *Journal of Comparative Physiology B, 165*(6), 445-449.

Livak, K. J., & Schmittgen, T. D. (2001). Analysis of relative gene expression data using real-time quantitative PCR and the 2− ΔΔCT method. *methods, 25*(4), 402-408.
Løvenskiold, H. L. (1964). *Avifauna Svalbardensis* (Vol. 129). Norwegian Polar Institute.
Mehlem, A., Hagberg, C. E., Muhl, L., Eriksson, U., & Falkevall, A. (2013). Imaging of neutral lipids by oil red O for analyzing the metabolic status in health and disease. *Nature protocols, 8*(6), 1149-1154.
Morin, P., & Storey, K. B. (2009). Mammalian hibernation: differential gene expression and novel application of epigenetic controls. *International Journal of Developmental Biology, 53*(2-3), 433-442.
Mortensen, A., & Blix, A. S. (1985). Seasonal changes in the effects of starvation of metabolic rate and regulation of body weight in Svalbard ptarmigan. *Ornis Scandinavica, 16*(1), 20-24. https://doi.org/10.2307/3676570
Mortensen, A., & Blix, A. S. (1989). Seasonal changes in energy intake, energy expenditure, and digestibility in captive Svalbard rock ptarmigan and Norwegian willow ptarmigan. *Ornis Scandinavica, 20*(1), 22-28. https://doi.org/10.2307/3676703
Mortensen, A., Unander, S., Kolstad, M., & Blix, A. S. (1983). Seasonal changes in body composition and crop content of Spitzbergen ptarmigan Lagopus mutus hyperboreus. *Ornis Scandinavica, 14*(2), 144-148.
Mostafa, N., Everett, D., Chou, S., Kong, P., Florant, G., & Coleman, R. (1993). Seasonal changes in critical enzymes of lipogenesis and triacylglycerol synthesis in the marmot (Marmota flaviventris). *Journal of Comparative Physiology B, 163*(6), 463-469.
Mrosovsky, N., & Fisher, K. (1970). Sliding set points for body weight in ground squirrels during the hibernation season. *Canadian Journal of Zoology, 48*(2), 241-247.
Mrosovsky, N., Nash, P., & Faust, I. (1987). Protection against fat cell hyperplasia in a hibernator, Glis glis. *American Journal of Physiology-Regulatory, Integrative and Comparative Physiology, 253*(4), R580-R586.
Mrosovsky, N., & Powley, T. L. (1977). Set points for body weight and fat. *Behavioral Biology, 20*(2), 205-223. https://doi.org/10.1016/S0091-6773(77)90773-8
Nicholls, T., Goldsmith, A., & Dawson, A. (1988). Photorefractoriness in birds and comparison with mammals. *Physiological reviews, 68*(1), 133-176.
NSIDC. (04-05-2020). *What is the Arctic?* Retrieved 26-01-2021 from https://nsidc.org/cryosphere/arctic-meteorology/arctic.html
Odum, E. P. (1960). Premigratory hyperphagia in birds. *The American Journal of Clinical Nutrition, 8*(5), 621-629.
Odum, E. P., & Perkinson Jr, J. D. (1951). Relation of lipid metabolism to migration in birds seasonal variation in body lipids of the migratory white-throated sparrow. *Physiological zoology, 24*(3), 216-230.
Olsen, L., Thum, E., & Rohner, N. (2021, 2021/03/16/). Lipid metabolism in adaptation to extreme nutritional challenges. *Developmental Cell, 56*. https://doi.org/https://doi.org/10.1016/j.devcel.2021.02.024
Parker, H., & Mehlum, F. (1991). Influence of sea-ice on nesting density in the Common Eider Somateria mollissima in Svalbard. *Norsk Polarinstitutt Skrifter, 195*, 31-36.
Parlee, S. D., Lentz, S. I., Mori, H., & MacDougald, O. A. (2014). Quantifying size and number of adipocytes in adipose tissue. *Methods in enzymology, 537*, 93-122.
Pedersen, Å. Ø., Overrein, Ø., Unander, S., & Fuglei, E. (2005). *Svalbard rock ptarmigan (Lagopus mutus hyperboreus): a status report*.

Prats, C., Gomez-Cabello, A., Nordby, P., Andersen, J. L., Helge, J. W., Dela, F., . . . Ploug, T. (2013). An optimized histochemical method to assess skeletal muscle glycogen and lipid stores reveals two metabolically distinct populations of type I muscle fibers. *PLoS ONE, 8*(10), e77774-e77774. https://doi.org/10.1371/journal.pone.0077774

Prestrud, P., Strøm, H., & Goldman, H. V. (2004). *A catalogue of the terrestrial and marine animals of Svalbard*. Norwegian Polar Institute.

Promega Corporation. (2020). *Tm for oligos calculator*. https://no.promega.com/resources/tools/biomath/tm-calculator/

Pulliainen, E., & Tunkkari, P. S. (1984). Seasonal changes in the weight and composition of the liver of the willow grouse (Lagopus lagopus) in the far north of Finland. *Annales Zoologici Fennici, 21*, 153-156.

Pummoung, S., Werawatganon, D., Chayanupatkul, M., Klaikeaw, N., & Siriviriyakul, P. (2021). Genistein modulated lipid metabolism, hepatic PPARγ, and adiponectin expression in bilateral ovariectomized rats with nonalcoholic steatohepatitis (NASH). *Antioxidants, 10*(1), 24. https://www.mdpi.com/2076-3921/10/1/24

Ramirez-Zacarias, J., Castro-Munozledo, F., & Kuri-Harcuch, W. (1992). Quantitation of adipose conversion and triglycerides by staining intracytoplasmic lipids with Oil red O. *Histochemistry, 97*(6), 493-497.

Sahlman, T., Segelbacher, G., & Hoglund, J. (2009). Islands in the ice: colonisation routes for rock ptarmigan to the Svalbard archipelago. *Ecography, 32*(5), 840-848.

Schneider, C. A., Rasband, W. S., & Eliceiri, K. W. (2012). NIH Image to ImageJ: 25 years of image analysis. *Nature methods, 9*(7), 671-675.

Sharma, A., & Kumar, V. (2019). Metabolic plasticity mediates differential responses to spring and autumn migrations: Evidence from gene expression patterns in migratory buntings. *Experimental Physiology, 104*(12), 1841-1857.

Siitari, H., Alatalo, R. V., Halme, P., Buchanan, K. L., & Kilpimaa, J. (2007). Color signals in the black grouse (Tetrao tetrix): signal properties and their condition dependency. *the american naturalist, 169*(S1), S81-S92.

Sockman, K. W., & Hurlbert, A. H. (2020). How the effects of latitude on daylight availability may have influenced the evolution of migration and photoperiodism. *Functional Ecology, 34*(9), 1752-1766.

Spangenburg, E. E., Pratt, S. J. P., Wohlers, L. M., & Lovering, R. M. (2011, 2011/09/25). Use of BODIPY (493/503) to visualize intramuscular lipid droplets in skeletal muscle. *Journal of Biomedicine and Biotechnology, 2011*, 598358. https://doi.org/10.1155/2011/598358

Steen, J. B., & Unander, S. (1985). Breeding biology of the Svalbard Rock Ptarmigan Lagopus mutus hyperboreus. *Ornis Scandinavica*, 191-197.

Stokkan, K.-A., Lindgård, K., & Reierth, E. (1995). Photoperiodic and ambient temperature control of the annual body mass cycle in Svalbard ptarmigan. *Journal of Comparative Physiology B, 165*(5), 359-365.

Stokkan, K. A., Mortensen, A., & Blix, A. S. (1986a). Food intake, feeding rhythm, and body mass regulation in Svalbard rock ptarmigan. *American Journal of Physiology - Regulatory Integrative and Comparative Physiology, 251*(2), R264-R267. https://doi.org/10.1152/ajpregu.1986.251.2.r264

Stokkan, K. A., Sharp, P. J., Dunn, I. C., & Lea, R. W. (1988). Endocrine changes in photostimulated willow ptarmigan (Lagopus lagopus lagopus) and Svalbard

ptarmigan (Lagopus mutus hyperboreus). *General and Comparative Endocrinology, 70*(1), 169-177. https://doi.org/10.1016/0016-6480(88)90107-4
Stokkan, K. A., Sharp, P. J., & Unander, S. (1986b). The annual breeding cycle of the high-arctic Svalbard ptarmigan (Lagopus mutus hyperboreus). *General and Comparative Endocrinology, 61*(3), 446-451. https://doi.org/10.1016/0016-6480(86)90232-7
Storch, I. (2000). WPA/Birdlife/SSC Grouse Specialist Group, IUCN; Reading: the World Pheasant Association; Gland, Switzerland; Cambridge, UK: 2000. *Grouse status survey and conservation action plan, 2004*, 112.
Unander, S., Mortensen, A., & Elvebakk, A. (1985). Seasonal changes in crop content of the Svalbard ptarmigan Lagopus mutus hyperboreus. *Polar Research, 3*(2), 239-245. https://doi.org/10.3402/polar.v3i2.6955
Unander, S., & Steen, J. B. (1985). Behaviour and social structure in Svalbard rock ptarmigan Lagopus mutus hyperboreus. *Ornis Scandinavica, 16*(3), 198-204.
Untergasser, A., Cutcutache, I., Koressaar, T., Ye, J., Faircloth, B. C., Remm, M., & Rozen, S. G. (2012). Primer3—new capabilities and interfaces. *Nucleic acids research, 40*(15), e115-e115.
Viscarra, J. A., & Ortiz, R. M. (2013). Cellular mechanisms regulating fuel metabolism in mammals: Role of adipose tissue and lipids during prolonged food deprivation. *Metabolism, 62*(7), 889-897.
Viscarra, J. A., Vázquez-Medina, J. P., Rodriguez, R., Champagne, C. D., Adams, S. H., Crocker, D. E., & Ortiz, R. M. (2012). Decreased expression of adipose CD36 and FATP1 are associated with increased plasma non-esterified fatty acids during prolonged fasting in northern elephant seal pups (*Mirounga angustirostris*). *The Journal of experimental biology, 215*(Pt 14), 2455-2464. https://doi.org/10.1242/jeb.069070
Weber, J.-M. (2009). The physiology of long-distance migration: extending the limits of endurance metabolism. *Journal of Experimental Biology, 212*(5), 593-597.
Wei, T., Simko, V., Levy, M., Xie, Y., Jin, Y., & Zemla, J. (2017). Package 'corrplot'. *Statistician, 56*(316), e24.
Wickström, S., Jonassen, M. O., Cassano, J. J., & Vihma, T. (2020). Present Temperature, Precipitation, and Rain‐on‐Snow Climate in Svalbard. *Journal of Geophysical Research: Atmospheres, 125*(14), e2019JD032155.
Yates, A. D., Achuthan, P., Akanni, W., Allen, J., Allen, J., Alvarez-Jarreta, J., . . . Flicek, P. (2020). Ensembl 2020. *Nucleic acids research, 48*(D1), D682-D688. https://doi.org/10.1093/nar/gkz966
Ye, J., Coulouris, G., Zaretskaya, I., Cutcutache, I., Rozen, S., & Madden, T. L. (2012). Primer-BLAST: a tool to design target-specific primers for polymerase chain reaction. *BMC bioinformatics, 13*(1), 1-11.
Zaefarian, F., Abdollahi, M. R., Cowieson, A., & Ravindran, V. (2019). Avian liver: the forgotten organ. *Animals, 9*(2), 63.
Zajac, D. M., Cerasale, D. J., Landman, S., & Guglielmo, C. G. (2011). Behavioral and physiological effects of photoperiod-induced migratory state and leptin on Zonotrichia albicollis: II. Effects on fatty acid metabolism. *General and Comparative Endocrinology, 174*(3), 269-275.

Appendix A – Raw data, statistics and qPCR results

Table A 1. Details on the birds in the study and raw data from samplings. The sampling point, bird-ID, room, position, gender, age, body mass (BM), liver mass, fat mass, fat as a percentage of BM, and the mass of the gonads of the 33 Svalbard ptarmigan studied for this project.

Sampling	Bird-ID	Room	Position	Gender	Age	BM (g)	Liver (g)	Fat (g)	Fat (%BM)	Gonads (g)
1	R5	3	17	male	yearling	794	6.4	77.5	9.76	0.033
1	R9	3	16	female	yearling	610	5.2	53.5	8.77	0.12
1	299-98	3	14	male	old	949	6.3	129	13.59	0.089
1	183-98	2	9	female	old	736	4.1	81.1	11.02	0.135
1	R30	6	35	male	yearling	722	5.6	71.1	9.85	0.1
1	294-98	3	15	male	old	1003	7.9	159.9	15.94	0.07
1	R31	6	36	female	yearling	560	4.6	34	6.07	0.186
2	R10	4	19	male	yearling	668	5.1	53.7	8.04	0.099
2	119-98	4	22	female	old	750	2.9	93	12.40	0.39
2	R13	4	20	female	yearling	501	4.1	10.4	2.08	0.108
2	184-98	4	24	male	old	791	5.5	87.4	11.05	0.103
2	R11	4	21	male	yearling	660	5	61.6	9.33	0.093
2	185-98	2	11	male	old	946	5.5	160.8	17.00	0.207
2	R26	1	4	female	yearling	753	5.3	83	11.02	0.144
2	187-98	5	30	male	old	846	3.8	90.1	10.65	0.087
3	R28	1	2	female	yearling	626	9	20.3	3.24	27.723
3	R27	1	6	male	yearling	525	4.9	15.6	2.97	1.789
3	190-98	2	12	male	old	541	5.9	19.1	3.53	2.573
3	296-98	5	27	male	old	660	5.5	54.8	8.30	2.72
3	126-98	5	28	female	old	638	10.2	13.6	2.13	16.454
3	R32	6	33	female	yearling	677	10	44.5	6.57	25.202
3	R34	6	34	male	yearling	524	6	9.3	1.77	1.095
4	135-98	5	26	male	old	703	8.4	41.8	5.95	0.491

4	270-98	5	29	female	old	720	8.9	75.7	10.51	0.279
4	R33	1	1	female	yearling	603	10.5	54.8	9.09	0.16
4	R7	1	3	male	yearling	720	13.3	53	7.36	0.188
4	G176	1	5	male	yearling	695	7	82.9	11.93	0.395
4	291-98	2	7	male	old	746	10.4	50.7	6.80	0.182
4	188-98	2	10	male	old	758	9.7	45.8	6.04	0.665
4	R29	6	31	female	yearling	591	7.7	43.6	7.38	0.582
Not sampled	R35	6	32	male	yearling	-	-	-	-	-
Not sampled	047-98	2	8	female	old	-	-	-	-	-
Not sampled	260-98	5	25	male	old	-	-	-	-	-

Table A 2. Testosterone measurements. The sampling point, bird-ID, and the measured testosterone in ng/ml in male captive Svalbard ptarmigan.

Sampling	**Bird-ID**	**Testosterone** (ng/ml)
1	R5	0
1	299-98	0
1	R30	0
1	294-98	0
2	R10	2.028868
2	184-98	0.174201
2	R11	2.526326
2	185-98	0.322909
2	187-98	0.406595
3	R27	2.555908
3	190-98	1.295841
3	296-98	10.64298 (outlier not included in analysis)
3	R34	2.565876
4	135-98	0
4	R7	0.017961
4	G176	0
4	291-98	0
4	188-98	0

Table A 3. Descriptive statistics for liver mass. The mean, standard error of the mean (SEM), and the sample size (N) for each sampling group.

Age	Sampling	Mean	SEM	N
Yearling	1	5.450	0.377	4
	2	4.875	0.266	4
	3	7.475	1.208	4
	4	9.625	1.440	4
Old	1	6.100	1.102	3
	2	4.425	0.647	4
	3	7.200	1.504	3
	4	9.350	0.441	4

Table A 4. ANOVA summary table for liver mass. Degrees of freedom (DF), mean of squares (MS) and F- and P- values with sampling group and age as the independent variables and liver mass as the dependent variable. The results of the Tukey's multiple comparisons test performed *post hoc*. *p<0.05, **p<0.01.

	DF	MS	F (DFn, DFd)	P	Tukey's multiple comparisons test
Interaction (age x sampling)	3	0.4408	0.1326 (3,22)	0.9396	Yearling: 1 vs 4: * 2 vs 4: ** Old: 2 vs 4: **
Sampling	3	36.64	10.42 (3,22)	0.0002***	
Age	1	0.05654	0.017 (1,22)	0.9396	

Table A 5. Descriptive statistics for fat mass. The mean, standard error of the mean (SEM), and the sample size (n) for each sampling group.

Age	Sampling	Mean	SEM	n
Yearling	1	59.025	9.763	4
	2	52.175	15.238	4
	3	22.425	7.696	4
	4	58.575	8.472	4
Old	1	123.333	22.923	3
	2	107.825	17.695	4
	3	29.167	12.915	3
	4	53.500	7.620	4

Table A 6. ANOVA summary table for fat mass. Degrees of freedom (DF), mean of squares (MS) and F- and P- values with sampling group and age as the independent variables and fat mass as the dependent variable. The results of the Tukey's multiple comparisons test performed *post hoc*. *p<0.05, **p<0.01, ***p<0.001.

	DF	**MS**	**F** (DFn, DFd)	**P**	**Tukey's multiple comparisons test**
Interaction (age x sampling)	3	2241	3.493 (3,22)	0.0327*	Old: 1 vs 3: *** 1 vs 4: ** 2 vs 3: ** 2 vs 4: *
Sampling	3	5875	9.160 (3,22)	0.0004***	
Age	1	6827	10.64 (1,22)	0.0036**	

Table A 7. qPCR results. The relative gene expression as log2 fold change from sampling group 1 of six key lipid metabolism enzymes in captive Svalbard ptarmigan sampled at four times in their body mass cycle.

		Liver						**Fat**					
Sampling	**ID**	**ACACA**	**FASN**	**ATGL**	**MGLL**	**ACSL1**	**CPTIA**	**ACACA**	**FASN**	**ATGL**	**MGLL**	**ACSL1**	**CPTIA**
1	R5	1.13	0.75	0.11	0.63	-0.15	-0.57	0.00	-0.12	-0.27	-0.12	0.20	0.00
1	R9	0.13	0.04	0.19	0.29	-0.07	0.32	0.21	0.63	-0.10	0.04	0.23	-0.15
1	299-98	-0.26	-0.04	-0.82	0.56	-1.10	-0.82	-0.07	0.21	-0.22	0.14	-0.12	0.50
1	183-98	0.95	0.64	0.87	-0.32	1.51	1.02	-0.18	-1.06	-1.29	1.12	-0.79	0.65
1	R30	-1.52	-1.36	0.62	-0.62	-0.04	0.24	0.14	0.50	-0.18	-0.97	0.24	-0.15
1	294-98	0.54	0.84	-0.78	-0.04	-0.65	-0.19	0.21	-0.01	0.72	-0.06	0.18	-0.36
1	R31	-0.95	-0.86	-0.20	-0.50	0.51	0.01	-0.30	-0.15	1.32	-0.15	0.06	-0.49
2	R10	-1.45	-2.57	-0.34	-1.75	-0.46	0.57	0.28	-0.43	0.79	-0.09	0.96	0.29
2	119-98	-0.98	-0.96	0.11	-0.40	-1.27	-0.50	-0.20	-0.67	-0.29	-0.94	-0.94	-0.42
2	R13	-1.49	-2.15	-0.73	-0.70	-1.49	-0.20	0.32	-0.67	1.84	0.58	0.58	-0.10
2	184-98	-1.89	-1.36	-0.42	-0.50	0.26	0.41	-0.30	-0.92	0.19	0.65	-0.45	0.10
2	R11	-1.16	-1.82	-0.10	-0.23	0.02	2.03	-0.22	-1.03	-0.74	0.41	-0.38	-0.74
2	185-98	-1.96	-2.47	-1.04	-0.65	-0.59	0.57	0.25	-0.42	0.16	0.44	-0.01	-0.12
2	R26	-0.54	-0.95	0.04	-0.16	-0.49	-0.33	0.19	-0.30	-0.69	0.15	-0.20	0.11
2	187-98	0.84	1.39	1.15	0.95	0.63	0.45	0.06	-0.60	-0.54	0.43	-0.03	-0.22
3	R28	-1.51	-1.34	-0.84	-0.39	-2.00	0.84	-0.07	-0.47	2.08	0.38	0.07	0.07
3	R27	-0.87	0.15	1.53	0.90	-1.11	-0.37	0.46	0.42	2.45	0.11	0.29	-0.45
3	190-98	0.57	-0.27	-0.06	0.29	-0.44	0.24	-0.09	-0.76	1.33	0.29	-0.04	0.79
3	296-98	0.26	-0.19	1.23	0.00	1.16	1.49	0.08	-0.51	0.44	0.38	-0.01	0.52
3	126-98	-1.22	-1.68	-0.83	-1.84	-3.63	-0.70	-0.04	-0.67	-0.27	-0.25	-1.25	-1.69
3	R32	-0.85	0.90	-2.02	0.08	-2.88	-1.77	-0.09	0.58	0.08	-0.10	-0.81	-1.69
3	R34	-1.01	-1.16	0.58	-0.47	-1.18	-0.89	0.12	0.29	2.14	-0.12	0.24	-0.47
4	135-98	-0.16	0.61	0.28	-0.62	-0.56	-0.78	0.18	0.31	-0.86	-1.12	-0.51	-1.29

4	270-98	0.88	0.82	-0.38	-0.56	-0.77	-0.31	-0.15	-0.49	-1.18	0.16	-0.62	-0.20
4	R33	0.40	0.38	-1.04	-0.42	-0.52	-1.94	0.41	0.85	-1.40	-0.74	0.20	-1.60
4	R7	-0.05	0.25	-0.41	0.29	-0.95	-1.66	0.37	0.08	-1.43	-0.38	0.06	-1.56
4	G176	-0.25	-0.84	-0.62	-1.32	-1.33	-2.43	0.03	0.42	-0.62	-0.64	-0.43	-1.32
4	291-98	0.03	0.04	-1.17	-1.15	-0.63	-1.28	0.26	0.28	-0.62	-0.14	-0.56	-1.60
4	188-98	0.07	0.03	0.14	-0.61	-0.66	-0.46	0.14	0.31	-0.89	0.15	-0.07	-0.86
4	R29	0.77	0.04	0.33	-0.38	0.37	0.26	0.26	0.26	-1.29	-1.15	-0.20	-0.81

Table A 8. Results of statistical analyses of qPCR. The F-value (DFn, DFd) and p-value results from a one-way ANOVA. If significant, a *post hoc* Tukey's multiple comparisons test was performed and p-values are presented if significant. Group 1 – fat winter birds (n=7), 2 – birds rapidly losing weight (n=8), 3 – lean summer birds, and 4 (n=7) – photorefractive birds gaining weight (n=8). *p<0.05, **p<0.01.

Tissue	**Gene**	**One-way ANOVA results** F(DFn, DFd)	***post hoc* Tukey's multiple comparisons test**
Liver	ACACA	F(3,26) = 2. 99	ns
		P = 0.049*	
	FASN	F(3,26) = 1.38	
		P = 0.272	
	ATGL	F(3,26) = 0.715	
		P = 0.552	
	MGLL	F(3,26) = 1.16	
		P = 0.346	
	ACSL1	F(3,26) = 1.28	
		P = 0.301	
	CPT1A	F(3,26) = 2.13	
		P = 0.121	
Fat	ACACA	F(3,26) = 1.11	
		P = 0.361	
	FASN	F(3,26) = 5.07	2 vs 4: 0.0042**
		P = 0.0068**	
	ATGL	F(3,26) = 6.04	1 vs 3: 0.036* 2 vs 3: 0.049* 3 vs 4: 0.0017**
		P = 0.0029**	
	MGLL	F(3,26) = 2.46	
		P = 0.086	
	ACSL1	F(3,26) = 0.644	
		P = 0.594	
	CPT1A	F(3,26) = 4.25	1 vs 4: 0.015*
		P = 0.0014*	

Appendix B – Results of ORO

Table B 1. ORO results liver. The percentage of a section of liver tissue stained with ORO.

Sampling	ID	% of section stained with ORO
1	R5	25.12
1	R9	37.67
1	299-98	36.38
1	183-98	14.65
1	R30	55.91
1	294-98	71.17
1	R31	17.59
2	R10	7.42
2	119-98	17.33
2	R13	15.57
2	184-98	22.96
2	R11	29.79
2	185-98	15.35
2	R26	12.51
2	187-98	14.91
3	R28	4.77
3	R27	18.58
3	190-98	18.84
3	296-98	13.27
3	126-98	9.66
3	R32	8.67
3	R34	14.81
4	135-98	14.86
4	270-98	10.49
4	R33	43.74
4	R7	49.49
4	G176	13.28
4	291-98	15.99
4	188-98	23.99
4	R29	37.48

Table B 2. ORO results heart. The percentage of a section of heart tissue stained with ORO.

Sampling	ID	% of section stained with ORO
1	R5	4.97
1	R9	3.05
1	299-98	0.31
1	183-98	0.27
1	R30	1.20

1	294-98	0.05
1	R31	0.75
2	R10	0.32
2	119-98	2.61
2	R13	0.25
2	184-98	0.60
2	R11	0.17
2	185-98	1.06
2	R26	1.59
2	187-98	0.65
3	R28	1.93
3	R27	0.48
3	190-98	0.99
3	296-98	1.01
3	126-98	3.12
3	R32	5.71
3	R34	0.75
4	135-98	2.96
4	270-98	3.20
4	R33	1.71
4	R7	1.61
4	G176	0.96
4	291-98	1.68
4	188-98	4.66
4	R29	2.18

Table B 3. ORO results muscle. The percentage of a section of muscle tissue stained with ORO.

Sampling	ID	% of section stained with ORO
1	R5	1.33
1	R9	3.36
1	299-98	0.31
1	183-98	3.42
1	R30	3.16
1	294-98	6.08
1	R31	0.90
2	R10	5.51
2	119-98	2.08
2	R13	2.19
2	184-98	6.34
2	R11	13.70
2	185-98	1.92
2	R26	3.37
2	187-98	3.09

3	R28	4.83
3	R27	6.27
3	190-98	20.81
3	296-98	5.49
3	126-98	1.44
3	R32	7.93
3	R34	13.49
4	135-98	11.73
4	270-98	2.66
4	R33	4.54
4	R7	2.36
4	G176	17.69
4	291-98	8.62
4	188-98	3.45
4	R29	9.36

Table B 4. Results of ORO staining of fat. The percent body fat and the mean ±SEM cell area in μm^2. The cell area was measured on ORO stained fat sections from captive Svalbard ptarmigan. Lean birds: ≤6% body fat and fat birds ≥11% body fat.

	ID	**% body fat**	**Mean ±SEM cell area (μm^2)**	**The number of cells measured**
Lean	R13	2.08	3075 ±263	13
	188-98	6.04	2451 ±220	18
	R34	1.77	2774 ±250	14
	135-98	5.95	1868 ±174	15
	R28	3.24	3659 ±276	7
	R27	2.97	2048 ±239	15
	126-98	2.13	2907 ±434	13
	190-98	3.53	2370 ±203	12
Fat	183-98	11.02	3753 ±247	21
	185-98	17.0	7567 ±1027	9
	119-98	12.4	4520 ±278	17
	294-98	15.94	7267 ±1031	9
	G176	11.93	4213 ±202	18
	184-98	11.05	4400 ±273	14
	R26	11.02	4735 ±571	11

Appendix C – Correlation plots and R script

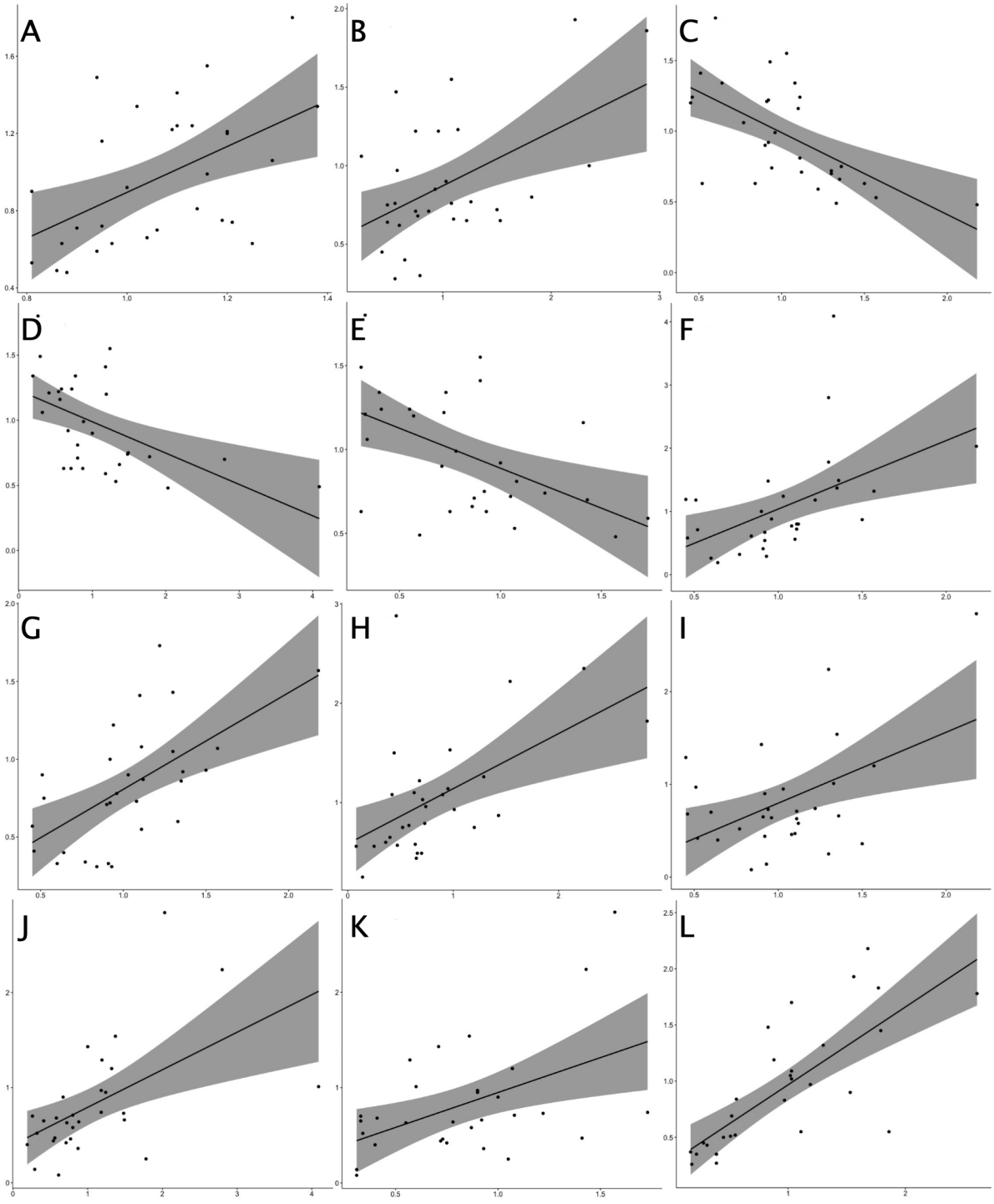

Figure C. 1. Correlation plots – gene expression. Results presented as fold change with 95% confidence interval. **A:** FASN fat x ACACA fat (R=0.52 , p<0.01); **B:** MGLL liver x ATGL liver (R=0.51, p<0.01); **C:** FASN fat x MGLL fat (R= -0.61, p<0.001); **D:** FASN fat x CPT1A liver (R= -0.54, p<0.01); **E:** FASN fat x CPTIA fat (R= -0.51, p<0.01); **F:** CPTIA liver x MGLL fat (R=0.5, P<0.01); **G:** CPTIA fat x MGLL fat (R=0.6, p<0.001); **H:** ATGL liver x ACSL1 liver (R=0.53, p<0.01); **I:** ACSL1 liver x MGLL fat (R=0.49, p<0.01); **J:** ACSL1 liver x CPTIA liver (R=0.54, p<0.01); **K:** ACSL1 liver x CPTIA fat (R=0.48, p<0.01); **L:** ACACA liver x FASN liver (R=0.76, p<0.0001).

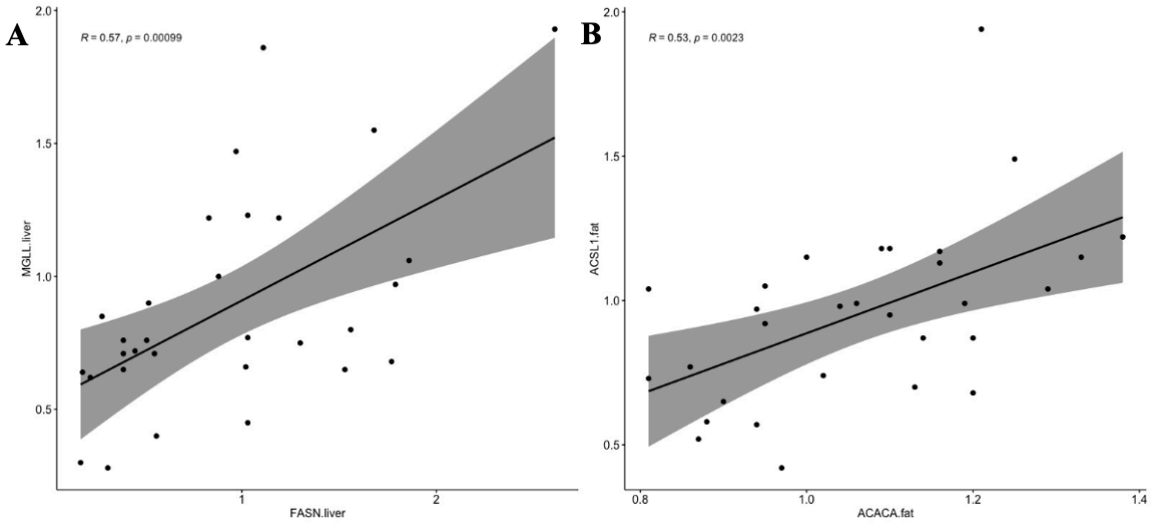

Figure C. 2. Expression of FA synthesis genes correlates with expression of lipolysis and FA oxidation genes. (**A**) MGLL gene expression plotted against FASN gene expression in fold change in liver tissue (R=0.57, p<0.001) and (**B**) ACSL1 gene expression plotted against ACACA gene expression in fold change in fat tissue (R=0.53, p<0.01) with 95% confidence intervals.

r script – correlation matrix and plots

```
ptarmigan <- read.delim("ptarmigan.txt")

ptarmatrix <- ptarmigan[c(-1,-2,-3,-4)]

#CORRELATION MATRIX:

library("Hmisc")

res <- cor(ptarmatrix, use= "complete.obs")

res

round(res, 2)

res2 <- rcorr(as.matrix(ptarmatrix))

res2

#The visualization of the matrix:

library(corrplot)

corrplot(res, type="upper", method="circle")
```

```
cor_5 <- rcorr(as.matrix(ptarmatrix))
M <- cor_5$r
p_mat <- cor_5$P
corrplot(M, type = "upper", order = "hclust",
         p.mat = p_mat, sig.level = 0.01, insig = "blank")

corrplot(res, type="upper", method="number")



res.aov2 <- aov(fFASN ~ factor(Group)*VFI, data = ptarmigan)
summary(res.aov2)

#INDIVIDUAL CORRELATION PLOTS:
library("ggpubr")
ggscatter(ptarmigan, x = "FASN.fat", y = "VFI",
          add = "reg.line", conf.int = TRUE,
          cor.coef = TRUE, cor.method = "pearson",
          xlab = "FASN.fat", ylab = "VFI")

ggscatter(ptarmigan, x = "MGLL.fat", y = "VFI",
          add = "reg.line", conf.int = TRUE,
          cor.coef = TRUE, cor.method = "pearson",
          xlab = "MGLL.fat", ylab = "VFI")

ggscatter(ptarmigan, x = "CPT1A.fat", y = "VFI",
          add = "reg.line", conf.int = TRUE,
          cor.coef = TRUE, cor.method = "pearson",
```

```
        xlab = "CPT1A.fat", ylab = "VFI")


ggscatter(ptarmigan, x = "CPT1A.liver", y = "VFI",
        add = "reg.line", conf.int = TRUE,
        cor.coef = TRUE, cor.method = "pearson",
        xlab = "CPT1A.liver", ylab = "VFI")
```